FINAL PROJECT REPORT # 00047948

GRANT: DTRT13-G-UTC45
Project Period: 8/1/2014 – 12/31/19

Volume II: Strengthening and Repair of Structural Concrete with a Fabric-Reinforced-Cementitious-Matrix (FRCM): Field Studies

Participating Consortium Member:
Missouri University of Science and Technology

Authors:
Dr. John J. Myers, Ph.D., P.E., (PI)
Dr. Eli S. Hernandez, Ph.D.
Michael A. Janke
Missouri University of Science and Technology

RE-CAST:
REsearch on Concrete Applications for Sustainable Transportation
Tier 1 University Transportation Center

DISCLAIMER

The contents of this report reflect the views of the authors, who are responsible for the facts and the accuracy of the information presented herein. This document is disseminated under the sponsorship of the U.S. Department of Transportation's University Transportation Centers Program, in the interest of information exchange. The U.S. Government assumes no liability for the contents or use thereof.

TECHNICAL REPORT DOCUMENTATION PAGE

1. Report No. RECAST UTC # 00047948	**2. Government Accession No.**	**3. Recipient's Catalog No.**
4. Title and Subtitle Volume II: Strengthening and Repair of Structural Concrete with a Fabric-Reinforced-Cementitious-Matrix (FRCM): Field Studies		**5. Report Date** January 2020 **6. Performing Organization Code:**
7. Author(s) Dr. John J. Myers, Dr. Eli S. Hernandez, and Michael A. Janke		**8. Performing Organization Report No.** Project # 00047948
9. Performing Organization Name and Address RE-CAST – Missouri University of Science and Technology 500 W. 16th St., 223 ERL Rolla, MO 65409-0710		**10. Work Unit No.** **11. Contract or Grant No.** USDOT: DTRT13-G-UTC45
12. Sponsoring Agency Name and Address Office of the Assistant Secretary for Research and Technology U.S. Department of Transportation 1200 New Jersey Avenue, SE Washington, DC 20590		**13. Type of Report and Period Covered:** Final Report Period: 8/1/2014 – 12/31/19 **14. Sponsoring Agency Code:**

15. Supplementary Notes
The investigation was conducted in cooperation with the U. S. Department of Transportation.

16. Abstract
With infrastructure continuing to age, technologies are being developed to strengthen structures as a more sustainable option than replacement. The use of fiber reinforced cementitious matrix (FRCM) strengthening systems is a promising new technology for adding flexural and shear capacity to existing reinforced concrete members. While cement based systems with carbon, PBO, and steel have all been implemented in a lab setting, there is not research data available for installation in the field. FRCM composites have advantages over more widely used fiber reinforced polymer (FRP) composites such as heat resistance and compatibility with concrete substrate. FRP systems have previously been field tested, giving confidence for the growth of FRCM use. This study aimed to validate the use of cement-based systems for field implementation. Missouri Bridge P-0058, a structurally deficient bridge in southern Missouri, was recently selected and six of its twelve girders were identified for strengthening using four different composite systems, three of which are cement-based. A parametric study was conducted to help choose the final design that will give the best information in the future. A pre-strengthening load test was conducted to get a baseline of the bridge's stiffness, so that future tests can capture the change due to the strengthening as well as potential loss of stiffness over time. Future work desires for the bridge girders to be brought to the campus of Missouri University of Science and Technology when the bridge is decommissioned. On campus, destructive testing will give valuable information about the field strengthened and field conditioned beams.

17. Key Words Strengthening and Repair; Structural Concrete; Fabric-Reinforced-Cementitious-Matrix	**18. Distribution Statement** No restrictions. This document is available to the public.	
19. Security Classification (of this report) Unclassified	**20. Security Classification (of this page)** Unclassified	**21. No of Pages** 157

Form DOT F 1700.7 (8-72) Reproduction of form and completed page is authorized.

Report for

RE-CAST-Research on Concrete Applications for Sustainable Transportation Tier 1 University Transportation Center (UTC)

Grant: DTRT13-G-UTC45

Strengthening and Repair of Structural Concrete with a Fabric-Reinforced-Cementitious-Matrix (FRCM): Field Studies

by

Dr. John J. Myers, Ph.D., P.E., (PI)
Dr. Eli S. Hernandez, Ph.D.
Michael A. Janke

Missouri University of Science and Technology
Department of Civil, Architectural & Environmental Engineering

January 2020

EXECUTIVE SUMMARY

With infrastructure continuing to age, technologies are being developed to strengthen structures as a more sustainable option than replacement. The use of fiber-reinforced cementitious matrix (FRCM) strengthening systems is a promising new technology for adding flexural and shear capacity to existing reinforced concrete members. While cement based systems with carbon, PBO, and steel have all been implemented in a lab setting, there is not research data available for installation in the field. FRCM composites have advantages over more widely used fiber reinforced polymer (FRP) composites such as heat resistance and compatibility with concrete substrate. FRP systems have previously been field tested, giving confidence for the growth of FRCM use. This study aimed to validate the use of cement-based systems for field implementation. Missouri Bridge P-0058, a structurally deficient bridge in southern Missouri, was recently selected and six of its twelve girders were identified for strengthening using four different composite systems, three of which are cement-based. A parametric study was conducted to help choose the final design that will give the best information in the future. A pre-strengthening load test was conducted to get a baseline of the bridge's stiffness, so that future tests can capture the change due to the strengthening as well as potential loss of stiffness over time. Future work desires for the bridge girders to be brought to the campus of Missouri University of Science and Technology when the bridge is decommissioned. On campus, destructive testing will give valuable information about the field strengthened and field conditioned beams.

TABLE OF CONTENTS

Page

EXECUTIVE SUMMARY iv

TABLE OF CONTENTS v

LIST OF ILLUSTRATIONS viii

LIST OF TABLES x

NOMENCLATURE xi

1. INTRODUCTION 1

1.1. BACKGROUND 1

1.2. RESEARCH OBJECTIVE 2

1.3. SCOPE AND LIMITATIONS 2

1.4. REPORT ORGANIZATION 3

2. LITERATURE REVIEW 4

2.1. FIBER-REINFORCED POLYMER STRENGTHENING 4

2.1.1. Types of Externally Bonded FRP Systems. 4

2.1.1.1. Wet layup systems. 4

2.1.1.2. Prepreg systems. 4

2.1.1.3. Precured systems. 5

2.1.1.4. Near-surface-mounted (NSM) systems. 5

2.1.2. Constituent Materials and Properties. 5

2.1.2.1. Constituent materials. 5

2.1.2.2. Physical properties 8

2.1.2.3. Mechanical properties 9

2.1.2.4. Time-dependent properties. 10

2.1.3. FRP Failure Modes 10

2.1.4. Research on FRP Strengthening Systems 11

2.1.4.1. Holdener, Myers, & Nanni, (2004) 11

2.1.4.2. Rahman, Kingsley, & Kobayashi (2000). 14

2.1.4.3. Petrou, Parler, Harries, & Rizos (2008) 15

2.2. FABRIC-REINFORCED CEMENTICIOUS MATRIX STRENGTHENING 16

2.2.1. Tensile Characterization 17
2.2.2. Research on FRCM Strengthening Systems 19
2.2.2.1. Di Tommaso, Focacci, & Mantegazza (2008) 19
2.2.2.2. D'Ambrisi & Focacci (2011). 20
2.2.2.3. Loreto, Leardini, Arboleda, and Nanni (2013). 20
2.2.2.4. Babaeidarabad, Loreto, and Nanni (2014) 21
2.2.2.5. Ombres (2015). 22
2.2.2.6. Loreto, Babaeidarabad, Leardini, and Nanni (2015). 23
2.3. STEEL REINFORCED GROUT 24
2.3.1. Research on SRG Strengthening. 25
2.3.1.1. Huang et al. (2003). 25
2.3.1.2. Wobbe et al. (2004) 25
2.4. NON-DESTRUCTIVE TESTING 26
2.4.1. Load Testing 26
2.4.2. Surface Roughness 27
2.4.3. Fiber Alignment 28
2.4.4. FRP Delamination 28
3. DESIGN OF STRENGTHENING SYSTEM 29
3.1. BRIDGE DESCRIPTION 29
3.2. MATERIALS USED 30
3.2.1. Fiber-Reinforced Polymer 30
3.2.2. Fiber Reinforced Cementitious Matrix 31
3.3. ANALYSIS OF EXISTING CAPACITY 31
3.3.1. Flexure 33
3.3.2. Shear 35
3.4. GIRDER STRENGTHENING DESIGN 36
3.4.1. Fiber Reinforced Polymer 38
3.4.1.1. Flexure design 39
3.4.1.2. Shear designI 41
3.4.2. Fiber Reinforced Cementitious Matrix. 43
1.1.1.1. Flexure design. is 43

1.1.1.2. Shear design 44
3.4.3. Summary of Design. 45
4. INSTALLATION OF STRENGTHENING SYSTEM 47
4.1. PRE INSTALLATION 47
4.1.1. Substrate Repair 47
4.1.2. Surface Preparation 48
4.2. INSTALLATION 49
4.2.1. Mixing of Resin or Matrix 49
4.2.2. Manual Layup 50
1.1.2. Curing 52
4.2.3. Durability Study 52
5. LOAD TEST PROGRAM 53
5.1. INSTRUMENTATION 53
5.2. SETUP 54
5.3. PROCEDURE 56
5.4. RESULTS AND DISCUSSION 58
5.4.1. Data Analysis. 59
5.4.2. Theoretical Modeling. 59
5.4.3. Results. 60
5.5. LOAD TESTING RESULTS PRIOR TO STRENGTHENING 66
5.6. BRIDGE EVALUATION PRIOR TO STRENGTHENING 66
6. SUMMARY AND CONCLUSIONS 69
6.1. SUMMARY 69
6.2. FINDINGS AND CONCLUSIONS 70
6.3. RECOMMENDATIONS 71
6.4. CURRENT AND FUTURE FIELD DURABILITY STUDIES 72

LIST OF ILLUSTRATIONS

Figure Page

2-1. FRP Debonding Modes 12
2-2. Location of Bridges Strengthened 12
2-3. Loading Scheme 15
2-4. Stress-Strain Curve for Fully-Clamped FRCM in Tension. 18
2-5. Debonding Failure Modes 19
2-6. Steel Reinforcement. 24
2-7. Laser Profilometer 27
3-1. Bridge P-0058 Load Posting 30
3-2. Bridge P-00585 Approach and Profile View 30
3-3. Fibers Used in FRCM. 33
3-4. Cross Sections of Spans 34
3-5. Effective Flange Width 35
3-6. Internal Stress and Strain Distribution in Flexure 41
3-7. Shear Strengthening with FRP Nomenclature 42
4-1. Spalling on Girder 47
4-2. Surface Preparation by Sand Blasting 48
4-3. Rounding Corners 49
4-4. Mixing Resin and Cementitious Matrix 50
4-5. Preparation of CFRP Sheets 51
4-6. Manual Layup of CFRP 51
5-1. Span 1 Prism Layout 54
5-2. Span 4 Prism Layout 54
5-3. Data Acquisition System Setup. 55
5-4. Total Station Setup 56
5-5. H20 Dump Truck Axle Configuration 56
5-6. Load Test Truck Placements 57
5-7. Trucks on Span 1 for Load Test 58

5-8. Truck on Span 4 for Load Test 58
5-9. Span 1 Stop 1 Vertical Deflection 61
5-10. Span 1 Stop 2 Vertical Deflection 61
5-11. Span 1 Stop 3 Vertical Deflection 62
5-12. Span 1 Stop 1 Interior Girder Deflection Comparison 63
5-13. Span 1 Stop 1 Exterior Girder Deflection Comparison 63
5-14. Span 1 Stop 2 Interior Girder Deflection Comparison 64
5-15. Span 1 Stop 2 Exterior Girder Deflection Comparison 64
5-16. Span 1 Stop 3 Interior Girder Deflection Comparison 65
5-17. Span 1 Stop 3 Exterior Girder Deflection Comparison 65
6-1. Fabrication of Beam Specimens 72
6-2. Additional Specimens. 74
6-3. Beam Strengthening with SRG System 74
6-4. Beam Strengthening with PBO System 75
6-5. Experimental Program. 76

LIST OF TABLES

Table Page

2-1. Typical Tensile Properties of Fibers Used in FRP Systems 8
2-2. Typical Densities of FRP Materials 8
2-3. FRP Service Load Stress Limits 10
2-4. Details of Five Bridges Strengthened 13
2-5. Girder Strengthening Schedule and Analytical Capacity Increase 13
3-1. CFRP Properties from Manufacturer 31
3-2. FRCM Statistical Properties 32
3-3. Geometrical Properties 35
3-4. Flexural Internal Steel Reinforcement at Midspan 35
3-5. Existing Nominal Moment Capacity 36
3-6. Shear Internal Steel Reinforcement 36
3-7. Existing Nominal Shear Capacity 36
3-8. Moment Capacity Parametric Data 37
3-9. Creep and Fatigue Stress Limits 45
3-10. Summary of Strengthening System Design 45
5-1. Pre-Strengthening Load Test Axle Loads 59
5-2. Midspan load distribution factor (LFD) 67
5-3. Analytical moments (span 1) 67
5-4. Bridge load rating 67
6-1. Test Matrix for Strengthening System (Bending Test) 73

NOMENCLATURE

Symbol	Description
a	Depth of equivalent stress block (in)
a/d	Shear span-to-depth ratio (in/in)
A_c	Area of concrete section (in^2)
A_f	Area of FRP/FRCM reinforcement (in^2)
A_{fv}	Area of FRP/FRCM shear reinforcement, with spacing s (in^2)
A_s	Area of longitudinal steel (in^2)
b	Width of rectangular cross section (in)
b_w	Web thickness (in)
b_e	Effective width of the flange
c	Distance from extreme compressive fiber to neutral axis (in.)
C_E	Environmental reduction factor
d	Distance from extreme compression fiber to centroid of steel reinforcement (in)
d_b	Diameter of reinforcing bar (in)
d_f	Distance from extreme compression fiber to centroid of FRP/FRCM reinforcement (in)
d_{fv}	Effective depth of FRP/FRCM shear reinforcement
Ec	Modulus of elasticity of concrete (psi)
E_f	Design or guaranteed modulus of elasticity of FRP/FRCM defined as mean modulus of a sample of test specimens; for FRCM, characterizes cracked behavior (psi)
E_f^*	Uncracked modulus of elasticity for FRCM, obtained from a coupon test (psi)
Es	Modulus of elasticity of steel (psi)

f_c	Compressive stress in concrete (psi)
f`c	Specified design concrete compressive strength (psi)
f_f	Stress in FRP/FRCM reinforcement in tension (psi)
f_{fd}	Design stress of FRP/FRCM reinforcement (psi)
f_{fe}	Effective stress in FRP/FRCM, stress level attained at section failure (psi)
f_{fu}	design tensile strength of FRP/FRCM material, considering reductions for service environment (psi)
f^*_{fu}	Guaranteed tensile strength of FRP/FRCM (psi)
f_{fv}	Tensile strength of FRP/FRCM for shear design (psi)
f_{fs}	Stress in FRP/FRCM reinforcement under service load (psi)
f_s	Stress in steel reinforcement (psi)
f_{ss}	Stress in steel reinforcement under service load (psi)
fy	Specified yield strength of shear reinforcement (psi)
h	Total depth of member (in.)
h_f	Member flange thickness (in)
I	Moment of inertia (in^4)
I_{cr}	Moment of inertia of transformed, cracked section (in^4)
I_e	Effective moment of inertia (in^4)
Ig	Gross moment of inertia (in^4)
k	Ratio of depth of neutral axis to reinforcement depth measured from extreme compression fiber
l	Length of span (ft)
ln	Clear span length (ft)
Mcr	Flexural cracking moment (k-ft)

M_n	Nominal flexural capacity of section (k-ft)
M_{nf}	Contribution of FRP/FRCM reinforcement to nominal flexural strength (k-ft)
M_{ns}	Contribution of steel reinforcement to nominal flexural strength (k-ft)
Mu	Factored moment at a section (k-ft)
n	Number of plies of FRP/FRCM reinforcement
n_f	Modular ratio of elasticity between FRP/FRCM and concrete = E_f/E_c
n_s	Modular ratio of elasticity between steel and concrete = E_s/E_c
r	Radius of gyration of a section (in)
s	Center to center spacing of shear reinforcement (in.)
t_f	Nominal thickness of one ply of FRP/FRCM reinforcement (in)
T_g	Glass-transition temperature (degrees Fahrenheit)
Vc	Nominal concrete shear resistance (kips)
V_f	Nominal FRP/FRCM shear resistance (kips)
Vn	Nominal shear resistance (kips)
Vs	Nominal steel shear resistance (kips)
Vu	Factored shear force at section (kips)
w_f	Width of FRP/FRCM reinforcing plies (in)
α	Angle of inclination of shear reinforcement to longitudinal reinforcement (degree)
α_1	Multiplier on f ́c to determine intensity of an equivalent rectangular stress distribution for concrete
β_1	Ratio of depth of equivalent rectangular stress block to depth of neutral axis
ε_{bi}	Strain level in concrete substrate at time of FRP/FRCM installation (in/in)

ε_c	Strain level in concrete (in/in)
ε_{cu}	Maximum usable strain in concrete (in/in)
ε_f	Strain level in FRP/FRCM reinforcement (in/in)
ε_{fd}	Debonding strain of externally bonded FRP/FRCM reinforcement (in/in)
ε_{fe}	Effective strain level in FRP/FRCM reinforcement at failure (in/in)
ε_{fu}	Design rupture strain of FRP/FRCM reinforcement (in/in)
ε^*_{fu}	Ultimate rupture strain of FRP/FRCM reinforcement (in/in)
ε_s	Net longitudinal strain at centroid of longitudinal reinforcement (in/in)
ε_t	Net tensile strain in extreme tension steel at nominal strength (in/in)
ε_y	Strain corresponding with yielding of steel reinforcement (in/in)
λ	Reduction factor for lightweight concrete
ϕ	Strength reduction factor
ϕ_m	Strength reduction factor for flexure
ϕ_v	Strength reduction factor for shear
ρ_f	FRP/FRCM reinforcement ratio
ρ_s	Steel reinforcement ratio of flexural member = A_s/bd
σ	Standard deviation
ψ_f	FRP strength reduction factor
AASHTO	American Association of State Highway and Transportation Officials
ACI	American Concrete Institute
ASCE	American Society of Civil Engineers
C-FRCM	Carbon fabric-reinforced cementitious matrix
CFRP	Carbon Fiber-Reinforced Polymer

DAS	Data Acquisition System
DOT	Department of Transportation
EB	Externally Bonded
FRCM	Fabric-reinforced cementitious matrix
FRP	Fiber-reinforced polymer
LRFD	Load and resistance factored design
LVDT	Linear Variable Differential Transformer / Linear Variable Displacement Transformer
ML	Manual Layup
MoDOT	Missouri Department of Transportation
NDT	Nondestructive Testing
NSM	Near Surface Mounted
PBO	Polyparaphenylene Benzobisoxazole
RC	Reinforced concrete
RE-CAST	Research on Concrete Applications for Sustainable Transportation
SRG	Steel Reinforced Grout
SRP	Steel Reinforced Polymer
WL	Wet Layup

1. INTRODUCTION

1.1. BACKGROUND

Our nation is facing major concerns with an aging infrastructure that is vital to commerce and our economy as well as our quality of life. The American Society of Civil Engineers (ASCE) puts out a yearly infrastructure report card in an attempt to put this issue into terms that the general public can relate to well. In 2017, nationally, bridges received a C+ rating, and Missouri is below average, coming in at a C. A grade of C signifies "mediocre, requires attention." Missouri has the seventh largest number of bridges of all the states, 12.5% of which are considered structurally deficient (ASCE, 2017). Many factors contribute to bridges becoming structurally deficient, including long-term exposure to harsh environments, poor initial design or construction, increasing traffic loads, changing design standards, increased safety requirements, or catastrophic events such as earthquakes.

Replacing thousands of bridges is both time consuming and expensive, so repairing bridges has emerged as a better, more sustainable option. Strengthening or retrofitting concrete structures can add capacity and increase the service life by several decades. Traditional flexural strengthening techniques include externally bonded steel plates, steel or concrete jackets, external post-tensioning, and other methods. Shear strengthening methods include external stirrups and epoxy bonded steel plates. These methods leave materials exposed to the environment, making them vulnerable to corrosion.

Since the 1980s, composite materials have been an emerging technology as an alternative for strengthening concrete structures in the United States, Japan, Canada, and Europe. While many research projects have been conducted in university labs, more full-scale and in situ studies are needed, since departments of transportation (DOTs) are still hesitant to implement these innovative materials.

Composite materials consist of fibers that are incased in some sort of matrix. Common fiber types include carbon, glass, aramid, and polyparaphenylene benzobisoxazole (PBO). When a polymeric resin is used, the material is classified as a fiber-reinforced polymer (FRP). When a cementitious material is used, the material is

classified as a fiber-reinforced cementitious matrix (FRCM). Both classes of composites have advantages over traditional materials such as corrosion resistance and high tensile strength.

The following report describes the design, fabrication, and installation of strengthening systems using FRP and FRCM. This study was one task of the Research on Concrete Applications for Sustainable Transportation (RE-CAST) program project 3C. Task 11 of project 3C consists of field implementation and load testing of an FRCM strengthened bridge. Missouri Bridge P0058 was chosen from several candidates for the project.

1.2. RESEARCH OBJECTIVE

This research study was conducted in an attempt to validate the applicability of several composite systems for strengthening bridge girders in the field and to monitor them over time. The main objective is to demonstrate bridge girder strengthening using the FRCM and SRG technology, which to date have no reported field bridge applications in available literature. Analysis of the structure was completed, and design calculations were prepared for each strengthening system. Design guides by ACI committees 440-08 and 549-13 were used in the design of the systems. These reports also detailed the proper procedure for installation of the strengthening systems. Pre- and post-strengthening load tests were used to monitor the bridge's behavior in service, and how the behavior changed after strengthening.

This study is also allowing for long-term bond performance test bed preparing for future studies of how the strengthening systems are affected by field exposure over time. Some design decisions were made to better prepare for future testing of the bridge.

1.3. SCOPE AND LIMITATIONS

This project is a demonstration of the field installation of composite strengthening systems. The study focuses only on strengthening of the bridge girders. Additionally, only the girders on spans 1 and 4 were strengthened where the girders were accessible for strengthening. Other structural elements such as the slab and bents were not considered.

The strengthening system design is not intended to change the posted limitations on the bridge.

1.4. REPORT ORGANIZATION

This report is organized into six sections. Section 1 is an introduction to the study, including background information on bridge strengthening, the research objective, and the scope.

Section 2 contains background information that was needed to begin the study. The following subject areas were studied: properties of FRP, properties of FRCM, properties of SRG, strengthening of structural members for flexure and shear, and non-destructive testing of structures.

Section 3 details the design of the strengthening systems. This includes a description of the bridge and materials used, analysis of the pre-strengthened bridge, and the design of each system.

Section 4 describes the installation of composite strengthening systems. This includes the substrate repair and surface preparation needed before strengthening, as well as the installation of each system.

Section 5 describes the load testing done for this study prior to strengthening to provide a baseline to compare future load test data to after strengthening during service life. Instrumentation and other work done in preparation for load testing is described in addition to the pre- and post- strengthening tests.

Section 6 contains the conclusions reached in this study, as well as future research recommendations. Following Section 6 are Appendices A through F, which include supplemental details and information

2. LITERATURE REVIEW

2.1. FIBER-REINFORCED POLYMER STRENGTHENING

Fiber-reinforced polymer (FRP) is defined by ACI 440.2R as "a composite material comprising a polymer matrix reinforced with fibers in the form of fabric, mat, strands, or any other fiber form." In a composite, constituent materials remain distinct, but combine to form a material with properties not possessed by any of the constituent materials individually. In general, The FRP fibers carry load along the length of the fiber to provide strength and stiffness, and the matrix material transfers stresses between the fibers and protects them from environmental and mechanical damages. Advantages of FRP include high strength to weight ratio, high tensile strength, and corrosion resistance. (ACI Committee 440, 2008; Arboleda, 2014; Pino, 2016)

2.1.1. **Types of Externally Bonded FRP Systems.**

2.1.1.1. Wet layup systems. Wet layup (WL) FRP systems consist of dry unidirectional or multidirectional fiber sheets or fabrics that are impregnated with a saturating resin on site. This method is also sometimes referred to as manual layup (ML). The concrete substrate is primed and puttied, and then the saturating resin binds the fibers to the surface. A wet layup system is similar to cast-in-place concrete, in that they are saturated in place, and cured in place. (ACI Committee 440, 2008).

2.1.1.2. Prepreg systems. Prepreg FRP systems consist of partially cured unidirectional or multidirectional fiber sheets or fabrics that are pre-impregnated with a saturating resin in the manufacturer's facility. Once on site, they typically do not require additional resin to bond the system to the concrete surface. Prepreg systems are saturated off-site, such as wet layup systems, they are cured on site. A typical prepreg system requires additional heating for curing. The manufacturer of a prepreg system should be consulted for storage and shelf-life recommendations and curing procedures. (ACI Committee 440, 2008)

2.1.1.3. Precured systems. Precured FRP systems consist of various composite shapes manufactured in a plant off-site. Common types of precured systems include unidirectional plates, multidirectional grids, and curved shells. Typically, an adhesive, along with primer and putty, is used to bond the precured shapes to the concrete surface. Another technique is to mechanically fasten (MF) precured plates to the concrete with bolts. Precured systems are similar to precast concrete, as they are saturated and cured off site. (ACI Committee 440, 2008; Holdener, Myers, & Nanni, 2004)

2.1.1.4. Near-surface-mounted (NSM) systems. NSM systems consist of surface-embedded circular or rectangular bars or plates, which are installed and bonded into grooves made on the concrete surface. An adhesive recommended by the NSM manufacturer is used to bond the FRP bar into the groove and is cured in place. Bars and plates used in NSM are typically manufactured using the pultrusion process, which creates long, straight, constant cross-section parts. (ACI Committee 440, 2008)

2.1.2. Constituent Materials and Properties. The physical and mechanical properties of FRP composites need to be understood to properly use them for concrete strengthening. Properties are dependent on several factors, such as loading history and duration, temperature, and moisture (ACI Committee 440, 2008; Arboleda, 2014).

2.1.2.1. Constituent materials. The constituent materials are chosen to have a great impact on the composite properties, as various materials can fill a wide range of desired properties. The correct choice of fiber type, resin type, and, when applicable, protective coating are important in dictating performance of the composite. Additionally, changing the volume fraction of these constituents can have a big impact on composite properties (ACI Committee 440, 2008).

A wide range of Polymeric resins are available for use in FRP systems. The most common types are epoxy, vinyl esters, and polyesters and they have been formulated for use in a wide range of environments. The main qualities of resins that manufacturers desire are (ACI Committee 440, 2008):

- Development of appropriate mechanical properties for the FRP composite
- Compatibility with and adhesion to both the concrete and reinforcing fibers

- Resistance to environmental effects such as moisture, salt water, extreme temperature, and chemicals associated with concrete
- Filling ability
- Workability
- Pot life consistent with the application

Fibers are relied on to give the FRP system its strength and stiffness. The most common fiber materials are carbon, glass, and aramid. The fiber tensile properties can vary based on manufacturing process.

Table 2-1 shows typical ranges of properties for different fibers.

Protective coatings are also sometimes used to help minimize potential environmental or mechanical damage to the composite. Coatings are typically applied after the saturating resin has cured. There are a variety of forms of protecting systems including: polymer coatings, acrylic coatings, cementitious systems, and intumescent coatings. Ultraviolet light protection, fire protection, vandalism protection, impact or abrasion resistance, improve aesthetics, chemical resistance, and to prevent chemicals from leaving the system if submerged in potable water are all viable reasons why protective systems may be desired for FRP strengthened concrete (ACI Committee 440, 2008).

Table 2-1. Typical Tensile Properties of Fibers Used in FRP Systems (ACI Committee 440, 2008)

Fiber type	Elastic modulus		Ultimate strength		Rupture strain, minimum, %
	10^3 ksi	GPa	ksi	MPa	
Carbon					
General purpose	32 to 34	220 to 240	300 to 550	2050 to 3790	1.2
High-strength	32 to 34	220 to 240	550 to 700	3790 to 4820	1.4
Ultra-high-strength	32 to 34	220 to 240	700 to 900	4820 to 6200	1.5
High-modulus	50 to 75	340 to 520	250 to 450	1720 to 3100	0.5
Ultra-high-modulus	75 to 100	520 to 690	200 to 350	1380 to 2400	0.2
Glass					
E-glass	10 to 10.5	69 to 72	270 to 390	1860 to 2680	4.5
S-glass	12.5 to 13	86 to 90	500 to 700	3440 to 4140	5.4
Aramid					
General purpose	10 to 12	69 to 83	500 to 600	3440 to 4140	2.5
High-performance	16 to 18	110 to 124	500 to 600	3440 to 4140	1.6

2.1.2.2. Physical properties. The physical properties of FRP's are much different than steel, and in most cases this is advantageous. The density of FRP materials ranges from 75 to 130 lb/ft^3 (1.2 to 2.1 g/cm^3), which is four to six times lower than steel. This makes FRP easier to transport, reduces dead load on the structure, and makes them easier to handle on the project location. Table 2-2 shows the density ranges for various types of FRP and includes steel for comparison (ACI Committee 440, 2008).

Table 2-2. Typical Densities of FRP Materials (ACI Committee 440, 2008)

Steel	GFRP	CFRP	AFRP
490 (7.9)	75 to 130 (1.2 to 2.1)	90 to 100 (1.5 to 1.6)	75 to 90 (1.2 to 1.5)

Units: lb/ft^3 (g/cm^3)

Thermal properties must be considered for many FRP applications. The coefficient of thermal expansion of composites differs in the longitudinal and transverse directions for a unidirectional laminate. The design of the laminate can be altered to get desired thermal properties in a given direction by changing the types of fiber, resin, and volume fraction of fiber. If the application of a composite system will experience substantial temperature fluctuations, then caution should be taken to choose an FRP

system that has similar thermal properties to the concrete it is strengthening. (ACI Committee 440, 2008).

Another important thermal property of FRP composites is their glass transition temperature (T_g). The value of T_g depends on the type of resin but is normally in the region of 140 to 180 °F (60 to 82.2 °C). Beyond the T_g, the molecular structure changes, and the elastic modulus of the polymer is significantly reduced. At this point, the fibers can continue to support some load in the longitudinal direction, but the system is significantly less stiff in the transverse direction, and in shear. This effect of high temperature reduces shear transfer, so other properties such as flexure strength are also affected. (ACI Committee 440, 2008).

2.1.2.3. Mechanical properties. The mechanical properties of all FRP systems, regardless of form, should be based on the testing of laminate samples with known fiber content. The properties of an FRP system should be characterized as a composite, recognizing not just the material properties of the individual fibers, but also the efficiency of the fiber-resin system, the fabric architecture, and the method used to create the composite. (ACI Committee 440, 2008)

When unidirectional FRP materials are loaded in tension, they do not exhibit any plastic behavior (yielding) like observed in steel. The stress-strain behavior of FRP is linear elastic up until failure, which is sudden and brittle. The tensile properties of a composite depend on many factors, most of which are fiber related. The type of fiber, the orientation of fibers, the quantity of fibers, and the method and conditions in which the composite is produced affect the tensile properties of the FRP material. The tensile properties can be reported in two ways: gross-laminate area (using total composite area with relatively lower strength and modulus) or net-fiber area (using known area of fiber and relatively higher strength and stiffness). Regardless of the basis for the reported values, the load-carrying strength ($f_{fu}*A_f$) and axial stiffness (A_f*E_f) of the composite remain constant. A commercial FRP should have an ultimate tensile strength and ultimate rupture strain reported by the manufacturer. These guaranteed properties are defined by the mean of a sample of test specimens minus three times the standard deviation. This approach gives a 99.87% probability that the actual properties will exceed the reported values. (ACI Committee 440, 2008)

Coupon tests on FRP laminates have shown that the compressive strength of FRP is lower than the tensile strength. Depending on the materials composing the specimen, FRP in longitudinal compression can fail in many ways, including transverse tensile failure, fiber microbuckling, or shear failure. Externally bonded systems with FRP should not be used as compression reinforcement. (ACI Committee 440, 2008)

2.1.2.4. Time-dependent properties. As most structures are intended to last decades, it is important to consider time dependent properties such as creep and fatigue. While research in labs has simulated long term effects, more studies are needed to verify the long term effects of FRP when exposed to field conditions, with different environmental factors. (ACI Committee 440, 2008).

Creep rupture is a sudden failure of a material subject to a constant load after a period of time known as the endurance time. In general, carbon fibers are the least susceptible to creep rupture, followed by aramid, and lastly glass. Fatigue in composites has had more research than creep rupture, because it is critical for aerospace industry applications. Similar to creep, carbon fibers perform the best in fatigue loading. ACI provides recommended sustained stress limits for each fiber type, shown in Table 2-3. (ACI Committee 440, 2008).

Table 2-3. FRP Service Load Stress Limits (ACI Committee 440, 2008)

	Fiber type		
Stress type	GFRP	AFRP	CFRP
Sustained plus cyclic stress limit	$0.20f_{fu}$	$0.30f_{fu}$	$0.55f_{fu}$

2.1.3. FRP Failure Modes. While FRP materials generally have a high tensile strength, their ultimate rupture strength is rarely achieved. Instead, failure is most commonly due to a loss of strengthening action due to various types of fiber debonding. In FRP strengthened RC, it is most common that the strengthening system delaminates due to a fracture within the concrete cover (area between reinforcing steel and concrete surface). The initial debonding may occur at a crack, or at the termination of the reinforcement. Figure 2-1 shows the locations that debonding is most likely to occur at and how the failure propagates. The main method for preventing debonding is to limit the

design strain in the fibers or to limit the bond shear. Aram et al. recommend limiting the fiber strain to .008, as well as limiting the shear stress to the tensile strength of the concrete. (ACI Committee 440, 2008; Aram, Czaderski, & Motavalli, 2008; Hind, Özakçab, & Ekmekyaparc, 2016).

2.1.4. Research on FRP Strengthening Systems. Various studies have been conducted around the world, using FRP to strengthen bridges, buildings, or components of structures. Included in this section are studies most relevant to the work done for this report.

2.1.4.1. Holdener, Myers, & Nanni, (2004). From 2003 to 2008, a research team From the University of Missouri-Rolla (UMR, now Missouri S&T) undertook a project to field strengthen bridges in order to validate FRP composite technology. The study is referred to as the five-bridge project, and officially titled: “Preservation of Missouri Transportation Infrastructure: Validation of FRP Composite Technology through Field Testing”.

Five structurally deficient bridges around Missouri were chosen and retrofitted with various FRP systems on their girders and slabs. Figure 2-2 shows the location of the bridges within Missouri’s DOT districts. The types of strengthening systems used are manual layup, NSM, steel-reinforced polymer (SRP), and precured laminates attached with epoxy or mechanically fastened (MF).

Table 2-4 breaks down the system types used on each bridge, and provides additional bridge details and geometry.

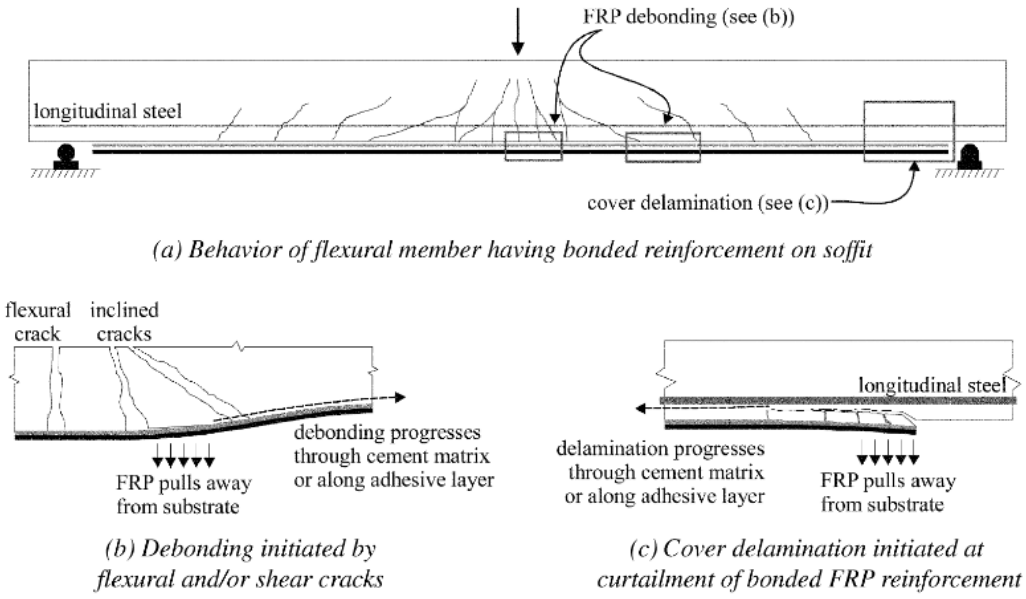

Figure 2-1. FRP Debonding Modes (ACI Committee 440, 2008)

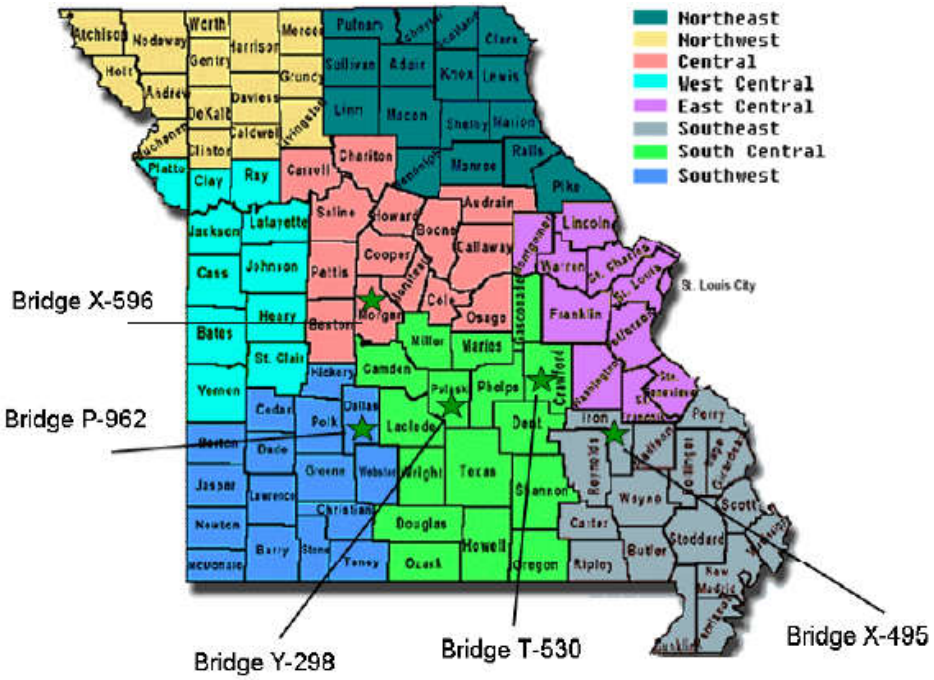

Figure 2-2. Location of Bridges Strengthened (Holdener et al., 2004)

The five-bridge project upgraded each bridge to meet the ultimate factored loading considering three loading conditions: HS20-44 truck load, 3S2 truck load, and lane load. These load cases satisfy both AASHTO and MoDOT requests.

Table 2-4. Details of Five Bridges Strengthened

Name	Location	Style	# Girders	Girder Spacing	Length Span Lengths	Age	Strengthening
T-0530	Crawford county	T-beam	4 (23ft wide)	6.5ft	237ft 5x 47.5ft spans	1937	CFRP wet layup, pre-cured cfrp laminates
X-0495	Iron County	T-beam	3 (24 ft wide)	9ft	137.5ft 42.5/ 52.5/ 42.5 ft	1948	CFRP wet layup, NSM bars
X-0596	Morgan County	T-beam	3 (20ft wide)	9ft	137.5ft 42.5/ 52.5/ 42.5 ft	1946	CFRP wet layup, NSM bars
P-0962	Dallas County	T-beam	3 (23 ft wide)	9ft	127.5ft 3x 42.5ft	1956	CFRP wet layup, NSM bars, SRP manual layup
Y-0298	Pulaski County	Solid slab	n/a (27ft wide)	n/a	30ft 2x 15ft spans	1937	CFRP wet layup, MF FRP laminates

Table 2-5 presents a detailed reference for the type and amount of strengthening applied to each girder and the analytical capacity increase in flexure gained by adding the composites. Holdener, Myers, and Nanni also presented details for slab flexural strengthening and girder shear strengthening, with their respective analytical capacity increase.

Table 2-5. Girder Strengthening Schedule and Analytical Capacity Increase (Holdener et al., 2004)

Bridge ID	Span #	Girder	Flexural Reinforcing Description (Girder)	Capacity Increase
X-596[g]	2	Interior	ML: 4 Plies 20" Wide; NSM Bars: 4 Total	42%
X-596[g]	2	Exterior	None	NA
X-596[g]	1, 3	Interior	ML: 4 Plies 20" Wide; NSM Bars: 4 Total	44%
X-596[g]	1, 3	Exterior	ML: 2 Plies 16" Wide	16%
T-530[g]	1, 3, 5	Interior	ML: 4 Plies 16" Wide	29%
T-530[g]	1, 3, 5	Exterior	ML: 2 Plies 16" Wide	15%
T-530[g]	2, 4	Interior	1 Laminate Plate: 12" Wide	29%
T-530[g]	2, 4	Exterior	1 Laminate Plate: 12" Wide	15%
X-495[g]	2	Interior	ML: 5 Plies 20" Wide	40%
X-495[g]	2	Exterior	None	NA
X-495[g]	1, 3	Interior	ML: 5 Plies 16" Wide; NSM Bars: 2 total	44%
X-495[g]	1, 3	Exterior	ML: 2 Plies 16" Wide	16%
P-962[g]	1, 2	Interior	ML: 5 Plies 16" Wide plus 4 NSM Bars	56%
P-962[g]	1, 2	Exterior	ML: 3 Plies 16" Wide	25%
P-962[g]	3	Interior	SRP 3X2: 3 Plies 16" Wide	54%
P-962[g]	3	Exterior	SRP 3X2: 3 Plies 16" Wide	49%

After strengthening, Holdener et al. conducted several nondestructive tests (NDT) in order to monitor the performance of the FRP systems without damaging the system or the RC structural elements. Load testing was a vital step in validating the effectiveness of

the strengthening. The bridge sites made it difficult for traditional deflection monitoring equipment, such as linear variable differential transformers (LVDT), to be used. Instead, optical laser surveying equipment was determined to be the best measure of deflection. NDT results conducted thus far on the five bridges project have shown satisfactory results with no growth in intentional or unintentional defects

Holdener, Myers, and Nanni's study is a valuable comparison, as most of the bridges strengthened are similar in geometry to bridge P0058 in this report. Additionally, the five bridges are other examples of composite strengthening in the field, whereas most research available was conducted in lab settings.

2.1.4.2. Rahman, Kingsley, & Kobayashi (2000). This study investigated a full-scale model of a bridge deck slab isotopically reinforced with FRP. The slab studied was 7.28 in (185mm) thick and 19.69 ft (6 m) wide. The total length of the slab was 19.69 ft (6 m) with three girders used to create two 6.56 ft (2 m) spans and a 3.28 ft (1 m) cantilever on each end. The slab was loaded in the midpoint of the two spans simultaneously, and loaded at three separate points along the width of the slab as shown in Figure 2-3. The strengthening material used was a two-dimensional carbon fiber grid. The slab was loaded monotonically to crack the concrete, then loaded cyclically to simulate 50 years of service loading, and finally loaded monotonically to failure. Strain gauges and LVDT were used to monitor the response through each load phase.

Rahman et al. found that the ultimate load of their slab was 120 kip (534 kN), more than five times the design service load. The dominant failure mode observed was punching shear. The exception was under the north jack when loaded at the west end, where a flexural crack developed and crushing of the concrete occurred. This study showed that FRP has satisfactory constructability, and its behavior in service conditions is also satisfactory. Rahman et al. concluded that the carbon FRP grid system is suitable for use in strengthening but advised for more research to be conducted considering other factors such as more extreme environmental changes and fatigue paired with chemical exposure.

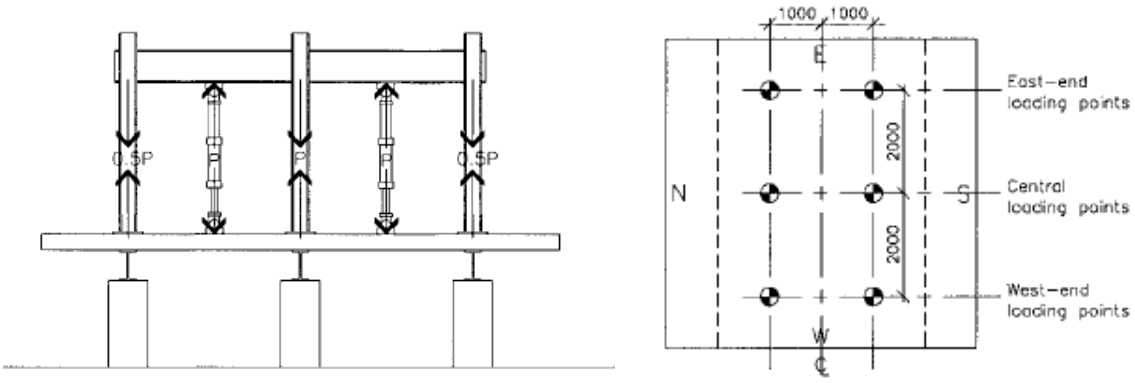

Figure 2-3. Loading Scheme (Rahman et al., 2000) (Dimensions shown are mm. Conversion: 25.4 mm = 1 in)

2.1.4.3. Petrou, Parler, Harries, & Rizos (2008). This study investigated the monotonic and fatigue behavior of one-way and two-way reinforced concrete slabs strengthened with carbon fiber-reinforced polymer (CFRP) materials. Five one-way reinforced concrete (RC) slab specimens were removed from a decommissioned bridge in South Carolina. Additionally, six half-scale, two-way RC slab specimens were constructed to represent a bridge deck designed using the requirements of AASHTO LRFD Bridge Design Manual.

The one-way specimens were 8.5inch (215.9 mm) thick rectangles, 14 feet (4.27 m) long and 5 feet (1.52 m) wide. Three specimens were retrofitted using CFRP strips, and two were left unstrengthened for comparison. For both monotonic and fatigue tests, the slabs were simply supported over a 13 foot (3.96 m) span, and subjected to three point bending with the load applied at midspan.

The two-way specimens were 3.75 inch (95.25 mm) thick squares, with 52 inch (1320.8 mm) sides. Two different retrofit techniques were carried out on the two-way specimens: a CFRP grid, and CFRP strips. Two slabs were strengthened with each technique, and two were left unstrengthened for comparison. For both monotonic and fatigue tests, the slabs were simply supported on all sides, resulting in a 48 inch (1219.2 mm) square test region.

The results of the monotonic testing are most relevant to this report. Petrou, Parler, Harries, & Rizos made the following conclusions from the monotonic tests:

- Monotonically tested one-way retrofit specimens achieved an increase in ultimate strength of 14.8% and 18.1%, over that of the unretrofit control specimen.
- The failure of the two monotonically tested retrofit one-way slabs was due to debonding of the CFRP that propagated outward from the midspan region as the applied load increased.
- For the monotonically tested two-way slabs, the CFRP strip retrofitted slab and the CFRP grid retrofitted slab achieved ultimate strength increases of 13.8% and 10.7%, respectively.
- The CFRP strip retrofitted two-way slab and the CFRP grid retrofitted two-way slab experienced increases in general cracking load of 8.7% and 34.8%, respectively.
- Punching signified the ultimate failure of all three monotonically tested two-way slabs.

2.2. FABRIC-REINFORCED CEMENTICIOUS MATRIX STRENGTHENING

FRCM systems share some of the advantageous properties of FRP, and overcome some of its limitations. In comparison, FRCM has superior heat resistance and compatibility with concrete substrate. Advantageous features of FRCM as noted by ACI 549 include (ACI Committee 549, 2013):

a) Compatibility with chemical, physical, and mechanical properties of the concrete or masonry substrate

b) Ease of installation due to the use of traditional plastering or trowel

c) Porous matrix structure that allows air and moisture transport both into and out of the substrate

d) Good performance at elevated temperatures in addition to partial fire resistance

e) Ease of reversibility (that is, the ability to undo the repair without harming the original structure)

There are also a few limitations when using of FRCM composites for strengthening. Since the systems are based on inorganic matrixes, it is not possible to fully impregnate individual fibers. For this reason, the fiber sheets typically used in FRP that are installed by manual layup are replaced in FRCM with a structural reinforcing mesh (fabric). The strands of the FRCM reinforcing mesh are typically made of fibers that are individually coated, but are not bonded together by a polymeric resin. If a polymer is used to either cover or bond the strands, such polymer does not fully penetrate and impregnate the fibers as it would in FRP. For these reasons, the term "dry fiber" is used to characterize an FRCM mesh (ACI Committee 549, 2013). Due to the lack of penetration, the bond cannot be assumed as perfect, which affects the theoretical behavior of FRCM (Arboleda, 2014).

Throughout its development, FRCM has been referred to by several different names or acronyms. The technology was first introduced in Europe as textile-reinforced concrete (TRC). The emphasis on textile was to signify that dry fibers are arranged in the direction of tension, rather than randomly distributed short fibers. A report by RILEM Technical Committee was one of the first to include information on strengthening with TRC (Brameshuber, 2006). Additionally, FRCM has been referred to as textile-reinforced mortar (TRM), fiber-reinforced concrete (FRC), and mineral based composites (MBC). (ACI Committee 549, 2013; Gonzalez-Libreros, Sabau, Sneed, Pellegrino, & Sas, 2017)

2.2.1. Tensile Characterization

Various researchers have studied the mechanical properties of FRCM materials. FRCM tensile properties are determined according to the test procedure specified in Annex A of AC434 (2013), in which tensile coupons are used to observe stress-strain behavior. Figure 2-4 adapted from Loreto et al. 2013 shows the behavior of a hydraulically gripped tensile coupon. The stress-strain behavior is broken down into three states: I, IIa, and IIb. State I is labeled as the uncracked zone because the strain is below the cracking strain of the matrix and the composite stiffness is governed by the reinforcement stiffness. Once the first crack develops, load is transferred through the

fabric back to the matrix and a multiple cracking pattern develops. This is shown in state IIa. At the end of this state is state IIb, where the load is carried completely by the fabric until its tensile strength is reached. In this state, the composite stiffness is governed by the reinforcement stiffness. The insert on the right of Figure 2-4 shows the reduction to an idealized tensile stress-strain curve for FRCM. The idealized curve is bilinear with a bend-over point corresponding to the intersection point obtained by continuing the initial and secondary linear segments of the response curve. The initial linear segment is uncracked linear elastic behavior and is characterized by the uncracked modulus of elasticity (E_f^*). The second linear segment is cracked behavior, and is characterized by the cracked modulus of elasticity (E_f).(ACI Committee 549, 2013; Arboleda, 2014; Loreto, Babaeidarabad, Leardini, & Nanni, 2015; Loreto, Leardini, Arboleda, & Nanni, 2013)

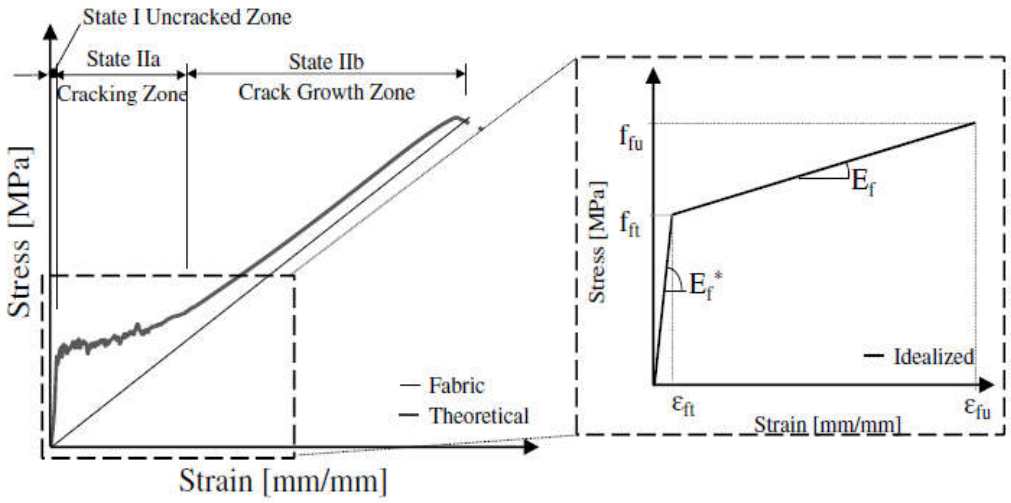

Figure 2-4. Stress-Strain Curve for Fully-Clamped FRCM in Tension (Loreto et al. 2013)

FRCM Failure Modes.

Similarly to FRP, it has been observed that FRCM fibers lose strength due to various forms of debonding before the fibers reach their ultimate rupture strength Figure 2-5 shows the four types of debonding failure modes that can occur, which are:

a) Sudden detaching with fracture surface within concrete

b) Gradual fiber slippage within the matrix

c) Sudden detaching with fracture at matrix/ concrete interface

d) Sudden detaching with fracture within matrix on a fiber plane.

In most cases, the debonding occurs within the matrix, which is different than FRP which tends to debond within the concrete cover (D'Ambrisi & Focacci, 2011; Di Tommaso, Focacci, & Mantegazza, 2008).

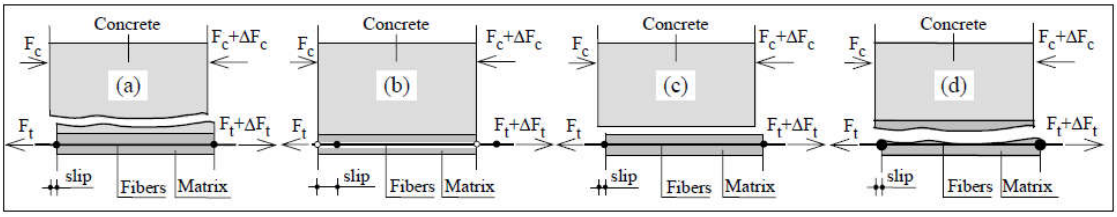

Figure 2-5. Debonding Failure Modes (Di Tommaso et al. 2008)

2.2.2. Research on FRCM Strengthening Systems

Several studies have been conducted on the effectiveness of FRCM systems for strengthening. Some of the most relevant studies to this report have been included.

2.2.2.1. Di Tommaso, Focacci, & Mantegazza (2008). This early study looked at the mechanics of adhesion and efficiency of strengthening RC beams with PBO-FRCM. Ten beams were tested under four-point bending, with a clear span of 86.6 inches (2200 mm). The specimens had a rectangular cross section 9.84 inches (250 mm) deep and 15.75 inches (400mm) wide. Specimens were strengthened with up to three layers of flexural strengthening and with either continuous U wrapping or a single wrap at each end.

Di Tommaso et al. found that FRCM materials are an effective way to strengthen RC beams, achieving up to 55% enhancement. They observed that failure was always caused by a loss of strengthening actions due to one of the types of fiber debonding, which typically includes slippage between fibers and matrix.

2.2.2.2. D'Ambrisi & Focacci (2011). In this study, externally bonded FRCM systems were used to strengthen reinforced concrete beams. Systems made using carbon fiber nets and PBO fiber nets were used, varying the net shape, cementitious matrices, and number of layers of reinforcement. Additionally some specimens were strengthened with carbon FRP in order to compare the performance of the FRCM systems. Specimens also had two different span lengths, and were tested in both three and four point bending. The long beams [86.6 in. (2200 mm) span] were expected to fail in shear, and tested in four-point bending configuration. The short beams [63 in. (1600 mm) span] were tested in three-point bending configuration. All beams tested had a depth of 9.84 in. (250 mm) and a width of 15.75 in. (400 mm). A total of 25 long beams and 10 short beams were tested throughout three experimental programs.

D'Ambrisi and Focacci found that for the considered cross sections, beams strengthened with PBO-FRCM materials had a flexural capacity increase (up to 54.3%) in the same order of magnitude as beams strengthened with FRP materials. The PBO FRCM systems performed better than carbon FRCM systems (up to 17.8% increase for carbon).

They also found that the failure of FRCM strengthened beams is typically caused by a loss of strengthening action as a result of one of four modes of debonding. For most cases, the debonding happens within the matrix or at the concrete-matrix interface rather than within the concrete as is common with FRP, proving that the matrix type, as well as its interface with the concrete and fibers are important factors in FRCM systems. As the number of FRCM plies increases, the debonding strain decreases, but as not as rapidly as observed in FRP. This is likely due to the difference in debonding mechanisms.

2.2.2.3. Loreto, Leardini, Arboleda, and Nanni (2013). This project studied the performance of FRCM systems used to strengthen RC slab-type elements. The specimens strengthened in this study simulated a unit slab strip 72 inches (1828.8 mm) long and had a rectangular cross section 12 inches (304.8 mm) wide and 6 inches (152.4 mm) deep. PBO FRCM was used to strengthen the slabs, with the number of plies as a test variable (0, 1, or 4 plies). Another test variable was the concrete compressive strength, as specimens with both high [5800 psi (39.99 MPa)] and low [4000psi (27.58 MPa)] strength concrete were tested. A total of 18 specimens (three of each condition)

were tested in three point bending with a clear span of 60 inches (1524 mm). The loading pattern consisted of two cycles up to concrete cracking, two cycles up to steel yielding, two cycles within the plastic range of the slab, and finally loading to failure.

Loreto et al. found that FRCM with PBO is a viable technology for strengthening RC slabs. For low strength concrete, they found that the average flexural capacity increase was 141% and 205% for one and four plies respectively. For high strength concrete, the average flexural capacity increase was 135% and 212% for one and four plies respectively. The study also showed that while adding plies increases the strength, there is a loss in ductility as a result. They also observed that the failure mode is related to the number of plies of strengthening. Specimens strengthened with one ply failed by fabric slippage within the matrix, whereas four ply specimens failed due to delamination from the substrate.

Loreto et al also performed an analysis based on the (at the time only proposed) ACI 549 (2013) design guide. They found that "the prediction [by ACI 549, 2013] is satisfactory and underestimates the enhancement attributable to FRCM strengthening because the tensile properties used in the analysis do not depend on fiber rupture but are based on the performance of the FRCM tensile coupon during the crack formation zone." As ACI 549 2013 was used in this report for strengthening design, it is safe to assume the calculations for strength increase are conservative.

2.2.2.4. Babaeidarabad, Loreto, and Nanni (2014). This project studied RC beams strengthened in flexure with PBO-FRCM systems. For the study, 18 beams were tested in three point bending, with a clear span of 60 inches (1524 mm). The specimens were 72 inches (1828.8 mm) long with a rectangular cross-section 12 inches (304.8 mm) deep and 6 inches (152.4 mm) wide. Variables studied in this project are the influence of concrete strength [4200 psi or 6200 psi (28.96 MPa or 42.75 MPa)], and number of layers (0, 1, or 4) of FRCM reinforcement. Babaeidarabad et al. investigated the flexural capacity, pseudoductility, and failure mechanisms of the specimens.

Babaeidarabad et al observed that the strengthening produced average enhancements of 32% and 92% for the low strength concrete with one and four plies respectively. Similarly they observed average enhancements of 13% and 73% for the high strength concrete with one and four plies respectively when compared to the control

sets. ACI 549 limits the capacity increase to 50% of the unstrengthened capacity, so the reported design capacities in this study would be limited in field use. The researchers also observed that the failure mode is governed by the number of plies of FRCM reinforcement, with one ply specimens failing by slippage of the fabric within the matrix, and four ply specimens failing by FRCM delamination from the substrate. Babaeidarabad et al. created load-deflection diagrams, and observed that FRCM is effective in increasing the flexural capacity, but also decreases pseudoductility. As expected, pseudoductility is higher for the lower FRCM amount.

Babaeidarabad et al. also conducted sectional analysis following methodology according to ACI 318 (2011) and ACI 549 (2013). Their analysis showed that predicted flexural strength underestimates the experimental results, but with a reasonable accuracy and the design values become more conservative after applying the appropriate strength reduction factor and the 50% limit on strength increase.

2.2.2.5. Ombres (2015). Ombres studied the structural performance of RC beams strengthened in shear with PBO-FRCM. A total of 9 beams were tested in two series. All beams were 9.84 ft (3000 mm) long and had rectangular sections 9.84 inches (250 mm) deep and 5.91 inches (150 mm) wide. All tests were simply supported with a clear span of 8.86 ft (2700 mm). The first series aimed to evaluate the compatibility and effectiveness of PBO-FRCM and estimate the influence of strengthening configuration on structural performance. They did so by comparing one unstrengthened beam to two strengthened beams with different U-wrap configuration (continuous and discontinuous). For this series, both three point and four point bending schemes were used with a shear span-to-depth ratio (a/d) of 3.0 for each scheme.

The second series consisted of six beams, all of which were strengthened in flexure with three plies of PBO, in order to force failure by shear. Five of these specimens were also strengthened in shear with configurations attempting to observe the effects of reinforcement ratio (number of plies) and strengthening configuration (continuous vs discontinuous wraps). For this series, only the three point bending scheme was used with with a shear span-to-depth ratio (a/d) of 2.78.

After completion of the experimental program, Ombres drew the following conclusions:

- PBO-FRCM systems allow for significant improvement of shear capacity of RC beams if an adequate strengthening configuration is used.
- When using a discontinuous U-wrap scheme, a proper ratio of strip width to strip spacing must be chosen to permit correct activation of the strips, and better allow them to contribute to the shear capacity.
- There is a clear interaction between the externally bonded FRCM strips and the internal steel stirrups.

2.2.2.6. Loreto, Babaeidarabad, Leardini, and Nanni (2015). This project studied RC beams that were strengthened in shear with FRCM. This study used 18 beams that were heavily reinforced in flexure to ensure a shear failure. The beams were strengthened in shear with PBO-FRCM and tested under three-point bending. Parameters considered were concrete compressive strength [low 4060psi and high 5800psi (27.99 MPa and 39.99 MPa)] and number of plies (0, 1, or 4) with three replications made for each combination. The specimens were 72 inches (1828.8 mm) long and had a rectangular cross section 12 inches (304.8 mm) deep and 6 inches (152.4 mm) wide. The specimens were tested with a shear span-to-depth ratio of 3.0 for all beams.

Loreto et al. found that FRCM increases shear strength, but not proportionally to the number of plies. The average strength enhancement for low strength concrete compared to the control beam was 121% and 151% for one and four plies respectively. For the high strength concrete specimens, the increases were 126% and 161% for one and four plies respectively. They also found that the failure mode differed based on the number of plies of strengthening. Specimens with one ply failed due to fiber slippage within the matrix, whereas the four ply specimens failed by delamination from the substrate.

This study also included analysis of the ultimate shear capacity based on the procedures in ACI 318 (2011) and ACI 549.4R (2013) in order to compare with the experimental results. Loreto et al. found that the analysis underestimates the enhancement

due to FRCM strengthening. This demonstrates that ACI549 is conservative for both flexure and shear design.

2.3. STEEL REINFORCED GROUT

Steel reinforced grout (SRG) is another type of strengthening system being studied for applications in strengthening RC. Similarly to the FRCM system, the SRG systems use an inorganic, cementitious matrix, but high-strength steel cords are used as the fibers. These cords are made into a fabric that is much more cost efficient than carbon or PBO. The cords used in SRG systems are manufactured by the same process used for making reinforcement of automobile tires. (Huang et al. 2005)

The performance of SRG systems depend heavily on the stress transfer between the wires and the matrix. For this reason, various configurations of twisted wires are used, which provides a mechanical interlock performing much better than a single wire. These twisted cords are often made into a unidirectional fabric using a backing to keep the cords in line. The most common cords and fabrics used are manufactured by Hardwire LLC. Figure 2-6 shows a fabric and two types of cords used. (Barton et al., 2005; Huang et al., 2003).

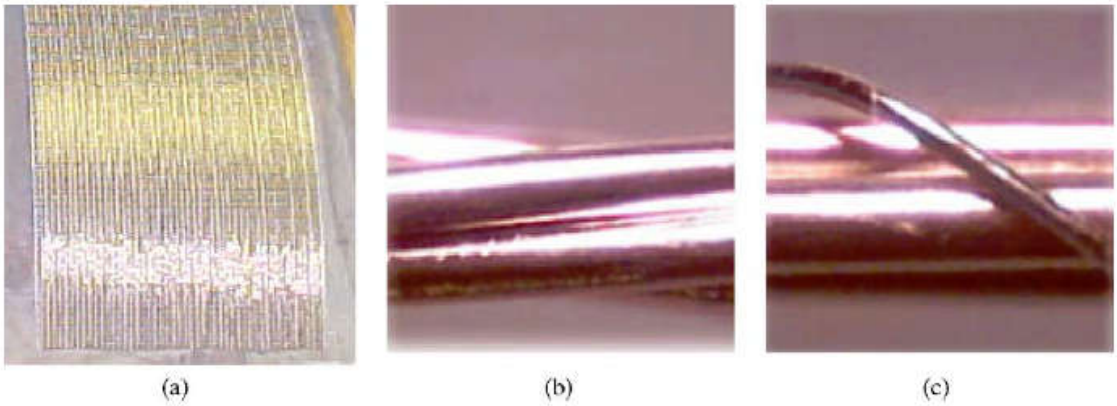

Figure 2-6. Steel Reinforcement: (a) steel fabric, (b) 3X2 cord and (c) 3SX cord. (Barton et al. 2005)

2.3.1. Research on SRG Strengthening.

Research is ongoing in the field of strengthening RC with SRG systems. Some of the most relevant studies to this report have been included.

2.3.1.1. Huang et al. (2003). Huang et al. studied the properties and potential application of SRG and steel reinforced polymer (SRP). Their experimental work included testing of SRG and SRP strengthened beams, with an unstrengthened beam for comparison. The three beams had a tee shaped cross section, with a flange width of 15 inches (381 mm) and a web width of 6 inches (152.4 mm). The flange depth was 4 inches (101.6 mm) and the overall depth of the beams was 16 inches (406.4 mm). The 10 foot (3.05 m) long beams were tested in four point bending with a simply supported clear span of 8 feet (2.44 m). Huang et al. observed a 30% and 20% ultimate capacity increase for the SRP and SRG strengthened specimens respectively when compared to the control. Both beams failed at midspan by debonding of the system. They concluded that both systems have potential for structural applications.

2.3.1.2. Wobbe et al. (2004). This team studied the flexural capacity of RC beams externally strengthened with SRP and SRG. The unidirectional cords used were 3x2 and 3SX, both manufactured by Hardwire and shown above in Figure 2-6. The 3x2 cord type consists of 5 wires; three straights with two wrapped around. The 3SX chord consists of three identical wires twisted and then overwrapped with a single smaller wire. Sheets with 3SX cords have a lower density of cords, allowing better penetration of matrix which makes them better for use with SRG. Four 8 foot (2.44 m) long beams were cast with rectangular cross section 12 inches (304.8 mm) deep and 8 inches (203.2 mm) wide. One beam was left un-strengthened as a control. Two specimens were strengthened with SRP using 3x2 cords, using one ply on one beam and two plies on the other. The final specimen was strengthened with two plies of SRG using 3SX cords.

The beams were tested in four point bending with a simply supported span length of 80 inches (2.03 m). Each beam was monotonically loaded to failure with midspan deflection and strain at several points being monitored. Compared to the control beam, the specimen strengthened with one ply of SRP had an ultimate strength increase of 42% and the specimen with two plies of SRG had an increase of 33%. These two beams had a

similar total number of strands, since the density of the two types of cord differ, which explains their similar behavior. The beam strengthened with two plies of SRP had an ultimate strength increase of 67% compared to the control. All three retrofitted beams failed due to concrete cover delamination. Wobbe et al. (2004) concluded that both SRP and SRG have great potential for flexural strengthening of RC structures.

2.4. NON-DESTRUCTIVE TESTING

Nondestructive testing (NDT) techniques are a valuable way to get feedback on the quality of installation of externally bonded composite systems. NDT allows for gathering information without damaging the structural element or strengthening system. The following tests have been researched previously and were considered for use in this strengthening project.

2.4.1. Load Testing

Load testing is a valuable way to validate the effectiveness of a composite strengthening system in the field. An initial load test should be conducted before the installation of a system, in order to have base values for comparison. Ideally, after the strengthening system is installed, a series of load tests should be conducted in order to observe the increased stiffness from strengthening and monitor any changes in stiffness over time. (Holdener et al., 2004; Merkle, 2004; Missouri Department of Transportation, 2005; J J Myers, Holdener, Merkle, & Hernandez, 2008)

The most common method for load tests involves using loaded dump trucks, which move to predetermined stop locations along the bridge. These stops are locations that cause maximum shear or moment for the spans. At each stop, the bridge is given time to settle, with deflection readings taken periodically. (Holdener et al., 2004)

Deflection measurements can be taken by either contact, or non-contact monitoring. Contact methods such as LVDT's and String Transducers are the traditional methods. These devices can be tedious to set up, and depending on the terrain, may be unusable for some applications. The devices were designed for laboratory use, and their adaptations for field use produce complications and sources for error. Once set up and calibrated, they can take continuous data readings. The non-contact alternative is optical

laser surveying equipment, consisting of prisms installed and a total station to take the readings. This method takes much less time to set up, but readings can only be taken about every one minute. Merkle and Myers showed that the Leica TCA 2003 Total Station is accurate to .005 inches (0.127 mm) at distances of 200 ft (60.96 m) to the target or less (Merkle and Myers, 2004). This accuracy is comparable to the accuracy of contact monitoring methods. (Holdener et al., 2004; Merkle, 2004)

2.4.2. Surface Roughness

Having the optimum surface roughness is critical for FRP and FRCM systems because the bond will be poor if the surface is too rough or too smooth. For use in the five bridge project, a new technology was developed at UMR to measure the surface roughness. The optimum surface roughness was identified with a profilometer utilizing image analysis techniques, which is the first existing roughness measuring device for use in the field. Holdner et al. described how the device works as follows: “The laser profilometer projects thin strips of laser light at an angle of 45 degrees onto concrete surface5. A high resolution camera perpendicular to the concrete surface then records a video that is digitized and sent to a computer for analysis. The roughness can then be quantified based upon the average pixel to pixel angles; this is called an average inclination angle.” Figure 2-7 shows the device in use. (Holdener et al., 2004; Missouri Department of Transportation, 2005).

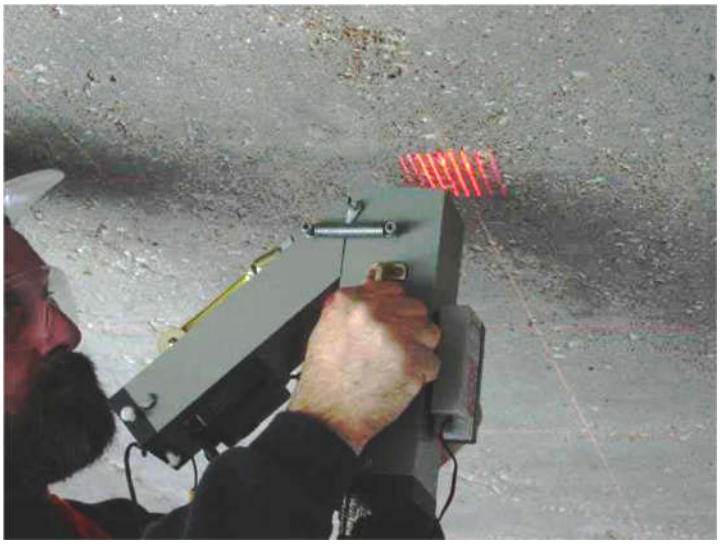

Figure 2-7. Laser Profilometer (Holdener et al. 2004)

2.4.3. Fiber Alignment

Proper fiber alignment is critical to the performance of an FRP or FRCM system because the fibers are strongest along their length. Both ACI 440.2R and ACI 549.4R design guides state that variations as little as 5 degrees can have a large impact on system performance. In order to monitor the variance, FRP is installed with a tracer woven into the fiber that can be seen through the matrix. A chord can then be stretched across the installed system in the desired alignment, and imaging software is used to determine the angle differences. (Holdener et al., 2004; ACI Committee 440, 2008; ACI Committee 549, 2013)

2.4.4. FRP Delamination.

Surface delaminations or voids between either the system and the concrete surface or between layers of reinforcement can drastically reduce the strength of an FRP or FRCM system. Causes of such delaminations include moisture (in FRP), fluctuating temperatures, and improper installment. According to ACI 440.2R and ACI 549.4R, delaminations over 25 square inches (16129 square mm) should be repaired by cutting away and patching. The system should then be reevaluated to ensure repairs were properly installed. NDT methods used to detect delaminations include acoustic sounding (hammer sounding), impact-echo, impulse response, ultrasonics, infrared thermography, and near-field microwave techniques. (Holdener et al., 2004; ACI Committee 440, 2008; ACI Committee 549, 2013)

3. DESIGN OF STRENGTHENING SYSTEM

This section contains the analysis and design procedures used in the strengthening of Missouri Bridge P-0058 located in south central Missouri near Lanton, Missouri. A description of the bridge and materials are included. For this project, spans 1 and 4 were strengthened and spans 2 and 3 were left unstrengthened. The middle spans had very poor access, making it difficult to strengthen them. In addition, having unstrengthened spans for comparison can provide valuable information for the study's future intended work.

3.1. BRIDGE DESCRIPTION

Missouri Bridge P-0058 was selected from a list of candidate bridges in Missouri. The candidates were all considered structurally deficient according to MoDOT. Missouri bridges receive condition ratings periodically for their deck, superstructure (sup), and substructure (sub). In the most recent inspection report, bridge P-0058 received deck/sup/sub ratings of 4/4/6, with 4 meaning poor, and 6 meaning satisfactory. Due to the age and condition, bridge P-0058 is currently load posted as shown in Figure 3-1.

Bridge P-0058 is located on Highway 142 and spans the Myatt Creek in Howell County, Missouri. This bridge was originally constructed in 1951 and consists of four simply supported reinforced concrete spans. For this study, the spans were numbered 1 through 4 from west to east. The two spans farthest west (1 & 2) are 37.5 feet (11.43 m) long and the two to the east (3 & 4) are 27.5 feet (8.38 m), for a total bridge length of 130 feet (39.62 m). The desk is six inches thick and is supported by three tee beams spaced 7.0833 ft. (2.16 m) on center. For this project, the three beams are referred to as beam 1 through 3, with 1 being the northern most, and 3 farthest south. The total deck width is 17.1667 ft. (5.232 m) with a curb to curb roadway of 14 ft (4.267 m). Due to the narrow roadway, the bridge is limited to one lane of traffic with yield to oncoming traffic signs in each direction. Figure 3-2 shows the bridge's approach, and a profile view.

The longer spans have slightly different geometry from the shorter spans. Cross sections with dimensions for each span length can be found in Section 3.4

Figure 3-1. Bridge P-0058 Load Posting

Figure 3-2. Bridge P-00585 Approach and Profile View

3.2. MATERIALS USED

The four different strengthening systems used are described in this section. Properties for each material are given by the manufacturer or obtained through tests performed in a lab setting.

3.2.1. Fiber-Reinforced Polymer

Carbon FRP manufactured by Structural Technologies was chosen for use in this strengthening project. The product used is V-Wrap™ C200HM High Modulus Carbon Fiber Fabric (Structural Technologies, 2016b). The resin used is V-Wrap™770 Epoxy Adhesive which is also manufactured by Structural Technologies. It is a two-part epoxy

that is designed to be used in wet-layup composite strengthening (Structural Technologies, 2016a). As stated in ACI 440.2R-08 account for long term exposure to the environment and must be reduced based on the exposure of the application. Bridges are in the exterior exposure category, so the ultimate strain and ultimate strength of the carbon shown in Table 3-1 were reduced to 85% of the given values for design properties.

Table 3-1. CFRP Properties from Manufacturer

System	Eq. Thickness [in2/in]	Ultimate Strain [%]	Garunteed Ultimate Strength [ksi]	Modulus of Elasticity [ksi]
Carbon FRP	0.00650	1.67	550.00	33000.00

3.2.2. Fiber Reinforced Cementitious Matrix

Three different systems with cementitious matrix were used in this study. The fiber types used were carbon (C-FRCM), PBO, and steel cords. As described in Section 2.2.2, when designing with FRCM, the properties should come from an idealized bilinear stress strain curve, but the contribution of FRCM before cracking is neglected. The idealized curve should come from statistic data from a series of coupon tests. The properties used in this study were provided by a research team at the University of Miami and are displayed in Table 3-2 (Babaeidarabad et al. 2014).

The carbon FRCM system used is CSS-UCG Unidirectional Carbon Grid which is manufactured by Simpson Strong-Tie. It is designed to be field installed with CSS-CM cementitious matrix also manufactured by Simpson Strong-Tie. (Simpson Strong-Tie, 2017, 2018) The PBO FRCM system used consists of fibers and inorganic matrix both manufactured by Ruredil (Ruredil, 2012). The SRG system chosen uses GeoSteel G600® mesh with either GeoCalce® Fino or GeoLite® cementitious matrix, all of which are manufactured by Kerakoll S.p.A. (Kerakoll S.p.A., 2014). Figure 3-3 shows each fabric, and their layout of fibers.

3.3. ANALYSIS OF EXISTING CAPACITY

The analysis was performed according to ACI 318-14 (ACI Committee 318, 2014). ACI analysis was chosen over AASHTO because it is referenced by the composite strengthening design guides. The analysis was based on the following assumptions:

- Plane sections remain plane after loading
- Maximum strain at the extreme concrete compression fiber shall be assumed equal to 0.003
- Tensile strength of concrete shall be neglected in flexural and axial strength calculations

Original design drawings were referenced for dimensions and design material properties and are found in Appendix A. The flexural steel reinforcement in the bridge has a yield strength of 33 ksi (227.5 MPa) according to MoDOT drawings. This value was used in the analysis of the existing capacity as well as the design of strengthening systems. The concrete compressive strength was reported by MoDOT as 3 ksi (20.7 MPa), however, field tests showed that it is much higher. Schmidt hammer tests on each beam of spans 1 and 4 gave equivalent compressive strength readings ranging from 5800 psi (40.0 MPa) to 8500 psi (58.6 MPa), with an average of 7289 psi (50.26 MPa). 6000 psi (41.4 MPa) was used in analysis and design of strengthening, which exceeds two standard deviations below the average test value.

Table 3-2. FRCM Statistical Properties

System		Eq. Thickness [in2/in]	Ultimate Strain [%]	Ultimate Strength [ksi]	Cracked Modulus of Elasticity [ksi]
Carbon FRCM	mean	0.00618	1.64	202.20	9209.94
	St. dv		0.43	2.03	1902.88
PBO FRCM	mean	0.00180	1.76	241.34	18564.83
	St. dv		0.13	11.17	2175.57
SRG	mean	0.00333	1.40	196.40	13478.36
	St. dv		0.30	14.70	2487.40

Conversion: 1 in^2/in = 25.4 mm^2/mm; 1 ksi = 6.895 MPa

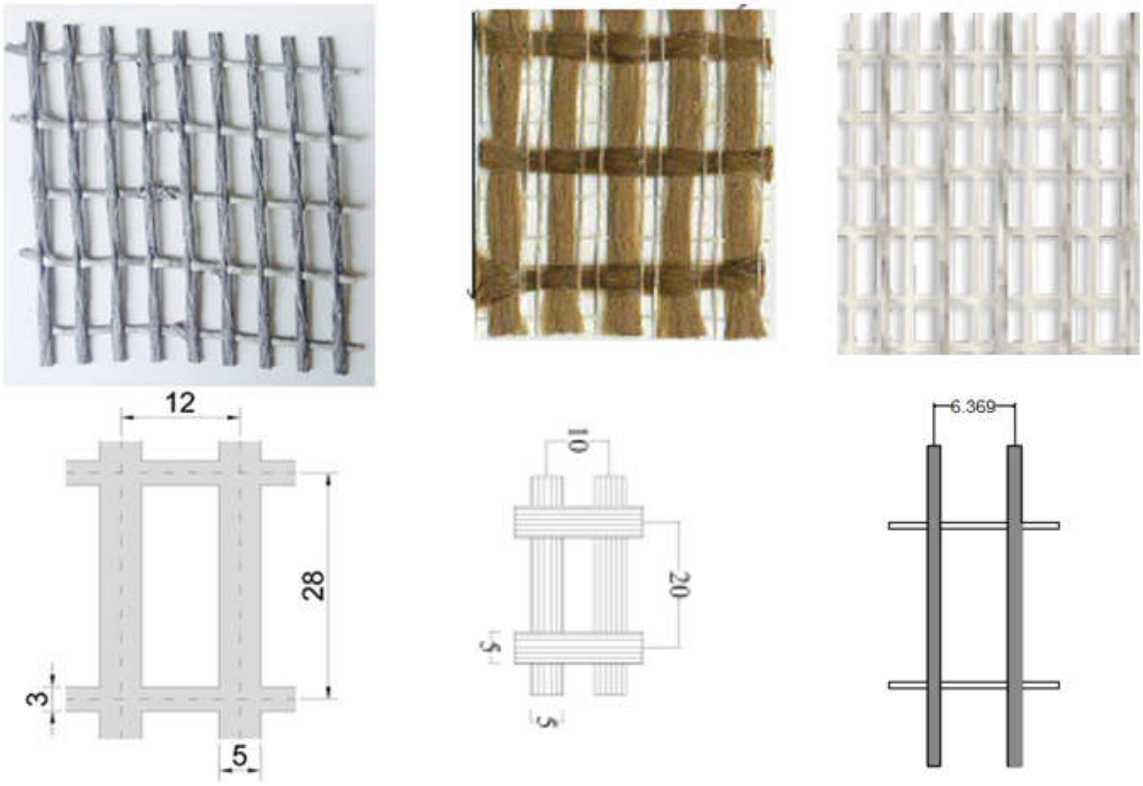

a) Carbon b) PBO c) SRG

Figure 3-3. Fibers Used in FRCM (Nanni, 2018). Dimensions in mm. 1in.=25.4mm.

3.3.1. Flexure

Since the bridge has simply supported spans, each girder type was analyzed individually as simply supported with positive moment only. Girder geometrical properties, shown in Figure 3-4 and

Table 3-3, were found in MoDOT's design drawings and then verified by measurements in the field. The effective flange width was calculated as per ACI 318 with the equations shown in Figure 3-5.

The tee beams were analyzed using the Whitney stress-block model, first assuming that the compression block fell within the flange. This assumption was verified for each case. It was also assumed, and later verified, that the steel yields at nominal

capacity. Table 3-4 shows the amount of internal flexural steel reinforcement for each girder type, as shown in MoDOT design drawings.

Table 3-5 shows the moment capacity for each girder type before strengthening. Full calculations can be found in Appendix A. The flexural strength reduction factor (Φ) for the nominal capacity is .9 for each beam, as per ACI 318 for beams that are tension controlled.

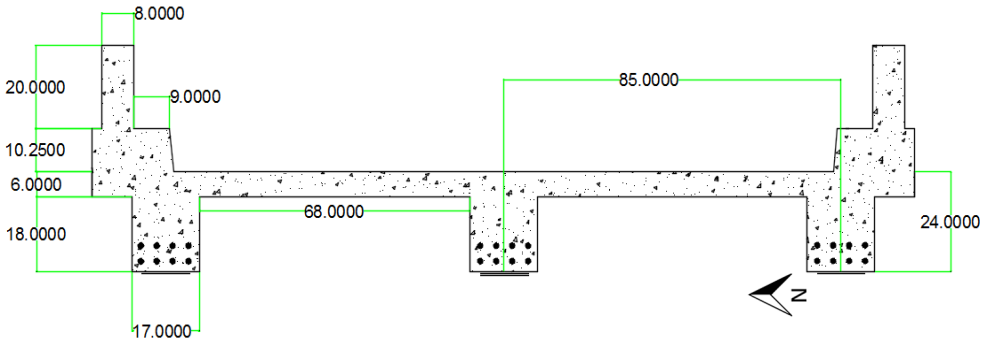

a) Spans 1 and 2 (units shown in inches) Conversion: 1 in. = 25.4 mm

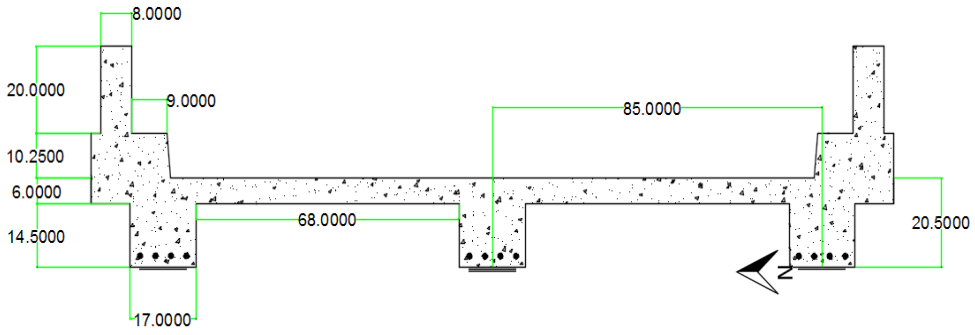

b) Spans 3 and 4 (units shown in inches) Conversion: 1 in. = 25.4 mm

Figure 3-4. Cross Sections of Spans

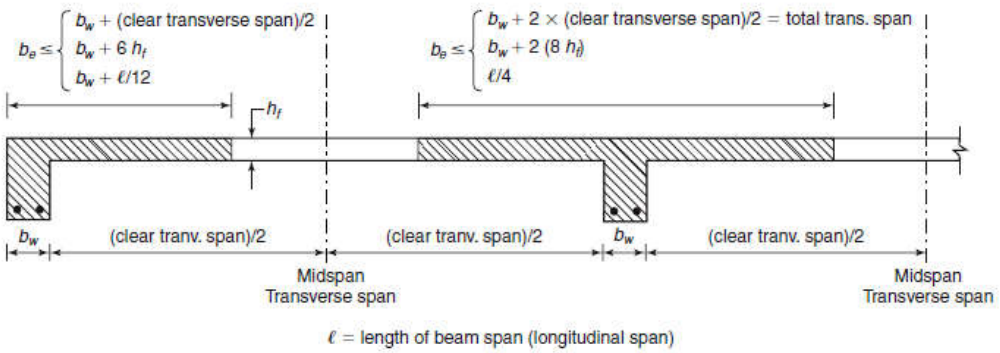

Figure 3-5. Effective Flange Width (Wight & Macgregor, 2012)

Table 3-3. Geometrical Properties

Span	Girder Type	Overall Height h, (in)	Width of the Web b, (in)	Width of the Flange b_e, (in)	Slab Thickness h_f, (in)
1 & 2	Interior	24	17	85	6
	Exterior	24	17	61	6
3 & 4	Interior	20.5	17	79	6
	Exterior	20.5	17	58	6

Conversion: 1 in. = 25.4 mm

Table 3-4. Flexural Internal Steel Reinforcement at Midspan

Span	Girder Type	Tensile Steel Area A_s, (in^2)	Effective Depth d, (in)
1 & 2	All	11.32	19.82
3 & 4	All	6.24	18

Conversion: 1 in. = 25.4 mm

3.3.2. Shear

Each girder type was analyzed for shear capacity as per ACI 318. Table 3-6 shows the internal steel shear reinforcement as originally constructed. This information was gathered from MoDOT design drawings. The total shear capacity of a beam type member is taken as the combination of the contributions from the concrete and the reinforcing steel. Both of the shear contributions were calculated in accordance with ACI

318 and are shown in Table 3-7. The shear strength reduction factor (Φ) for the nominal capacity is .75 as per ACI 318. Full calculations can be found in Appendix B.

Table 3-5. Existing Nominal Moment Capacity

Span	Girder Type	Nominal Moment Capacity Mn (kip-ft)
1 & 2	Interior	603.49
	Exterior	598.22
3 & 4	Interior	304.50
	Exterior	302.91

Conversion: 1 kip-ft = 1355.8 N-m

Table 3-6. Shear Internal Steel Reinforcement

Span	Girder Type	Shear Steel Area A_v, (in^2)	Stirrup Spacing s, (in)
1 & 2	All	0.4	15
3 & 4	All	0.4	12

Conversion: 1 in. = 25.4 mm

Table 3-7. Existing Nominal Shear Capacity

Span	Girder Type	Shear Contribution from Steel V_s (kip)	Shear Contribution from Concrete V_c (kip)	Nominal Shear Capacity Vn (kip)
1 & 2	All	17.44	52.19	69.63
3 & 4	All	19.80	47.41	67.21

Conversion: 1 kip = 4.448 kN

3.4. GIRDER STRENGTHENING DESIGN

With six girders to be strengthened using four different systems, decisions were made in an attempt to get the best information possible in the long term. Research field applications and data is presently not available on FRCM and SRG, so cementitious systems were chosen to be the main focus. Each girder type is controlled by flexure, so the focus of the strengthening is for flexure.

A parametric study was completed, varying the different span lengths (which have different section depths and areas of steel reinforcement), the different strengthening systems (Carbon FRCM, PBO FRCM, CFRP and SRG), the width of the plies, and different numbers of plies of strengthening up to four plies. This study showed which systems performed better than others on the long spans. It also made clear the expected result of multiple layers of each system. After consideration, it was decided to use two plies of each system, which will give valuable information with lower labor and material costs.

Table 3-8 shows a section of the data for the moment capacity parametric using 17 in. (43.2 cm) wide plies. This table also includes the percent difference of the percent increase in capacity for the same amount of strengthening applied to the long vs. short spans. A lower percentage here shows that the system is less effected by which span length they are installed on. While carbon FRP and Carbon FRCM were most impacted by the span length, their higher efficiency overall made them the best choice for strengthening the long spans. The full parametric study results with example calculations is given in Appendix C.

The focus of this study is flexural strengthening, but some shear strengthening was also provided. The effects of MoDOT posting vehicles H20 Legal and 3S2 were considered. Strengthening in shear to accommodate these trucks maintains that the girders are expected to fail in flexure after strengthening. The long spans are controlled by the Missouri 3S2 truck. The maximum shear exceeds the pre strengthening capacity by about 5 kips (22.2 kN) for the 2 feet (.61 m) closest to supports in the shear envelope. For the short spans, the H20 Legal truck controls. The short spans have adequate shear strength without strengthening. U-wraps, which are generally used for shear strengthening, also help anchor the flexural reinforcement and reduce the failure by deboning and also aid field installation by reducing ability of the flexural strengthening to sag, so they will be used on each span. The exact wrapping configuration was decided after consulting with the design teams of each manufacturer. The chosen wrapping scheme for each beam can be found in Appendix D.

Table 3-8. Moment Capacity Parametric Data

Moment Capacity Parametric (17 inch width)		Long Span % increase	Short Span % increase	Long vs Short span % difference	Average % difference
FRCM-PBO	1 Ply	1.84%	2.98%	61.9%	59.6%
	2 Ply	4.45%	7.10%	59.4%	
	3 Ply	7.07%	11.22%	58.7%	
	4 Ply	9.67%	15.33%	58.4%	
FRCM-Carbon	1 Ply	2.58%	5.15%	99.5%	83.2%
	2 Ply	6.29%	11.43%	81.6%	
	3 Ply	10.00%	17.70%	77.0%	
	4 Ply	13.71%	23.96%	74.8%	
SRG	1 Ply	0.99%	1.06%	6.5%	17.6%
	2 Ply	3.24%	3.88%	19.5%	
	3 Ply	5.50%	6.69%	21.8%	
	4 Ply	7.75%	9.51%	22.7%	
CFRP	1 Ply	11.46%	18.92%	65.1%	73.9%
	2 Ply	17.72%	31.31%	76.7%	
	3 Ply	21.62%	38.24%	76.9%	
	4 Ply	24.91%	44.07%	76.9%	

3.4.1. Fiber Reinforced Polymer

The design and analysis was performed according to ACI 318 (ACI, 2014) and ACI 440 (ACI Committee 440, 2008), based on the following assumptions:

- Design calculations are based on the dimensions, internal reinforcing steel, and material properties of existing member being strengthened
- Plane sections remain plane after loading, so strains are proportional to distance from the neutral axis
- The bond between FRP and concrete substrate as well as that of the fabric to the matrix is perfect
- Shear deformation within the adhesive is very small and is neglected
- The maximum usable compressive strain in the concrete (ε_{cu}) is 0.003 in/in
- Tensile strength of concrete is neglected

  The FRP has a linear elastic stress-strain relationship to failure.

3.4.1.1. Flexure design. ACI 440 imposes strengthening limits in order to guard against structure collapse should bond or other failure of the system occur due to damage, vandalism, or other causes. To make the structure able to still resist a reasonable level of load should a failure occur, Equation 3.1 must be satisfied. R_n is the nominal strength of a member and S_{DL} and S_{LL} are the dead load and live load effects.

$$(\Phi R_n)_{existing} \geq (1.1S_{DL} + 0.75S_{LL})_{new} \quad (3.1)$$

In order to reduce the failure by debonding, ACI 440 limits the effective strain in the FRP to a level in which debonding may occur (ε_{fd}), which is defined by Equation 3.2. The limit is based on the compressive strength of the concrete (f`c), the number of layers of fabric (n_f), the modulus of elasticity of the FRP (E_f), and the effective thickness of the fabric (t_f). This equation also limits the debonding strain to 90 percent of the ultimate strain (ε_{fu}). This equation was developed based on statistical analysis of a database of flexural test beams that failed by debonding (ACI Committee 440, 2008).

$$\varepsilon_{fd} = 0.083\sqrt{\frac{f`c}{n*E_f*t_f}} \leq .9\varepsilon_{fu} \quad (3.2)$$

The ultimate strength of a section is found based on the internal strain and stress distribution under flexure at the ultimate limit state. The procedure for obtaining the ultimate strength must satisfy strain compatibility and force equilibrium, as well as consider the governing mode of failure. The procedure chosen uses a trial-and-error method to find a solution. Figure 3-6 illustrates steps in the procedure described in the following.

The procedure for obtaining the ultimate strength begins by assuming a value of c, or the depth to the neutral axis. With this assumption, the strain level in the FRP (ε_{fe}) can be calculated using Equation 3.3. This equation considers the failure mode for the assumed neutral axis. If the left side of the inequality governs, then concrete crushing controls the flexural failure, and if the right side governs, then FRP failure by either debonding or rupture controls the section failure. In the equation, d_f is the depth of the fibers from the extreme compression face, which is taken as the height of the beam being strengthened. The strain level in the concrete surface at the time of FRP strengthening

(ε_{bi}) is considered in the equation, and it is calculated based on the properties and dimensions of the RC section and the moment caused by the dead load.

$$\varepsilon_{fe} = \varepsilon_{cu} * \left(\frac{(d_f - c)}{c}\right) - \varepsilon_{bi} \leq \varepsilon_{fd} \quad (3.3)$$

With the effective strain in the FRP known, the effective stress level (f_{fe}) can be calculated using Hooke's law, assuming perfectly elastic behavior. Based on the strain level in the FRP, the strain in the steel (ε_s) can also be found using the linear strain distribution. Then, the stress in the steel (f_s) is determined using its stress-strain curve. This method uses a rectangular equivalent compressive stress block as shown in Figure 3-6, where the distribution factors α_1 and β_1 are defined by Equations 3.7 and 3.6. With the strain and stress levels in the FRP and steel known for the assumed neutral axis depth, the internal equilibrium can be checked using Equations 3.4 through 3.8

$$E_c = 57000\sqrt{f`c} \quad (3.4)$$

$$\varepsilon`_c = \frac{1.7f`c}{E_c} \quad (3.5)$$

$$\beta_1 = \frac{4\varepsilon`_c - \varepsilon_c}{6\varepsilon`_c - 2\varepsilon_c} \quad (3.6)$$

$$\alpha_1 = \frac{3\varepsilon`_c\varepsilon_c - (\varepsilon_c)^2}{3\beta_1(\varepsilon`_c)^2} \quad (3.7)$$

$$c` = \frac{(A_s f_s + A_f f_{fe})}{\alpha_1 f`c \beta_1 b} \quad (3.8)$$

where E_c is the modulus of elasticity of the concrete, ε_c is the compressive strain level in concrete, $\varepsilon`_c$, is the compressive strain corresponding to f`c, A_s is the area of flexural steel reinforcement, and A_f is the area of flexural FRP fibers.

If the assumption of the neutral axis depth was correct, then the value for c assumed will be in agreeance with c` calculated from Equation 3.8, which shows that the tension and compression in the section are equal. If the assumption was incorrect, then iterations are done by changing the value of c and repeating the process of calculating strains and stresses. The correct value for the neutral axis depth is found when convergence occurs and the neutral axis depth is returned as c`.

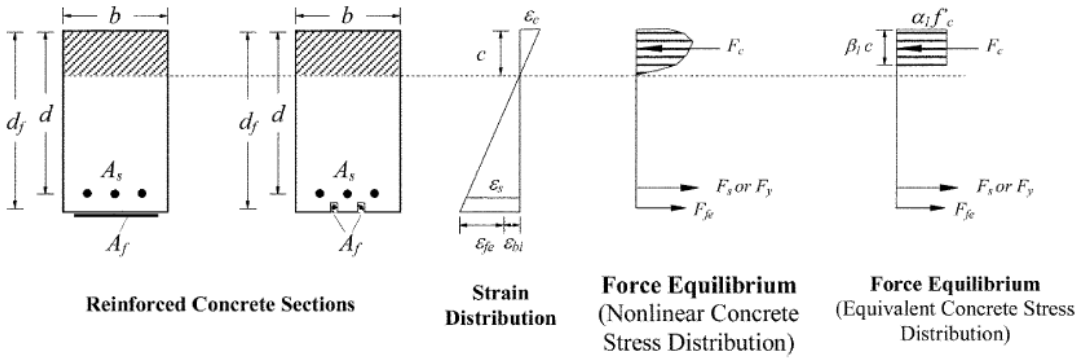

Figure 3-6. Internal Stress and Strain Distribution in Flexure (ACI Committee 440, 2008)

The nominal flexural strength of the section is computed using the force equivalent forces and the moment arm between them. Equation 3.9 shows the moment capacity provided by both the original RC section, and the added external FRP strengthening. For FRP contribution, an additional reduction factor, Ψ_f, is applied. For flexure, the value used is .85, which is based on reliability analysis and the inherent uncertainties of FRP compared to more widely used materials (ACI Committee 440, 2008).

$$M_n = A_s f_s \left(d - \frac{a}{2}\right) + \Psi_f A_f f_{fe} \left(d_f - \frac{a}{2}\right) \qquad (3.9)$$

ACI 440.2R also includes limits on the service load stress in the steel and FRP. The guide has equations based on cracked-section analysis of the FRP-strengthened reinforced concrete section that were used to check the service stresses against their limits. The stress limit for steel is 80% of the yield strength, and for carbon, the limit is 55% of the ultimate fiber strength.

3.4.1.2. Shear design. Three different wrapping schemes are discussed in ACI 440 for shear strengthening of RC members: complete wrapping, 3- sided “U-wrap”, and 2-sided. Complete wrapping is the most efficient technique, but it is rarely possible for girders, because the integral slab prevents access to the top side. U-wraps are the next efficient method, and were chosen for this project. Shear strengthening systems can also be installed continuously along the span, or placed as discrete strips, however, complete encasement is discouraged, as it prevents migration of moisture (ACI Committee 440,

2008). Figure 3-7 illustrates a cross sectional view of a girder strengthened with U-wraps (a), as well as side views of beams strengthened with discrete strips both vertical (b) and inclined (c). The figure also shows the dimensional variables used in strengthening calculations.

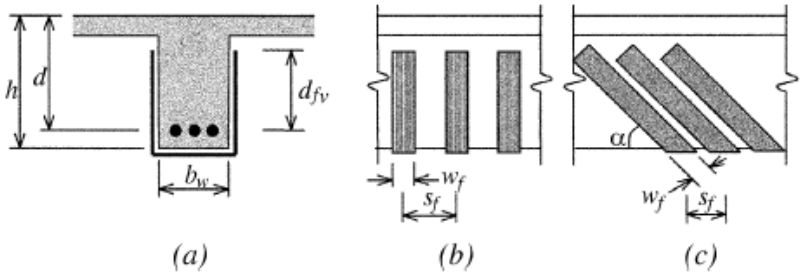

Figure 3-7. Shear Strengthening with FRP Nomenclature (ACI Committee 440, 2008)

The nominal shear capacity of an FRP strengthened reinforced concrete member is calculated with Equation 3.10. For shear reinforcement, Ψ_f has a value of .85 for U-wrapped members. As typical for shear design, Φ is taken as .75.

$$\Phi V_n = \Phi(V_c + V_s + \Psi_f V_f) \quad (3.10)$$

In Equation 3.10, the shear contributions from the concrete (V_c) and steel (V_s) are calculated as per ACI 318. The contribution from FRP is calculated based on fiber quantity and orientation, as well as an assumed crack pattern. Equation 3.11 gives the shear contribution of the FRP reinforcement based on the tensile stress in the FRP across the assumed crack.

$$V_f = \frac{(A_{fv} f_{fe}(sin\alpha + cos\alpha) d_{fv})}{s_f} \quad (3.11)$$

A_{fv} and f_{fe} are defined by Equations 3.12 and 3.13. Figure 3-7 shows the definition of the terms α (orientation of the strips), s_f (center to center spacing of strips), and d_{fv} (depth of flexural reinforcement from top of shear reinforcing fibers). In addition, the figure shows the variables used in calculating the area of shear reinforcing fibers: n (number of plies), t_f (effective thickness of one ply), and w_f (width of a strip).

$$A_{fv} = 2nt_f w_f \quad (3.12)$$
$$f_{fe} = \varepsilon_{fe} E_f \quad (3.13)$$

ACI 440 has different limitations on the effective strain in the FRP for shear than for flexure. There are also different limitations for completely wrapped beams than 2 or 3-sided since delamination is more likely to occur for the latter. For U-wrapped beams, Equation 3.14, which uses a bond reduction coefficient (κ_v), is used. This equation also limits the strain to 0.4%, which helps avoid the loss of aggregate interlock of the concrete.

$$\varepsilon_{fe} = \kappa_v \varepsilon_{fu} \leq 0.004 \qquad (3.14)$$

Shear design with FRP also has limits to how much strength enhancement can be added. In in-lb units, the limit for the contribution of steel and FRP combined is given by Equation 3.15.

$$V_s + V_f \leq 8\sqrt{f`c}\, b_w d \qquad (3.15)$$

3.4.2. Fiber Reinforced Cementitious Matrix.

The design and analysis were performed according to ACI 318-14 and ACI 549 (2013) based on the following assumptions:

- Plane sections remain plane after loading
- The bond between FRCM and concrete substrate as well as that of the fabric to the matrix is perfect
- The maximum usable compressive strain in the concrete is 0.003 in/in
- FRCM has a bilinear-elastic behavior up to failure, however, the contribution of FRCM before cracking is neglected

1.1.1.1. Flexure design. The procedure for FRCM design laid out in ACI 549 is similar to the FRP design in ACI 440. The initial step is to get material properties from coupon tests. Rather than using Equation 3.2 to limit strain to prevent debonding, ACI 549 uses statistics from coupon tests and defines the ultimate strain, ε_{fd}, as the average ε_{fu} minus one standard deviation. This ultimate tensile strain is then multiplied by

the cracked modulus of elasticity (E_f) to get the ultimate tensile strength of the FRCM. In order to prevent slippage of fibers within the matrix, the design tensile strain (ε_{fe}) is further limited to the smaller of ε_{fd} and 0.012.

The ultimate moment capacity is calculated based on the internal strain and stress distribution under flexure at the ultimate limit state. A trial-and-error method is used for obtaining the ultimate strength, which satisfies strain compatibility and force equilibrium and considers the governing mode of failure. Figure 3-6 illustrates steps in the procedure. Once iterations of Equations 3.4 through 3.8 are done to find the neutral axis depth, and internal stresses are found, the ultimate moment capacity is found using Equation 3.16.

$$M_n = A_s f_s \left(d - \frac{a}{2}\right) + A_f f_{fe} \left(d_f - \frac{a}{2}\right) \quad (3.16)$$

ACI 549.4R also has limitations on the amount of enhancement provided. The increase in flexural capacity strength provided by FRCM reinforcement should not exceed 50 percent of the existing flexural capacity. Additionally, the stresses in steel under service loads should be limited to 80 percent of the yield strength. In order to prevent concerns over creep rupture and fatigue, the service level tensile stress in the FRCM is limited to a percentage of the design tensile strength based on the fiber type as shown in Table 3-9.

1.1.1.2. Shear design. For shear strengthening with FRCM, the procedure based on ACI 549 is very similar to what was used for FRP. The statistical properties from coupon tests that were used in flexure design are again used in shear design. ACI 549 limits the design tensile strain in the FRCM for shear to the smaller of 0.004 and the ultimate strain from tests. Equations 3.12 through 3.14 are used to determine the shear contribution from the FRCM strengthening. The total shear strength of the RC section with added FRCM is then calculated using equation 3.17. As typical for shear design, a strength reduction factor, Φ, of .75 is applied to the nominal shear strength, V_n.

$$V_n = V_c + V_s + V_f \quad (3.17)$$

The total shear strength provided by the FRCM and steel is limited by equation 3.18. Additionally, the increase in shear strength after adding FRCM should not exceed 50 percent of the existing capacity.

$$V_s + V_f \leq 8\sqrt{f`c}\, b_w d \qquad (3.18)$$

3.3.4. Summary of Design.

Table 3-10 provides a summary of both flexural and shear strengthening added to bridge P-0058. All strips used for strengthening are 12 inches wide. Details of the shear strengthening wrapping scheme are located in Appendix D. Appendix E contains a detailed bill of materials as built.

Table 3-9. Creep and Fatigue Stress Limits (ACI Committee 549, 2013)

	Fiber type				
	AR glass	Aramid	Basalt	Carbon	PBO
Creep rupture and fatigue	$0.20f_{fd}$	$0.30f_{fd}$	$0.20f_{fd}$	$0.55f_{fd}$	$0.30f_{fd}$

Table 3-10. Summary of Strengthening System Design

	Span 1	**Span 2**
	Carbon FRCM/ CFRP	
	36.1875ft	36.1875ft
Girder 1	**CFRP:** Flexure: 2 ply Shear: one ply 17in spacing, 18 strips total	No Strengthening
Girder 2	**Carbon FRCM:** Flexure: 2 ply Shear: one ply 12in spacing, 20 strips total	No Strengthening
Girder 3	**Carbon FRCM:** Flexure: 2 ply Shear: one ply 12in spacing, 20 strips total	No Strengthening

	Span 3	Span 4
		PBO FRCM/ SRG
	26.375ft	26.375ft
Girder 1	No Strengthening	**SRG:** Flexure: 2 ply Shear: two ply 18in spacing, 13 strips total
Girder 2	No Strengthening	**SRG:** Flexure: 2 ply Shear: two ply 18in spacing, 13 strips total
Girder 3	No Strengthening	**PBO FRCM:** Flexure: 2 ply Shear: two ply 18in spacing, 13 strips total

4. INSTALLATION OF STRENGTHENING SYSTEM

The installation of strengthening systems requires an emphasis on attention to detail. The procedures used should agree with ACI 440, ACI 549, and the suggestions of the material manufacturers. This section describes the planned procedure for installing strengthening on Bridge P-0058. The installation of the strengthening systems follows the completion of this report

4.1. PRE INSTALLATION

Composite strengthening systems require some preparatory work before manual layup. The preinstallation helps with the performance of the system in the future.

4.1.1. Substrate Repair

The quality and strength of the substrate is important for performance of externally bonded strengthening systems. Areas that were damaged by concrete spalling were addressed to avoid compromising the integrity of the strengthening system. Figure 4-1 shows spalling on a girder. As shown in the figure, much of the damaged areas were below drop drains and were exposed to water regularly and salt concentrations in the winter. Cement mortars that are compatible with both the concrete substrate and the systems used for strengthening were used for the patching. For the carbon FRCM system, the cementitious matrix (CSS-CM) can be used to patch voids and defects that are no deeper than 2 in. (51 mm) (Simpson Strong-Tie, 2017).

Figure 4-1. Spalling on Girder

4.1.2. Surface Preparation

The surface of the substrate must be prepared accordingly to allow optimal bonding conditions for load transfer to the strengthening systems. Strengthening for both flexure and shear are bond critical, and thus require an adhesive bond between the system and the substrate. Sand blasting, shown in Figure 4-2, was used to remove all laitance, dust, dirt, oils, and other matter that could interfere with the bond of the system. This surface preparation also provides a rough surface that is critical for the resin or cementitious matrix to bond to. ACI 440 requires "a minimum concrete surface profile (CSP) 3 as defined by the ICRI (International Concrete Repair Institute) surface- profile chips." For the Simpson FRCM system, it is recommended to achieve a minimum ¼ in. (6 mm) amplitude which is a CSP-6-9 (Simpson Strong-Tie, 2017). Surface irregularities such as fins and form lines were also removed or taken down to 1/32 inch as per ACI 440.

Surface preparation also includes rounding of corners that the fabric will wrap around in order to prevent stress concentrations in the fibers. ACI 440 requires a minimum radius of .5 inches (12.7 mm) for FRP, whereas ACI 549 states a radius not less than 0.75 inch (19.1 mm) before FRCM shear strengthening. The guidelines of each manufacturer were in agreeance with these corner radius limits.

Figure 4-2. Surface Preparation by Sand Blasting

A radius of 0.75 inch (19.1 mm) was used for each girder that was rounded and was achieved by grinding with a special bit as shown in Figure 4-3. The exception were girders strengthened with SRG, which were left unrounded.

Figure 4-3. Rounding Corners

4.2. INSTALLATION

The fiend installation of strengthening systems requires a good plan to be made before the day of installation. Attention to detail is crucial to adhere to the guidelines of ACI design guides as well as the suggestions of each manufacturer. The plan for installing strengthening on Bridge P-0058 follows.

4.2.1. Mixing of Resin or Matrix

Mixing of the resin was done in accordance with the manufacturer's recommendations. The suggested mixing ratio was followed, and complete mixing (based on mix time and visual inspection) was achieved before use. Electric paddle mixing was used to prepare the batches as shown in Figure 4-4, and batch size was kept small so that the resin could be used up in the recommended pot life for ideal viscosity. V-Wrap 770 comes in two parts referred to as A and B. Part A was premixed for 2 minutes, then the full contents of Part B pail were added to the full contents of Part A pail. Part A and Part B were then blended with a mechanical mixer for 3 minutes until uniformly blended. (Structural Technologies, 2016a).

Mortars were also mixed as specified by the manufacturer's recommended batch size, mix ratio, method, and time. Figure 4-4 shows the mixing process. Batch sizes were small so that the mortar could be used within its plastic state. This allows for the best viscosity for the matrix to penetrate the fabric.

The recommended procedure for mixing both Ruredil's and Simpson Strong-Tie's mortars is as follows. To start, 90% of the total mixing water recommendation depending on the desired consistency of the mortar was added. The batch was then mixed with a mechanical mixer at least 3 minutes adding the remaining 10% of the recommended total water if necessary until a homogeneous mixture with the desired consistency is formed. The mixture was allowed to rest 1 minute and then remixed another 10 seconds before applying. No additional water was added after the setting process is started. (Simpson Strong-Tie, 2017; Ruredil, 2012)

Figure 4-4. Mixing Resin and Cementitious Matrix

4.2.2. Manual Layup

For each system, the sheets of fabric were pre-measured and cut in the Missouri S&T labs in order to reduce prep work in the field prior to installation. Figure 4-5 shows materials being cut in the lab. The carbon FRP sheets were applied by wet layup as shown in Figure 4.6. The sheets were properly aligned, avoiding deviations of more than 5 degrees in either direction of the girder line as given as the acceptable tolerance in ACI

440. The sheets were set into the surface saturant, and rollers were used to smooth the fabric and remove bubbles. After about 10 minutes of setting, another layer of resin was rolled over to complete impregnation.

Figure 4-5. Preparation of CFRP Sheets

Figure 4-6. Manual Layup of CFRP

For the FRCM and SRG systems, trowels were used to apply an even, ¼ to ½ inch (6–13 mm) thick layer of matrix over the surface. The fabric was then gently pressed into the matrix, and another ¼ to ½ inch (6–13 mm) thick layer of additional matrix was smoothed over the top. Figure 4-6 shows this process. For each system, two plies of flexural reinforcement were used, and the second layer was applied before complete curing of the first layer. The SRG system presented other issues due to its rigidness in

comparison to the other fabrics. For u-wraps, a machine is needed to aid bending before the system can be installed.

For each system, flexural reinforcement was fully installed before shear reinforcement. This allowed for the flattest surface possible for the flexural sheets. Additionally, having the U-wraps on the exterior created the best anchorage qualities to aid the flexural system.

1.1.2. Curing

For FRCM systems, it is important to properly cure the system to achieve the desired strength**.** Installation shall be kept humid and protected against heat and wind for 3 to 5 days by wet curing or using an ASTM C309 complaint water-based curing compound. The use of curing compounds may affect adhesion of subsequent surface treatments. SSD surface conditions and proper curing procedures are critical to prevent premature drying or cracking. (Ruredil, 2012; Simpson Strong-Tie, 2017).

4.2.3. Durability Study

For each system, additional strips were installed in areas other than the girders to serve as a durability study area. The strips are intended to be used for pull-off testing at different times in the future. Different types of testing will be done to monitor performance in pure tension as well as shear to observe different failure modes. These strips will be exposed to the same environmental conditions as the girder strengthening such as freeze and thaw cycles, and ultraviolet light. These conditions can cause durability concerns and effect the bond performance of the strengthening systems in the long term.

5. LOAD TEST PROGRAM

For this project, load testing was performed to record baseline serviceability behavior prior to strengthening and is expected to be repeated post-strengthening on spans 1 and 4 (furthest east and west). Load testing is observing and measuring the response of a structure subjected to controlled loads in the elastic range. Both static and dynamic tests were conducted. The pre-strengthening load test was performed on July 3rd 2018, and the static test is described in this section. Deflection data of the girders was collected with both LVDTs and surveying equipment. Repetition of load testing over the years following strengthening will allow for monitoring of the system's performance. Any major loss of the systems' strength or stiffness may be observed through load testing. (John J. Myers, Holdener, & Merkle, 2012).

5.1. INSTRUMENTATION

Field visits were taken prior to the first load test in order to install instrumentation for monitoring during the load tests. An epoxy was used to attach steel plates to the underside of the beams in spans 1 and 4. These plates were placed at locations where optical surveying prisms were later magnetically attached to be used to monitor deflection. Even at the highest points, the prisms were quickly and easily installed using a range pole. The deck was not to be monitored. A Leica TCA 2003 Automatic Total Station was used to save and read the coordinates. Research on total station use for load testing has shown that this total station can measure deformation accurate to 0.005 inches (.127 mm) or better at close range, which is comparable to LVDT's (Hernandez & Myers, 2018a; Myers et al., 2008). The layout of the prisms is shown in Figure 5-1 and Figure 5-2. A total of 22 prisms were used between the two spans, with 2 additional per span used as reference prisms.

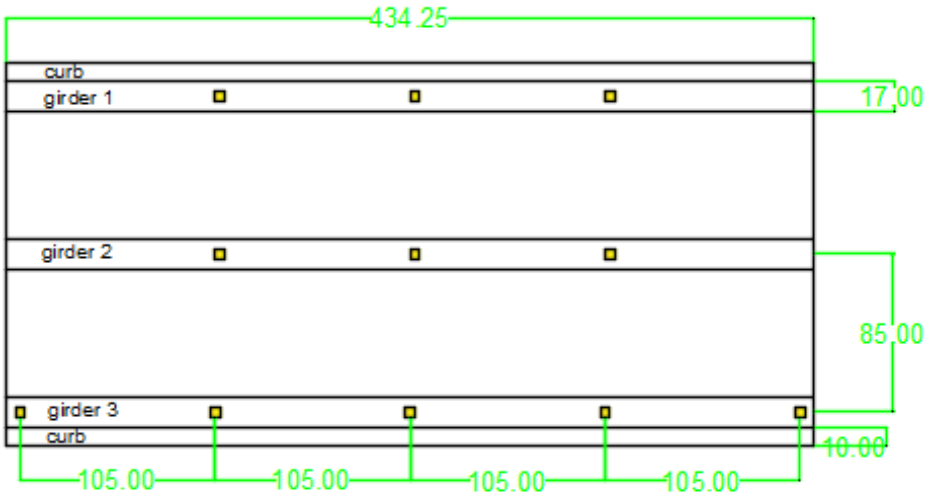

Figure 5-1. Span 1 Prism Layout (Dimensions shown in inches, 1 in. = 25.4 mm)

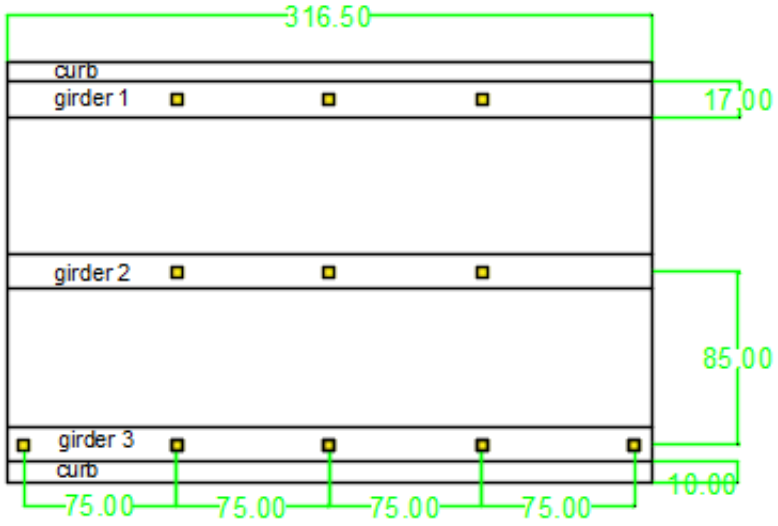

Figure 5-2. Span 4 Prism Layout (Dimensions shown in inches). Conversion Factor: 1 in. = 25.4 mm

5.2. SETUP

On the day of the test, equipment was set up and checked for functionality prior to starting the load test. LVDTs on stands were set up as another way to monitor deflection throughout the testing. They allowed for much more frequent readings than the total station. The LVDTs were used at midspan of each beam. Figure 5-3 shows the midspan

setup, including LVDTs and the data acquisition system (DAS) employed during the test. In addition, Figure 5-3 shows three prisms at midspan, and the total station is in the background.

Figure 5-4 shows the setup for the total station test. Once prisms were installed and the total station was setup on a secure tripod with a clear view of the targets, the device was programmed to mark the locations of each prism with respect to reference prisms. The reference prisms were also used to check if the total station had moved between readings. Each prism was named sequentially, and the names were documented in a field book. The total station was programmed to take three readings at each point, and an average value was used, neglecting any large variances.

Pre-test setup also included marking the physical truck stops to be used. These stops differed between the two spans due to the different geometry. The length and capacity of span 1 allowed for two loaded trucks to be used. In order to observe the maximum moment, the trucks were placed back to back, centered about the midspan. Span 4's smaller girders and shorter span length made a one truck setup necessary. Using the axle weights and distances between axles, the proper location of the truck for maximum moment was determined and marked.

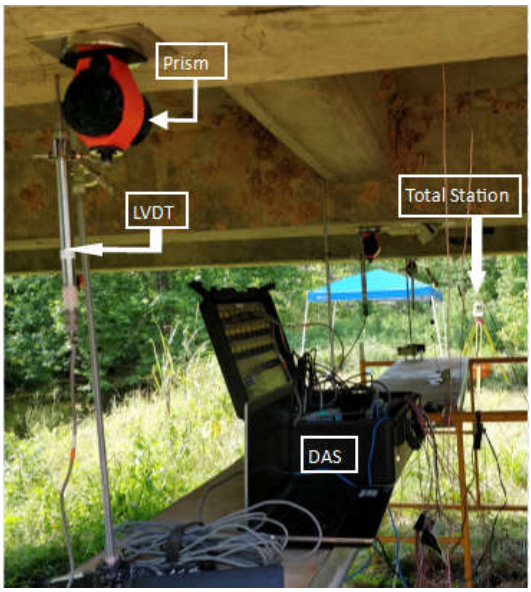

Figure 5-3. Data Acquisition System Setup. P1: Front Axle Weight; P2: Total Weight of Rear Axles. Conversion factor: 1 m = 3.28 ft

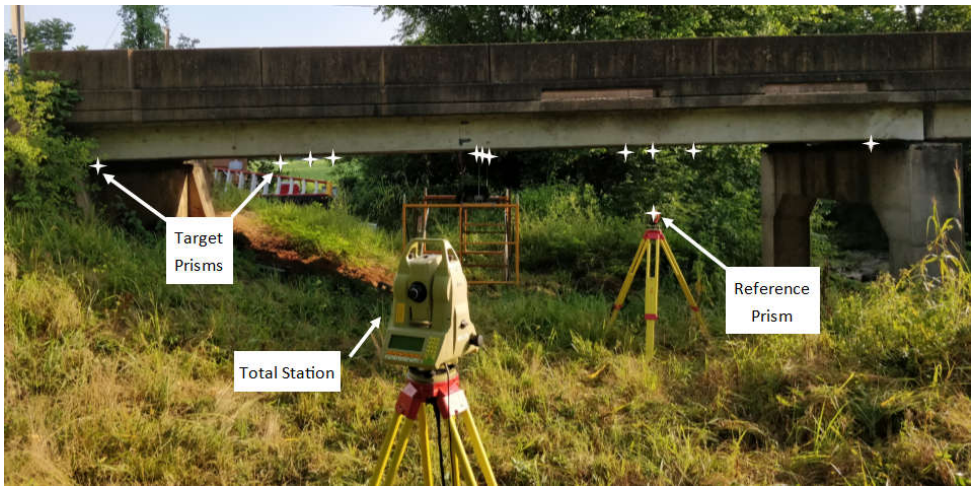

Figure 5-4. Total Station Setup

5.3. PROCEDURE

For each test described in the following, traffic control was used to ensure the results were due to the test trucks. Three H20 dump trucks were provided by MoDOT and labeled as trucks A, B, and C. Trucks A and B were loaded with gravel to be about 38 kips (169 kN) each and were used for the static load tests (Figure 5-5). Truck C was empty, and was only used for the dynamic load tests. shows the axle configuration of the trucks. The exact truck and axle weights were recorded so that variances in the weights on future load tests will be known for normalization and comparison.

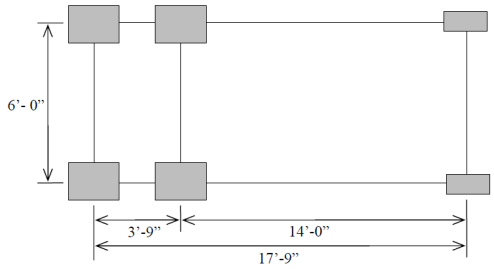

Figure 5-5. H20 Dump Truck Axle Configuration (Merkle, 2004). Conversion: 1 ft = 0.305 m; 1 in = 25.4 mm

For both spans, three different static tests were done, moving the trucks across the bridge from north to south. This allowed for observing the effect of different load distributions to each girder. Setups 1 and 3 produced an overload condition on the two

exterior girders, while setup two was symmetrically centered. All of the stops tested had the truck weight centered longitudinally on the span, to produce the maximum positive moment. The three positions are shown in Figure 5-6.

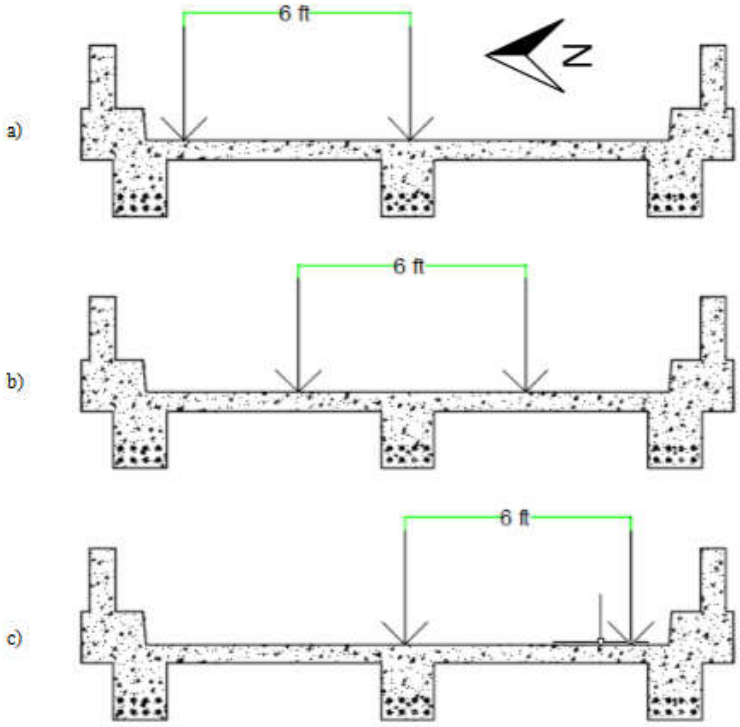

Figure 5-6. Load Test Truck Placements. (a) Setup 1; (b) Setup 2; (c) Setup 3

The testing began with span 1. An initial reading was taken with the total station, and the strain gauge and LVDT data began being collected at a rate of 1Hz. The total station was programmed to take three readings at each point, and an average value was used, neglecting any large variances. Next the trucks were positioned as close to the northern safety barrier as possible, as shown as position 1.

Figure 5-7 shows the trucks in position. Measurements were taken to know the exact location of the trucks, and the bridge was given time to respond to the load. After about 5 minutes, the total station was used to take readings of all the prisms on the span. This same procedure was repeated for placements 2 (centered on the span) and three (close to the south barrier). After these three static tests, the bridge was given time to relax, and final total station readings were taken.

Figure 5-7. Trucks on Span 1 for Load Test

The DAS and other equipment were then moved across the river to span 4, and a similar setup was completed. Initial total station readings were taken and LVDT data began collecting. Three stops were used on span 4, locating the single truck close to the north barrier, centered, and close to the south barrier. Figure 5-8 shows the loaded truck on span 4.

Figure 5-8. Truck on Span 4 for Load Test

5.4. RESULTS AND DISCUSSION

Upon completion of load testing, the data must be processed and condensed down to extract the useful information. Theoretical modeling were also performed and compared to the load test results.

5.4.1. Data Analysis.

The total station data was uploaded to a computer for further analysis. Each measurement was taken in sets of three readings, and these values were averaged, with any outliers removed. For each point, there was a control set from before loading and sets for each truck stop. Deflection was found by subtracting the control reading average from each truck stop reading average. A second control set was intended to be taken after the stops were concluded, but the total station was moved before the reading could happen. This additional control set would have helped verify that nothing moved undesirably, and the set would be used in adjusting for thermal effects. However, consistency of the reference points, and points where zero deflection was expected showed that total station settling wasn't an issue. While the temperature was rising throughout the tests, the total time for span one tests was only an hour and a half, and the increase in temperature was low over this time. An increase in temperature is known to cause an increase in camber, (upward deflection at midspan) however very minimal thermal adjustments were required for these load tests (Merkle, 2004). Once these adjustments were complete, deflections were plotted as a function of distance from the west support.

5.4.2. Theoretical Modeling.

Individual Tee-Beam analysis was performed for each girder, breaking the full cross section into three individual tee-beams. This model was to find the theoretical pre-strengthening deflection from the load test. The loads used were from the truck weight tickets collected during the load tests. The truck geometry was verified in the field, and this geometry along with the truck stop diagrams were used to locate the wheel loads, which were assumed to act as point loads. The loads are shown in Table 5-1.

Table 5-1. Pre-Strengthening Load Test Axle Loads

	Weight (kips)		
Truck	Front Axle	Rear Axles	Total
A	13,900	24,280	38,180
B	14,180	24,020	38,200

Conversion factor: 1 kip = 4,448 N.

Two Tee-Beam models were made, first ignoring any contribution from the barrier walls and then adding their influence by estimating their stiffness contribution to

the interior and exterior girders. MoDOT distribution factors were used to distribute the wheel loads to each girder and calculate the maximum influence each girder may see from the trucks. The Tee-Beams were analyzed as simply supported structures. Assumptions were required for beam stiffness properties. It was assumed that each beam was uncracked, and the gross moment of inertia was used. The modulus of elasticity was approximated based on the field-measured compressive strength of the concrete, as per ACI 318.

Bridge P-0058 has a tight girder spacing relative to many other RC bridges. Additionally, span 1 has a transverse diaphragm at midspan. Both factors increase the transfer of load between the girders and help the span act as a unit. This transfer can allow girders in better condition (therefore stiffer) to attract more load and compensate for weaker girders. The degree at which the load is transferred is difficult to estimate without full knowledge of cracking, corrosion, and other deterioration. For the model considering the barriers, it was estimated that 25% of the stiffness of a barrier was transferred to the interior girder while the remaining 75% of the stiffness influenced the exterior girder closest to the barrier. Since there are barriers on each side, the interior girder was given 50% of a barrier added stiffness, with 25% coming from each side. The excel spreadsheets used to calculate theoretical deflections are included in Appendix G.

5.4.3. Results.

Figures 5-9 through 5-11 show the plotted deflections along the length of each girder for the pre strengthening load tests on span 1. These deflection data points are all from the total station readings during testing. The values at midspan were compared to LVDT deflection readings to verify the accuracy of the readings.

Figure 5-9 shows the results of stop 1, which overloaded the north side, placing the wheel lines very close to directly over girders 1 and 2. The span behaved as expected and girders 1 and 2 saw most of the influence. This stop had the highest deflection seen of any stop at 0.077 inches (2.0 mm). Based on visual inspection, girder 1 is in the worst condition due to spalling. The load test also suggests that girder 1 is in the worst condition of the three based on the highest observed deflection being from stop 1.

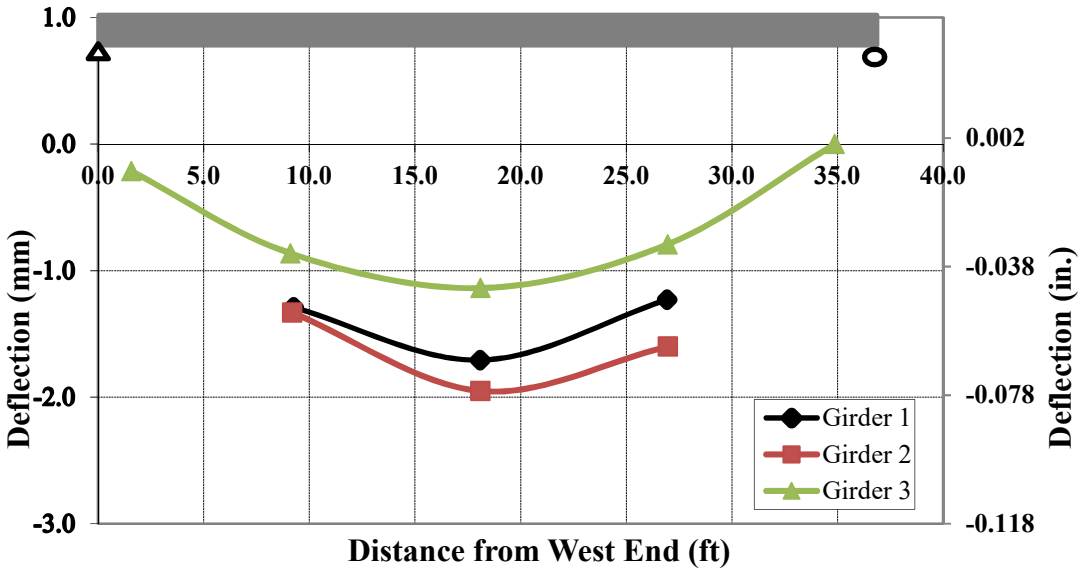

Figure 5-9. Span 1 Stop 1 Vertical Deflection

The results of stop two are shown in Figure 5-10. This stop had the trucks centered, straddling girder two. As expected, girder two deflected slightly more than the other two girders for this loading. Based on field measurements, the trucks were placed 4 inches (101.6 mm) south of being perfectly centered.

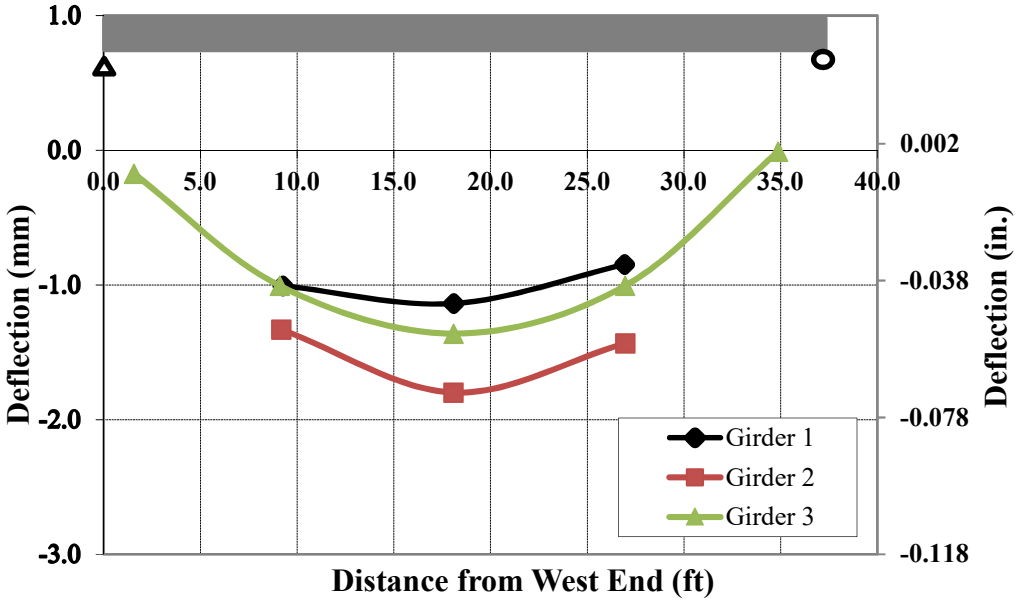

Figure 5-10. Span 1 Stop 2 Vertical Deflection

This lack of symmetry could have caused error in the results and could explain why girder 3 deflected more than girder 1 for this stop. Additionally, if girder 3 is in better condition than girder 1, then girder 3 would attract more load as the load is transferred transversely through the span.

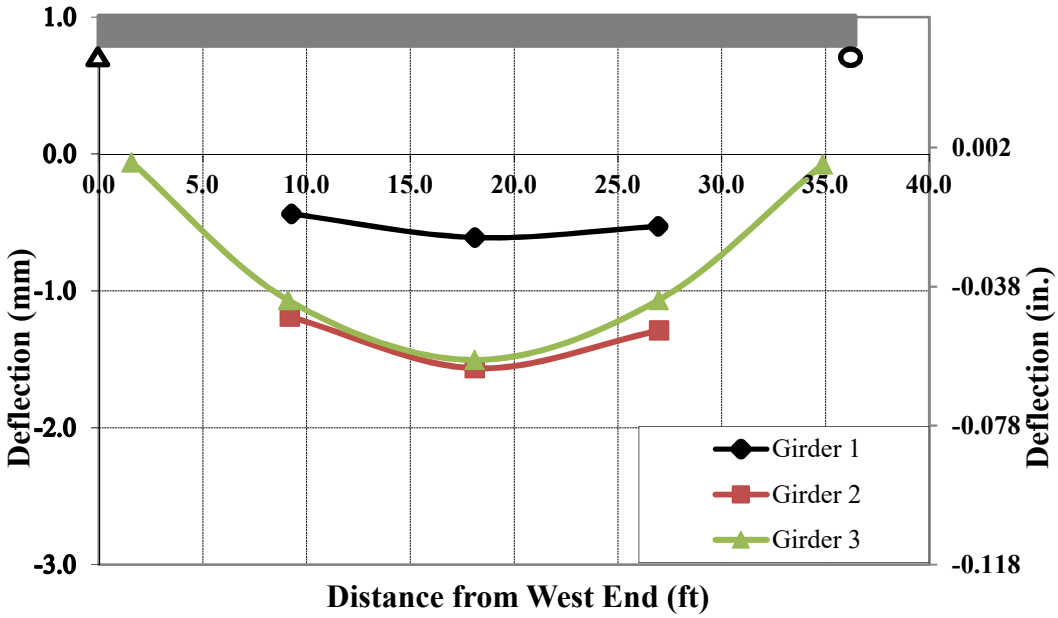

Figure 5-11. Span 1 Stop 3 Vertical Deflection

Stop 3, shown in Figure 5-11, overloaded the south of the bridge, with most of the weight over girders two and three. The results were as expected, with these overloaded girders having the highest deflection. Girder 1 had very little deflection from stop 3, which suggests that little load was transferred to it, as the other stiffer girders took the load.

Figures 5-12 through 5-17 show a comparison of the theoretical deflection models to the deflection values measured with the total station in the field. The plots are broken up by load test stop, as well as by interior and exterior girders.

The Tee-Beam analysis not considering the barriers predicted the maximum midspan deflection to be about 0.25 in. (6.3 mm) for the interior girder and about 0.28 in. (7.2 mm) for the exterior girders for each stop. These values are over 300% higher than any observed deflections. This model was overly conservative which suggests that the barrier walls and diaphragm have a large impact on the rigidity of the bridge working as a full unit.

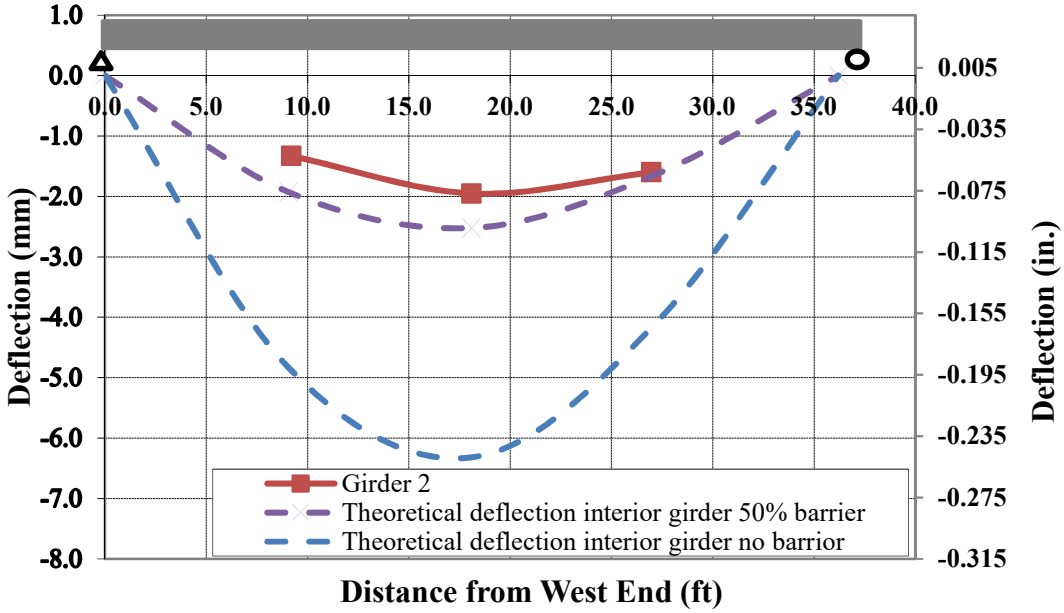

Figure 5-12. Span 1 Stop 1 Interior Girder Deflection Comparison

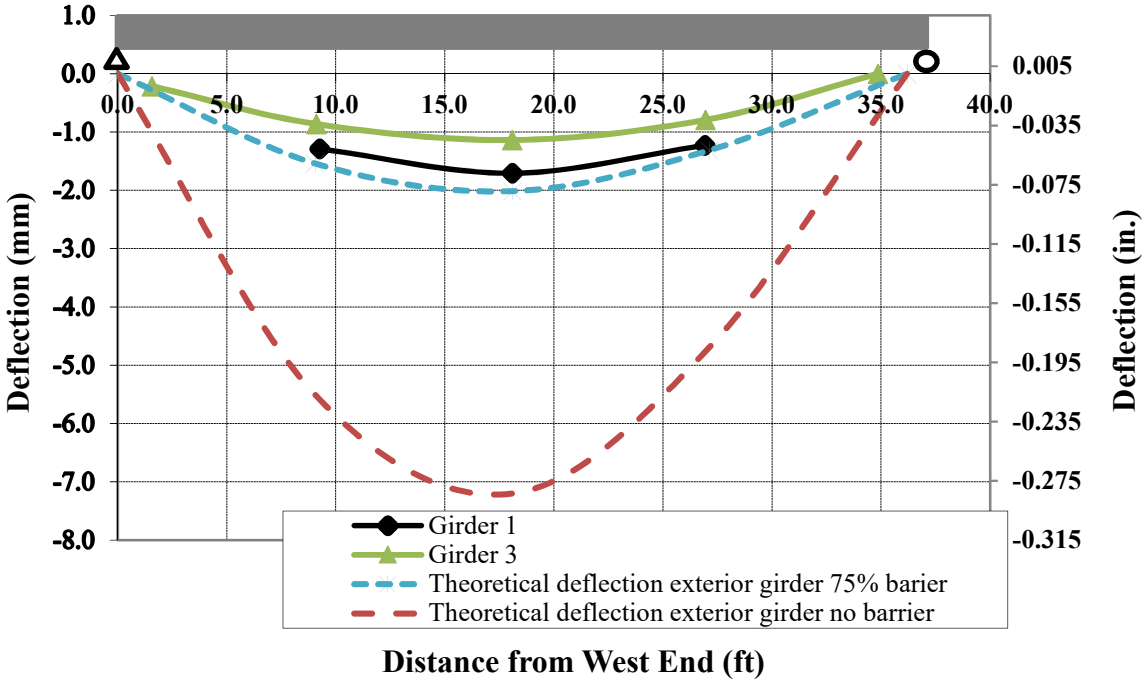

Figure 5-13. Span 1 Stop 1 Exterior Girder Deflection Comparison

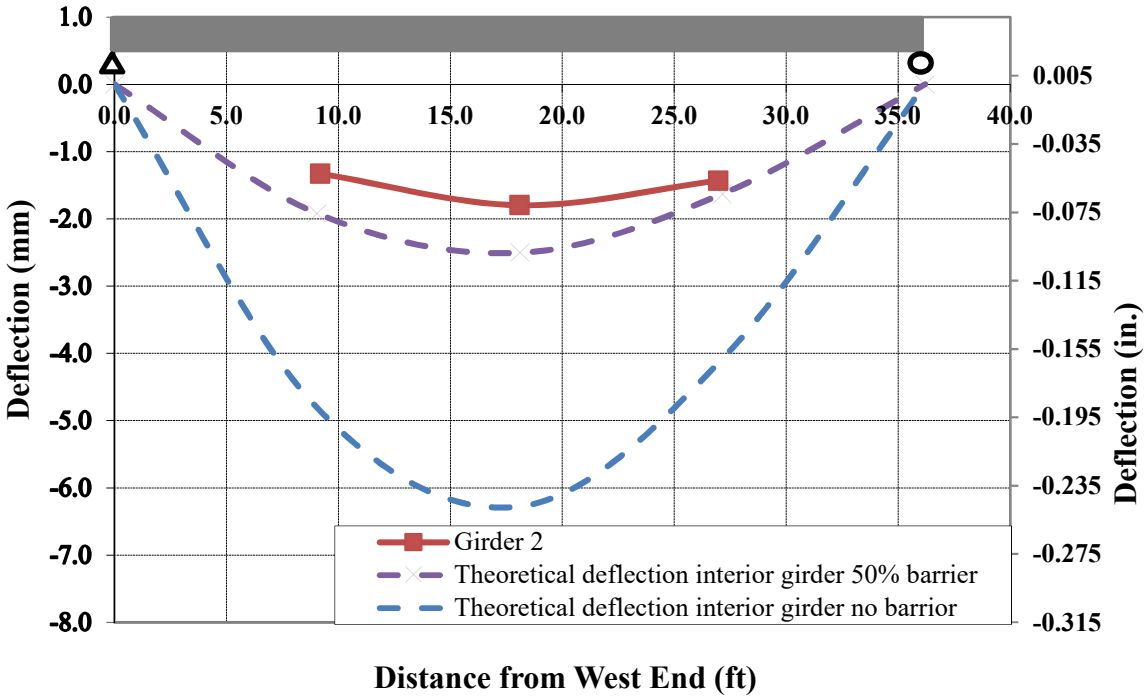

Figure 5-14. Span 1 Stop 2 Interior Girder Deflection Comparison

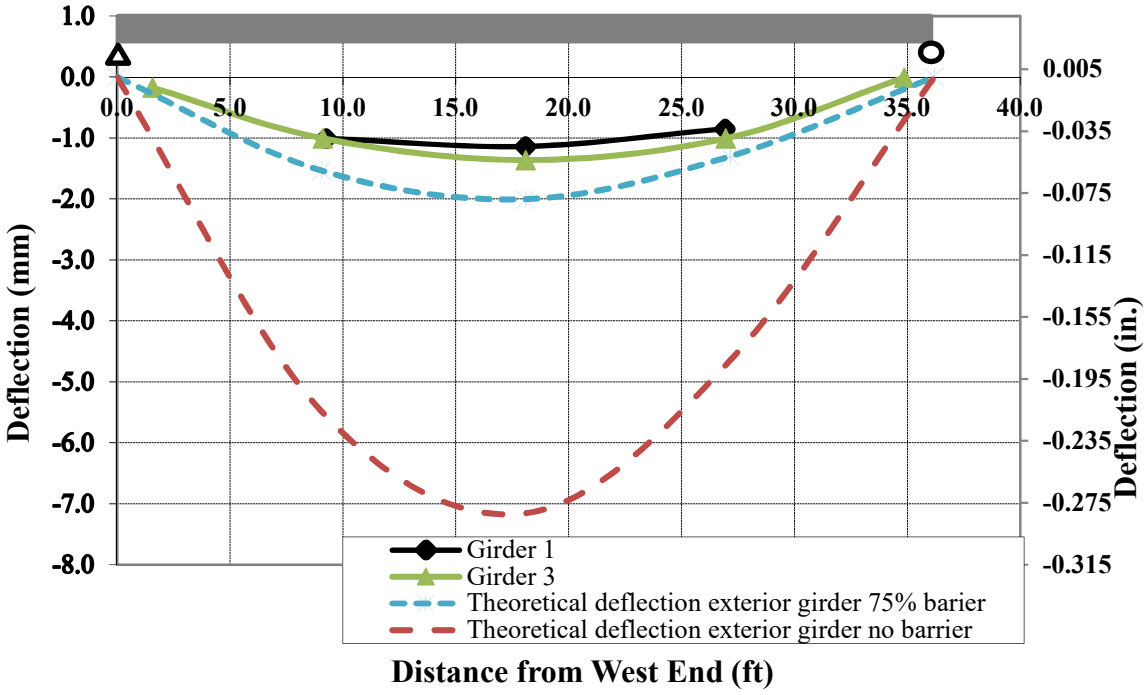

Figure 5-15. Span 1 Stop 2 Exterior Girder Deflection Comparison

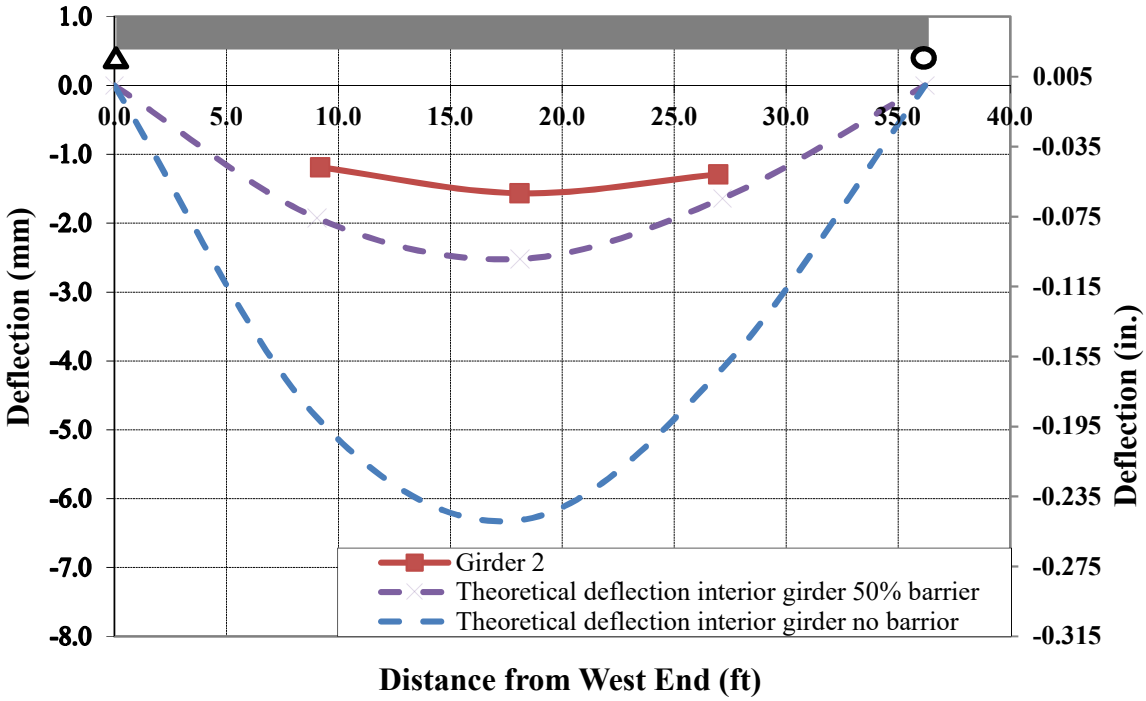

Figure 5-16. Span 1 Stop 3 Interior Girder Deflection Comparison

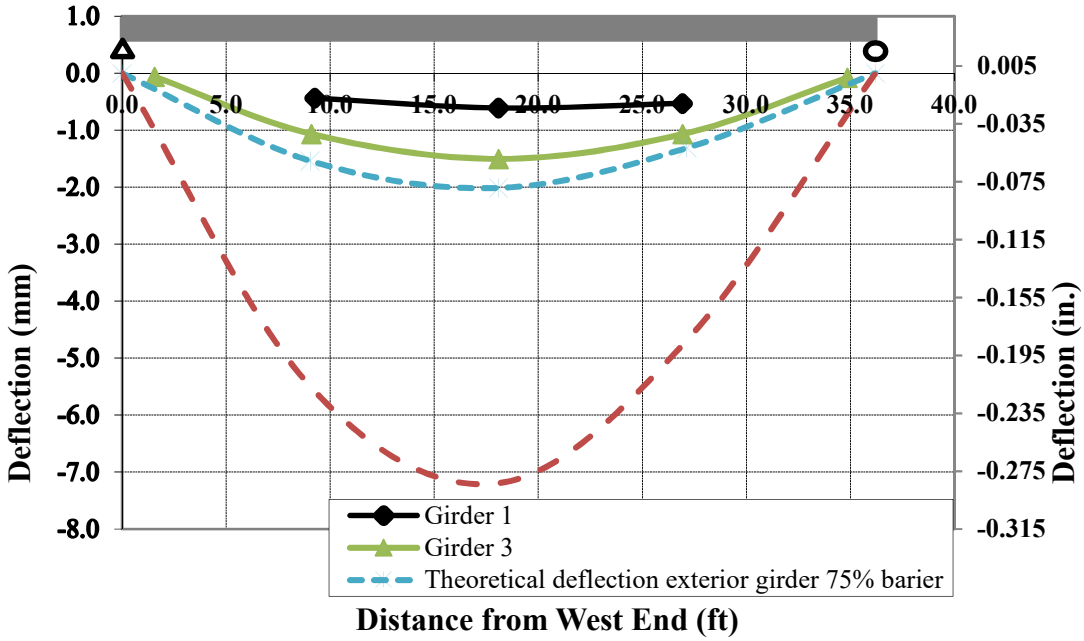

Figure 5-17. Span 1 Stop 3 Exterior Girder Deflection Comparison

The Tee-Beam analysis considering the barrier walls predicted the maximum deflection at midspan to be about 0.10 in. (2.5 mm) for the interior girder and about 0.08 in. (2.0 mm) for the exterior girders for each stop, which range from 18% to 80% higher

than the observed midspan deflections. With the estimated barrier wall stiffness contributions added, the model was still conservative. One potential contributing factor to the model being conservative is that the modulus of elasticity of the concrete was calculated based off of a conservative estimate of the concrete compressive strength, whereas these in situ properties may be higher. Regardless of how conservative the Tee-Beam analysis estimates were, the deflection results of the pre-strengthening load test showed that the girders are in good condition.

5.5. LOAD TESTING RESULTS PRIOR TO STRENGTHENING

During the static load tests, midspan's vertical deflections were recorded with LVDTs. The load distribution factor of the interior and exterior RC beams was estimated as follow (Hernandez & Myers, 2019):

$$LDF_i = n\frac{\delta_{Gi}}{\sum_{i=1}^{k}\delta_{Gi}} \tag{5.1}$$

where LDF_i = load distribution factor of *ith* girder obtained from field deflections; δ_{Gi} = vertical deflection of the *ith* girder at midspan; n = number of lanes loaded = 1; and k = number of girders. The experimental load distribution factors (LDF) that were employed to enhance the rating factor of Bridge P0058 are reported in Table 5-2

5.6. BRIDGE EVALUATION PRIOR TO STRENGTHENING

The rating factor of a bridge component can be estimated analytically using the AASHTO LFR approach (AASHTO 1994) in the following manner:

$$RF = \frac{M_n - A_1 M_D}{A_2 M_L (1+I) DF} \tag{5.2}$$

where RF = rating factor; M_n = nominal moment capacity; M_D = dead load moment; M_L = live load moment effect caused by the rating vehicle (HS20 truck); I = impact factor = $50 / (3.28L+125)$; L = span length (m); DF = distribution factor; A_1 and A_2 = factors for dead and live load, respectively. A_1 = 1.3 (operating and inventory levels); A_2 = 1.3 (operating level); and A_2 = 2.16 (inventory level). Some calculations are omitted for the sake of brevity. The LDF values are reported in Table 5-2. The values of the live load moment (M_L) were determined using the AASHTO LFD HS20 rating loading (inventory and operating levels).

Table 5-2. Midspan load distribution factor (LFD)

Span	LDF_1	LDF_2	LDF_3
1	0.38	0.39	0.23
1	0.28	0.41	0.31
1	0.22	0.40	0.38

Table 5-3 summarizes the analytical and experimental data used to determine the rating factor of the bridge.

Table 5-3. Analytical moments (span 1)

Parameter	Interior Girder	Exterior Girder
M_D (kN-m)	267.5	227.8
M_L (kN-m)	377.4	253.9

The experimental compressive strength reported in Table 5-4 was obtained using the Rebound Test (Schmidt Hammer) according to ASTM C805 (ASTM 2018). Analytical distribution factors were determined using the AASHTO Bridge Standard Specifications (AASHTO 2002) and following Art 3.23.2.2 [3] (footnote f). In addition, Table 5-4 presents the analytical and experimental rating factors.

Table 5-4. Bridge load rating

Parameter	Interior Girder (Span 1)	Exterior Girder (Span 1)
Analytical		
DF	1.153	0.776
f'c	21.0	21.0
M_n (kN-m)	719.7	706.8
Experimental		
DF	0.41	0.38
f'_c (MPa)	41.3	41.3
M_n (kN-m)	736.05	729.6
Analytical Rating Factor		
Inventory	0.45	0.75
Operating	0.76	1.24
Experimental Rating Factor		
Inventory	0.67	0.80
Operating	1.11	1.34

Similar to results reported by (Hernandez and Myers, 2018b), it was demonstrated that by using field data, the current load rating obtained following the AASHTO LFR procedure could be enhanced. However, the higher experimental load rating was not large enough to remove the load posting of the bridge, and consequently, the strengthening of the bridge was recommended to increase is flexural load capacity.

6. SUMMARY AND CONCLUSIONS

6.1. SUMMARY

The objective of this study was to validate cementitious composite systems for strengthening of RC in the field. Bridge P0058 in Howell County, Missouri was chosen from a list of structurally deficient candidate bridges to be the site for the demonstration of four composite strengthening systems. The systems used are FRP with carbon fibers, FRCM with carbon, FRCM with PBO, and SRG.

The original bridge design was reviewed, and geometry was verified in the field. Field measurements of the concrete compressive strength showed a significant increase. Each cross section was reanalyzed with this increase in compressive strength to obtain the pre-strengthening capacity.

A parametric study was completed to see which systems performed most efficiently on longer spans, and to observe the effect of adding additional plies of each system. From this study, a final design was chosen with each strengthened beam being enhanced by a minimum of 4% in flexure and 11% in shear. Each design followed the guidelines of ACI 440.2R-08 and ACI 549.4R-13 as applicable.

A pre-strengthening field load test was completed to obtain a baseline of the responses for comparison later on. Deflection data from static test stops were presented and will be used for comparison with future load tests.

This project showed that cement based composite strengthening systems are a viable technology for future use.

A pre-strengthening load test was successfully performed on the superstructure of Bridge P0058 to obtain an experimental load rating of the bridge's superstructure. The data collected experimentally enhanced the load rating obtained analytically according to the AASHTO LFR procedure. However, the experimental load rating was not large enough to remove the load posting of the bridge.

The strengthening systems proposed in this study helped validate cementitious composite systems for strengthening of RC members in the field. A parametric study was executed to compare the theoretical performance of the different strengthening systems. This study demonstrated that cement based composite strengthening systems are a viable

technology for field infrastructure applications. This project is the first planned field implementation of cement based strengthening systems that the authors are aware of in the US.

6.2. FINDINGS AND CONCLUSIONS

The design and installation process lead to several conclusions regarding field strengthening of bridge girders. The parametric study included in the design phase gave valuable comparisons in the theoretical performance of the four systems.

- If one equal width ply of each system is installed on four identical girders, Carbon FRP has the highest theoretical moment capacity increase, followed by carbon FRCM, then PBO FRCM, and finally SRG.
- All four systems are more efficient on the shorter spans, which have a shallower section containing less steel reinforcement.
- When comparing the capacity gained by adding the same area of fibers added to the deeper and shallower cross sections, the average added capacity was 18% higher on the shallow than the deep section for SRG. This is low compared to the other systems, which had increases of 60% for PBO, 83% for C-FRCM, and 74% for CFRP. While carbon FRP and Carbon FRCM were most impacted by the span length, their higher efficiency overall made them the best choice for strengthening the long spans.

The load tests also presented valuable information about the condition of the bridge. The girders are in good condition overall, especially when compared to the theoretical maximum midspan deflection values calculated using Tee-Beam Analysis. The load tests also suggested that girder 1 is the most damaged of the span 1 girders, which agreed with the visual inspection done during site visits.

It is anticipated that field installation will produce comparisons in the feasibility of each type of system for strengthening existing bridges. These expected findings are based on the specific strengthening systems chosen, and the conditions in which they were installed.

- Field application was successful for all four systems. This project is the first documented field implementation of cement based strengthening systems for

research. The study demonstrated that cementitious systems are easier to work with in the field than systems using epoxy or other resins. When installation takes place in late summer, the cementitious matrix is much less effected by, and easier to work with in the high heat.

- A durability study area was created, so that pull off tests can later show how the bonding of the systems have held up over time exposed to field conditions.
- A long-term study of the performance of these systems was created. The Missouri Department of Transportation has agreed to allow the bridge girders to be brought to Missouri S&T once the bridge is decommissioned in approximately in 3 to 4 years. This will allow for future studies discussed further in Section 6.4.

A long-term load testing study was also started by this project. Future load tests intended to be conducted about twice a year will show the increase in stiffness from the strengthening. The repeated tests will also capture potential loss of stiffness over time exposed to the environment.

6.3. RECOMMENDATIONS

This study showed that FRCM and SRG systems are a viable alternative to FRP and externally bonded steel systems but taught some factors that are important for consideration. When deciding if strengthening is the best choice for a bridge, it is important to check for access for lifts. With the naturally rough, rocky surface of a creek bed, it can be difficult to get equipment under the girders and it is labor intensive to set up scaffolding.

This study also showed the importance of preparatory work before starting the installation. Field cuts are difficult to make accurately, so precise measurement and cutting should be done before bringing materials on site. This is extra critical for SRG systems, since bends for U-wraps requires equipment that cannot be easily transported to the field.

6.4. CURRENT AND FUTURE FIELD DURABILITY STUDIES

A total of nine beam specimens (Figure 6-1) have been fabricated to evaluate the long-term behavior behavior of two strengthening systems. The systems that were selected to perform this study include the PBO and SRG strengthening techniques. Table 6-1 presents a summary of the test matrix employed and the age at which the specimens will be tested to failure. A set of three specimens, including a control beam (no strengthening system), a beam strengthened with SRG, and beam strengthened with PBO will be tested at the beginning of February 2020. Additional tests will be performed on two more sets of beams (three beams per set as listed on Table 6-1) after three and five years of field exposure.

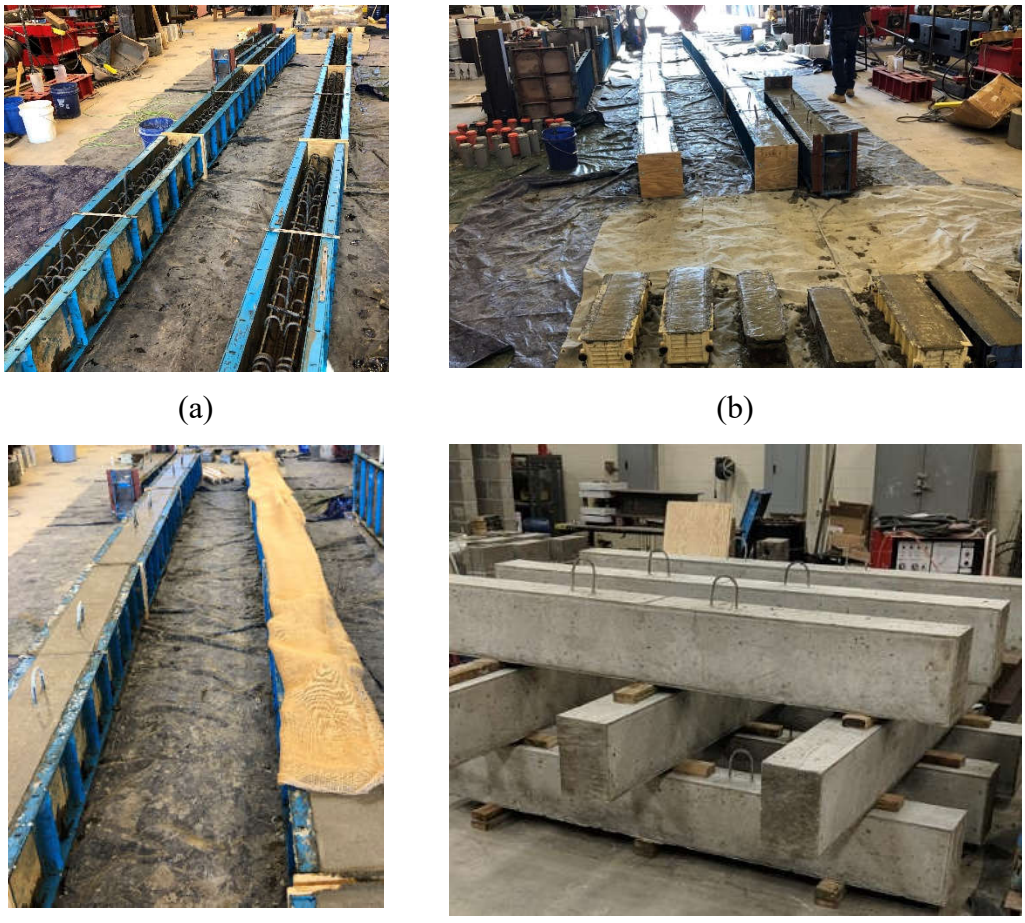

(a) (b)

(c) (d)

Figure 6-1. Fabrication of Beam Specimens. (a) Formwork; (b) Concrete Placement; (c) Curing; (d) Storage

The specimens, have been placed in an exterior environment on the S&T campus for a multi-year investigation, will be used to show the actual ultimate strength and durability after multiple years of field exposure. In addition, it is expected to show that the predictions of ultimate strength estimated using ACI 549 are conservative to evaluate the flexural behavior.

Table 6-1. Test Matrix for Strengthening System (Bending Test)

Specimen ID	Environmental Condition	Number of Plies	Strengthening System	Exposure Time
BC-1	NE	0	Control	NA
BC-2	NE	0	Control	3 years
BC-3	NE	0	Control	5years
BS-1	NE	2	SRG	NA
BS-2	NE	2	SRG	3 years
BS-3	NE	2	SRG	5years
BP-1	NE	2	PBO	NA
BP-2	NE	2	PBO	3 years
BP-3	NE	2	PBO	5years

NE: Field Exposure (Outside the Lab). BC: Control Beam. BS: Beam Strengthened with SRG System. BP: Beam Strengthened with PBO System.

Figure 6-1 illustrates the fabrication, curing and storing previous to strengthening of the nine beam specimens. Additional, specimens (Figure 6-2) that include thirty 4-in. by 8-in cylinders and eight MOR beams were fabricated. The MOR specimens will be used to evaluate the long-term bonding response of the chosen strengthening systems (PBO and SRG) after being field exposed. Figure 6-3 and Figure 6-4 illustrate the strengthening procedure of the beams using the SRG and PBO system, respectively. Figure 6-5 presents the flexural test setup that will be used to test the beam specimens to failure. Figure 6-5(b) shows details of the steel reinforcement used to fabricate the specimens.

(a)

(b)

Figure 6-2. Additional Specimens. (a) Compressive Strength; (b) Bond Test Specimens

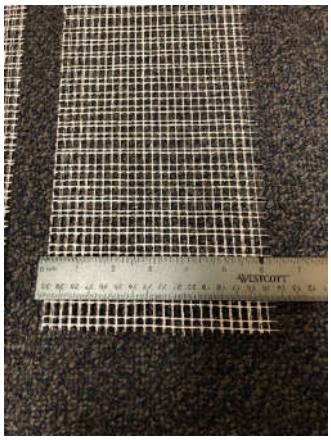

(a)

(b)

(c)

(d)

Figure 6-3. Beam Strengthening with SRG System; (a) SRG Preparation; (b) Surface Preparation (Sand Blasting); (c) Mortar Impregnation (First Layer); (d) Beam Strengthening Completed

(a)

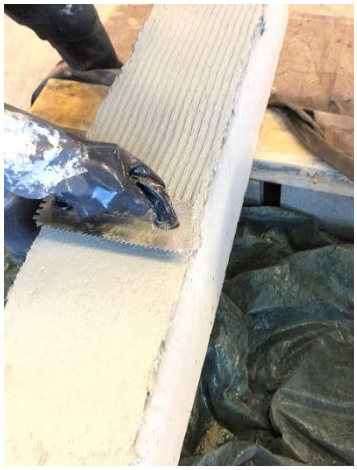

(b)

(c)

(d)

Figure 6-4. Beam Strengthening with PBO System; (a) PBO Preparation; (b) Application of First Layer of Mortar; (c) Application of First PBO Ply; (d) Mortar Impregnation (First Layer); (e) Application of Second PBO Ply (f) Beam Strengthening Completed

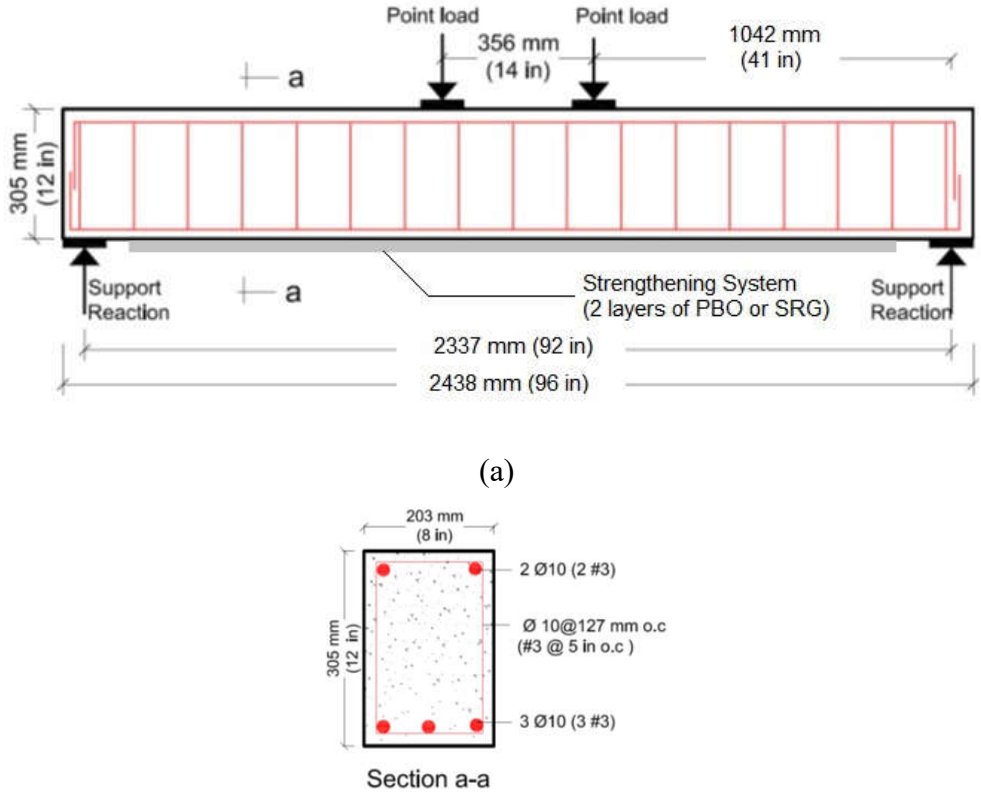

Figure 6-5. Experimental Program. (a) Beam Elevation; (b) Beam Cross Section

The Missouri Department of Transportation has indicated that Bridge P0058 is likely to decommissioned for a new bridge replacement in the coming 4-5 years. The strengthening systems have been designed with the hopes of being able to do destructive testing once the bridge is out of service. The intent is to saw cut the deck of each span to create three large Tee beams that could be transported to the Missouri S&T SERL. Once on campus, the six strengthened girders can be tested to failure to show the actual ultimate strength after field installation and several years of field exposure. This is expected to show that the predictions of ultimate strength of ACI 440 and ACI 549 are conservative. This project will be a unique and valuable study of girders that are strengthened in the field, and then exposed to actual service conditions.

The six unstrengthened girders will provide control for comparison, as well as give the ability to strengthen some in the lab to gain additional data. Potential studies include:

1. Using more plies of reinforcement.
2. Different shear wrapping schemes, including changing the angle of orientation.
3. Strengthening systems that use mechanical anchorage.
4. Using new emerging strengthening systems.

APPENDIX A.
MODOT DESIGN DRAWINGS

MISSOURI STATE HIGHWAY DEPARTMENT

FED. ROAD DIST. NO.	STATE	FED. AID PROJ. NO.	FISCAL YEAR	SHEET NO.	TOTAL SHEETS
5	MO.	S-938(2) Sec. A(50)	19		

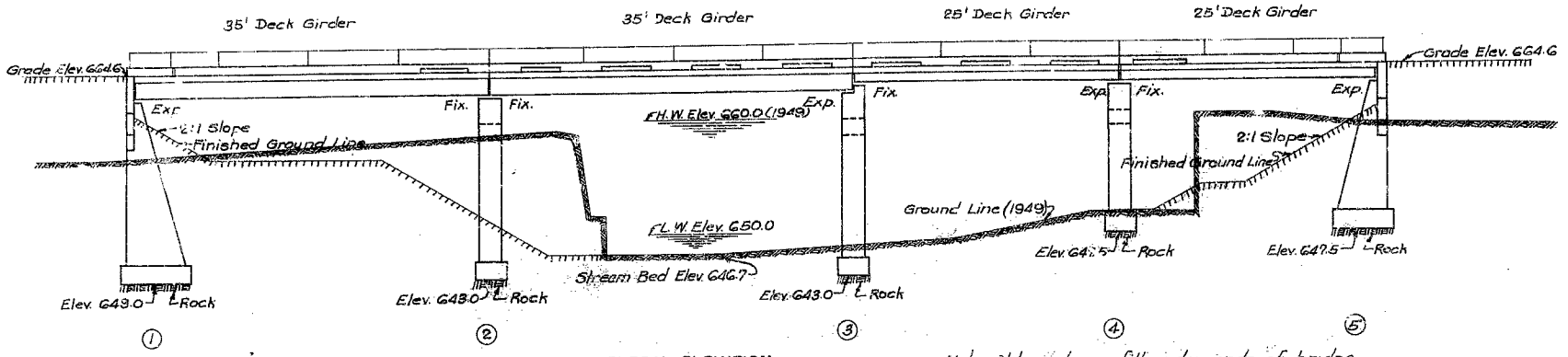

GENERAL ELEVATION

Note: All loose, shelly or disintegrated rock shall be removed and the footings placed on hard, solid undisturbed rock. If soft rock or shale is encountered the footings shall be carried at least 18" into and cast against vertical faces of same. In no case shall footings of Bents No. 2, 3 and 4 be placed higher than elevations shown.

Note: Old roadway fill under ends of bridge shall be removed to natural ground line.
Payment for this excavation outside limits of excavation for structure will be made at unit contract price for Roadway Excavation.

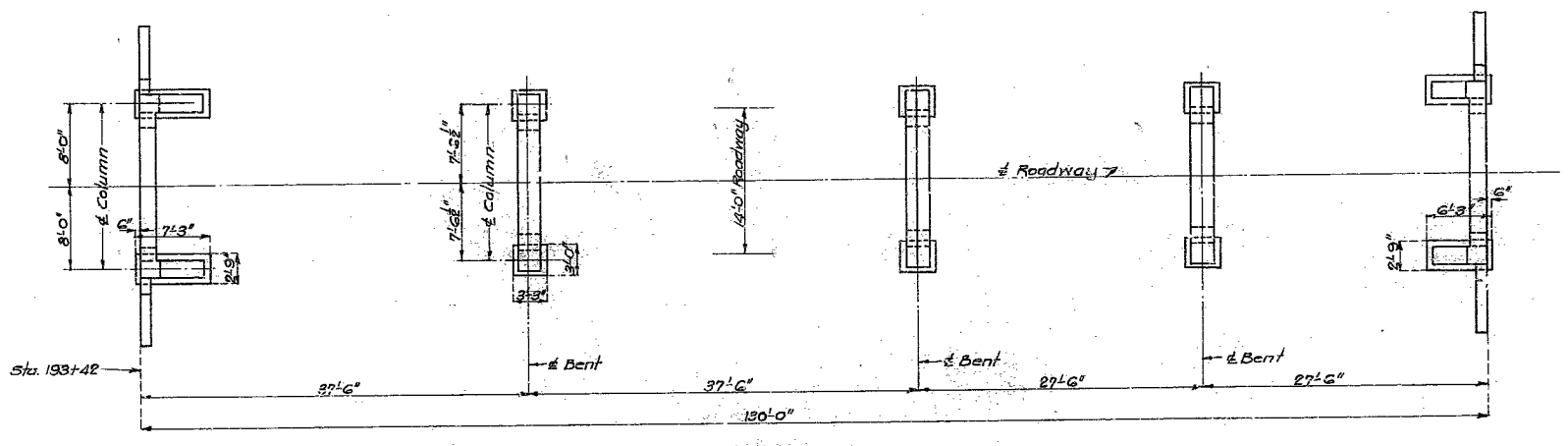

PLAN

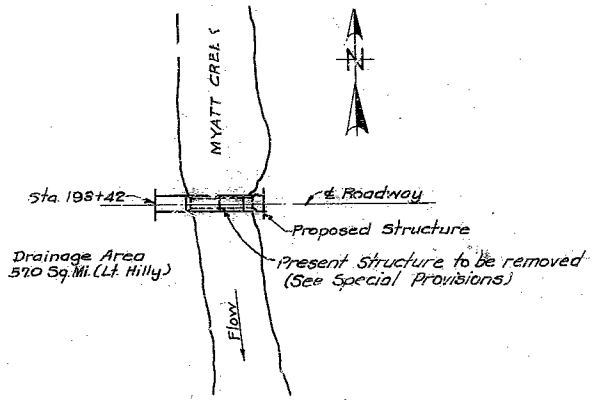

LOCATION SKETCH

ESTIMATED QUANTITIES

Item		Substr.	Superstr.	Total
Class 1 Excavation for Structures	Cu. Yds.	60		60
Class 2 Excavation for Structures	Cu. Yds.	100		100
Class "B" Concrete (Handrail)	Cu. Yds.		11.0	11.0
Class "B" Concrete (Except Handrail)	Cu. Yds.	61.1	83.9	145.0
Reinforcing Steel	Lbs.	6950	25110	32060
Structural Steel Bearing Plates	Lbs.		1650	1650

Note: Excavation for bridge made above Elev. 651.0 will be paid for as Class 1 Excavation for Structures.
Excavation for bridge made below Elev. 651.0 will be paid for as Class 2 Excavation for Structures.

COMPLETE BILL OF SUBSTRUCTURE REINFORCING STEEL

No	Size	Length	Mark	Location
End Bents No. 1 & 5				
28	¾" sq.	5'-3"	D1	Footing
16	¾" sq.	8'-0"	F1	Haunch
12	¾" sq.	17'-6"	H1	Beam
4	1" sq.	19'-6"	H2	Bm. Bl. #9
4	¾" sq.	17'-6"	H3	" " "
16	¾" sq.	12'-3"	H4	Wing
4	¾" sq.	19'-6"	H5	Bm. Bl. #5
8	¾" sq.	11'-6"	H6	Wing
6	¾" sq.	11'-9"	T1	"
8	¾" sq.	12'-6"	T2	"
18	¾" sq.	10'-3"	U1	Beam
18	¾" sq.	8'-8"	U2	"
10	¾" sq.	8'-6"	V1	Wing
6	¾" sq.	17'-6"	V2	Col. Bl. #7
8	¾" sq.	17'-0"	V3	" " #7
8	¾" sq.	11'-9"	V4	" " #7
24	¾" sq.	14'-0"	V5	" " #7
8	¾" sq.	12'-9"	V8	Col. Bl. #5
6	¾" sq.	13'-0"	V9	" " #5
16	¾" sq.	12'-9"	V10	" " #5
8	¾" sq.	7'-8"	V11	" " #5
6	¾" sq.	12'-3"	T3	Wing Bl. #5
18	¾" sq.	10'-9"	U6	Bm. Bl. #5
Int. Bents 2, 3 & 4				
48	¾" sq.	5'-3"	D1	Footing
24	¾" sq.	8'-0"	F1	Haunch
6	1" sq.	19'-8"	G1	Girder Bl. #9
9	¾" sq.	18'-9"	G2	" " " #9
6	1" sq.	18'-9"	G3	Bm. Bl. #4
6	¾" sq.	16'-9"	G4	" " "
2	¾" sq.	16'-8"	G5	Bm. Bl. #3
5	1" sq.	19'-8"	G6	" " "
51	¾" sq.	9'-9"	U3	Beam
18	¾" sq.	3'-0"	U4	"
28	¾" sq.	2'-0"	U5	Bm. Bl. #3
32	¾" sq.	17'-0"	V6	Col. Bl. #9
70	¾" sq.	8'-3"	V7	" " "
16	¾" sq.	12'-9"	V12	Col. Bl. #4

BAR SIZE EQUIVALENTS	
#2 = ¼" Rd.	#7 = ⅞" Rd.
#3 = ⅜" Rd.	#8 = 1" Rd.
#4 = ½" Rd.	#9 = 1" Sq.
#5 = ⅝" Rd.	#10 = 1⅛" Sq.
#6 = ¾" Rd.	#11 = 1¼" Sq.

Bending Sketches & Cutting Diagrams

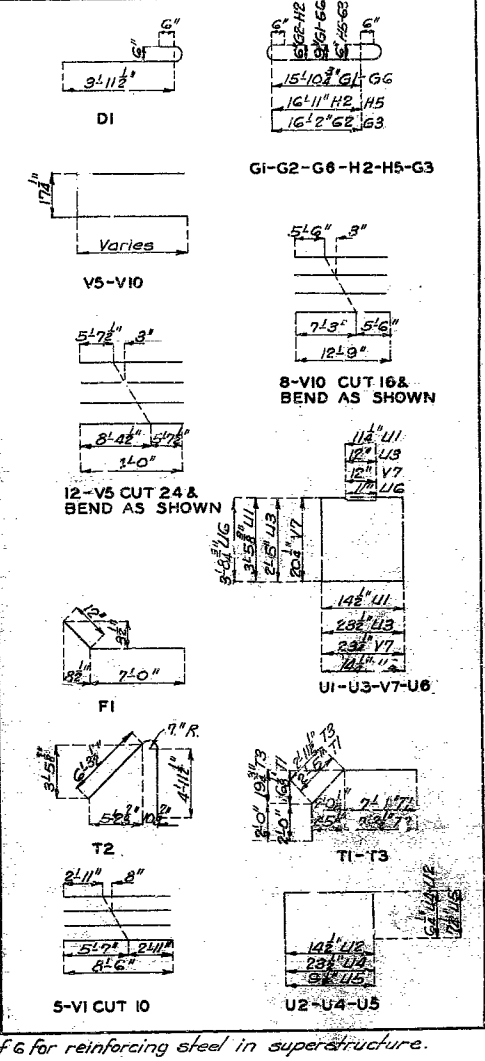

Note: See Sheets No. 4 and 5 of 6 for reinforcing steel in superstructure.

GENERAL NOTES:

Design Specifications A.A.S.H.O. 1949
Loading H10-44
Reinforcing Steel Stress 18,000#/a"
Class "B" Concrete Stress 1,000#/a"
All concrete shall be Class "B"
Where Joint Filler is specified on plans it shall conform with the requirements of Section 38-194 (1) h of the Standard Specifications for Premoulded Material for Filler.

B.M. Elev. 657.48 N.1.P.P. 162' Lt. Sta. 193+60

BRIDGE OVER MYATT CREEK

STATE ROAD FROM LANTON EAST TO ORECON CO. LINE.
ABOUT 12.3 MILES W. OF THAYER.
PROJECT NO. S-938(2)SEC.A (50) STA. 193+42

HOWELL COUNTY

FINISHED

SUBMITTED BY W. W. Emalon DATE 6/5/1951 BRIDGE ENGINEER
APPROVED BY C. W. Brown DATE 6/5/1951 CHIEF ENGINEER

FINISHED STD. C-8009
FINISHED STD. C-110 R3
P-58

Drawn Nov. 1950 by W.L.W.
Traced Dec. 1950 by M.E.L.
Checked Feb. 1951 by C.S.A.

Note. This drawing is not to scale. Follow dimensions.

SEE FINAL PLANS BROWN-LINES

106

"IMPERIAL" TYPING CLOTH, U. S. Blue, Chicago

2.

MISSOURI STATE HIGHWAY DEPARTMENT

F. ROAD DIST. NO.	STATE	FED. AID PROJ. NO.	FISCAL YEAR	SHEET NO.	TOTAL SHEETS
5	MO.	S-933(2) Sec.A(SO)	19		

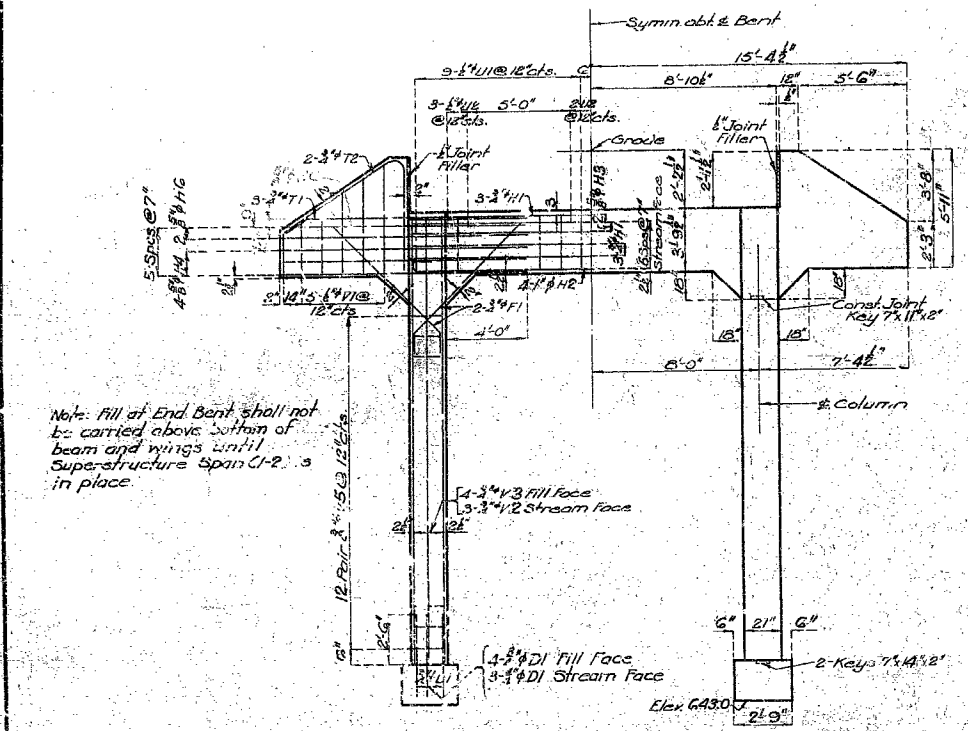

ELEVATION

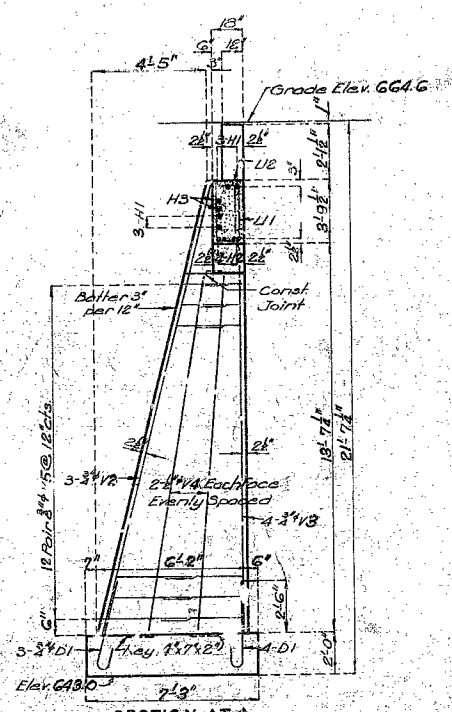

SECTION AT ℄

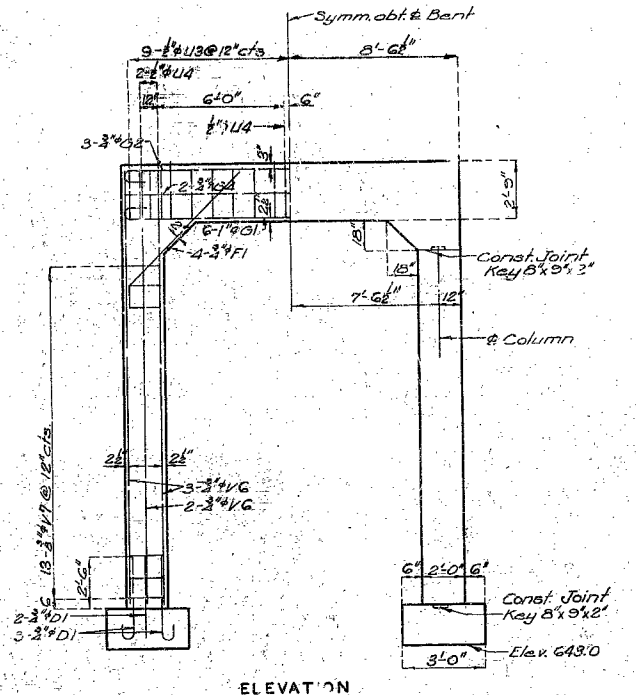

ELEVATION

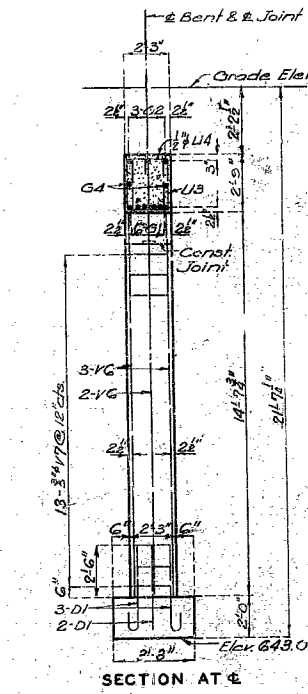

SECTION AT ℄

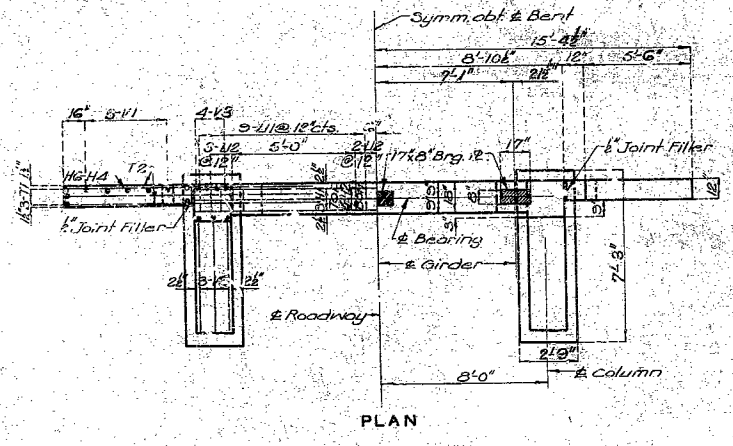

PLAN

DETAILS OF END BENT NO. 1

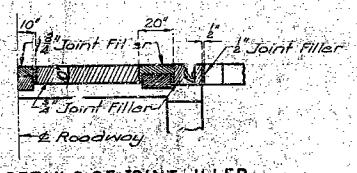

DETAILS OF JOINT FILLER AT END BENTS

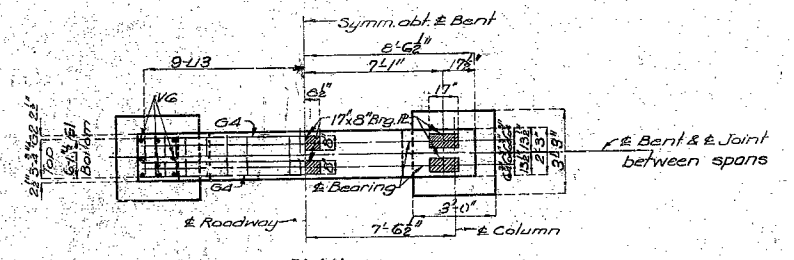

PLAN

DETAILS OF INTERMEDIATE BENT NO. 2

107

Drawn Nov. 1950 by W.L.W.
Traced Nov. 1950 by M.E.L.
Checked Feb. 1951 by C.S.B.

Note: This drawing is not to scale. Follow dimensions.

Sheet No. 2 of 6

BRIDGE OVER MYATT CREEK

STATE ROAD FROM LANTON EAST TO OREGON CO. LINE
ABOUT 12.3 MILES W. OF THAYER
PROJECT NO. S-933(2) SEC.A (SO) STA. 193+42

HOWELL COUNTY

FINISHED

FINISHED

FINISHED

P-58

MISSOURI STATE HIGHWAY DEPARTMENT

FED. ROAD DIST. NO.	STATE	FED. AID PROJ. NO.	FISCAL YEAR	SHEET NO.	TOTAL SHEETS
5	MO.	S-938 (2) Sec A(SO)	19		

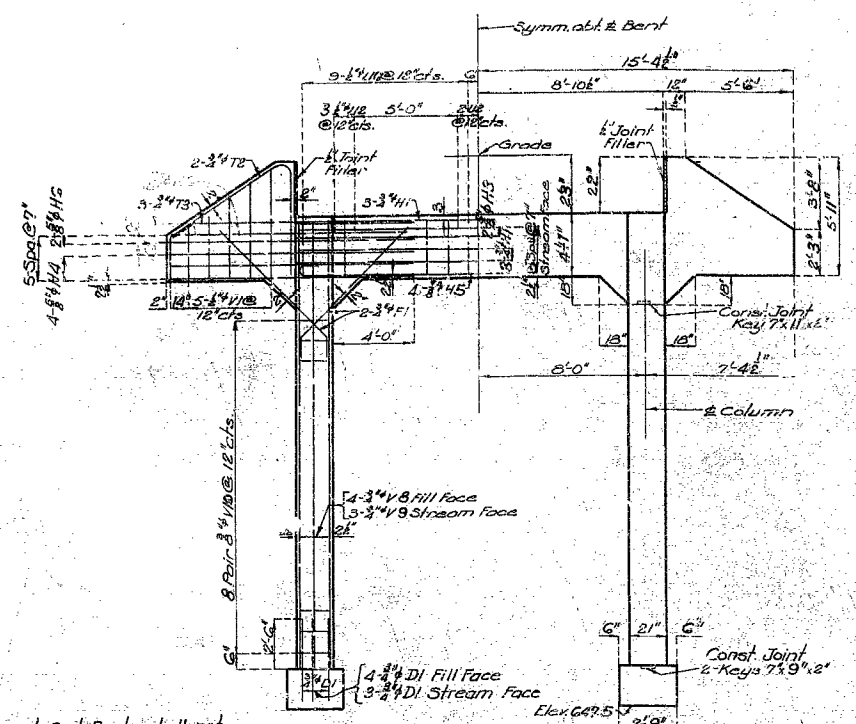

ELEVATION

No fill at End Bents shall not be carried above bottom of beam and wings until superstructure Span (4-5) is in place.

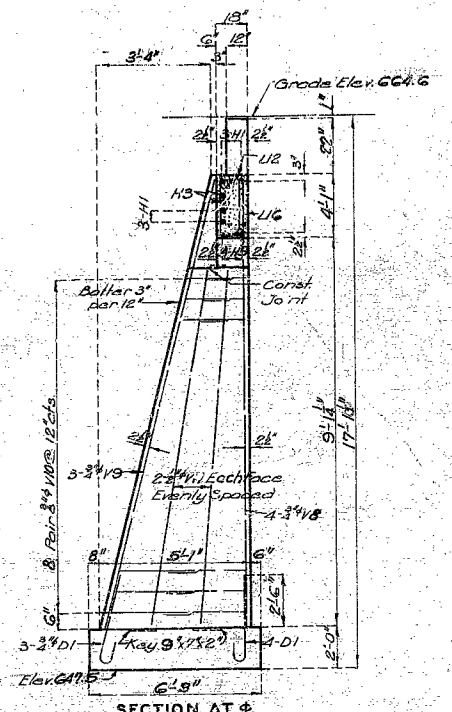

SECTION AT ℄

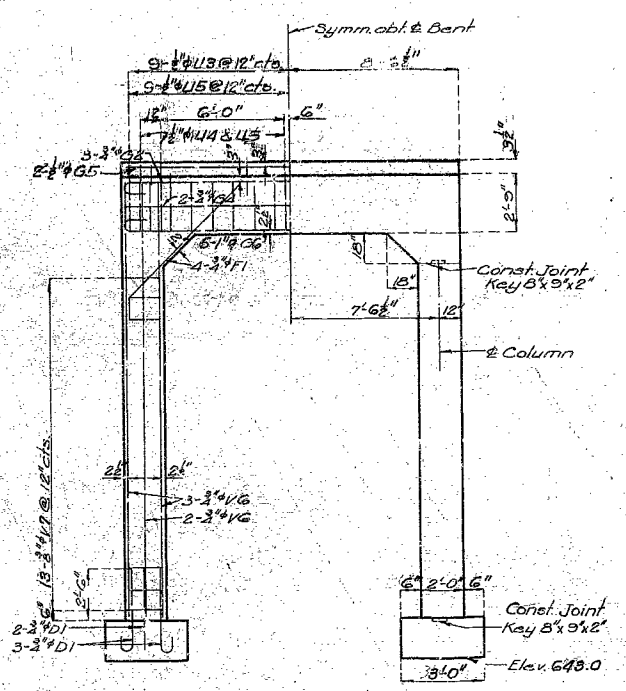

ELEVATION

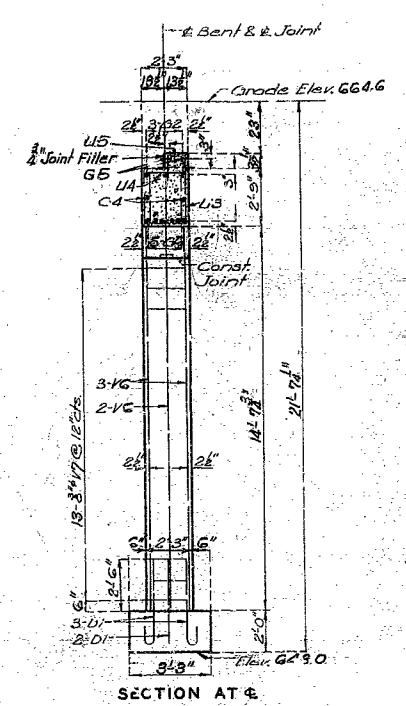

SECTION AT ℄

DETAILS OF INTERMEDIATE BENT NO. 3

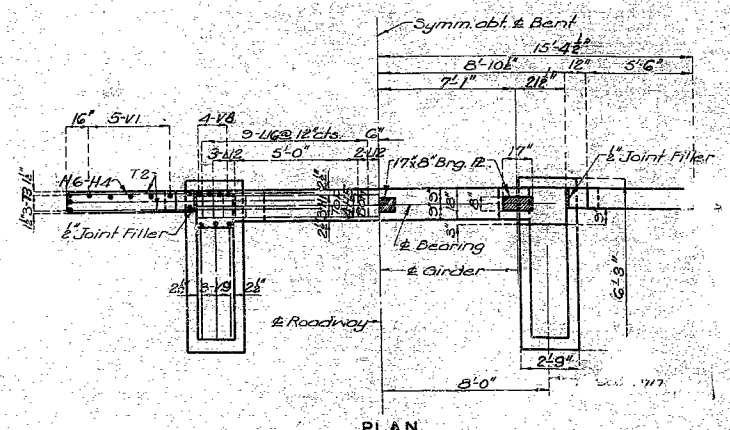

PLAN

DETAILS OF END BENT NO. 5

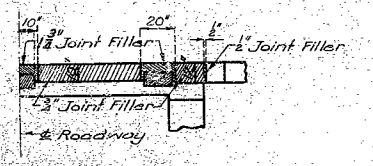

DETAILS OF JOINT FILLER AT END BENTS

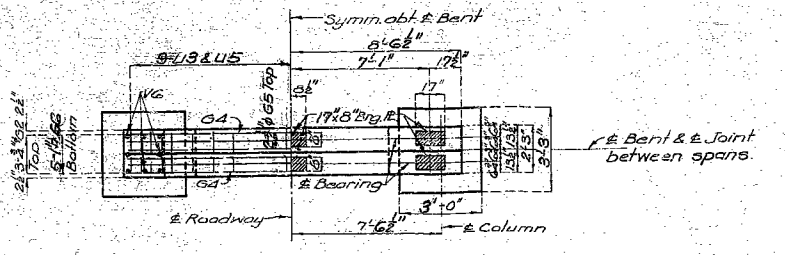

PLAN

DETAILS OF INTERMEDIATE BENT NO. 3

BRIDGE OVER MYATT CREEK

STATE ROAD FROM LANTON EAST TO OREGON CO. LINE.
ABOUT 12.3 MILES W. OF THAYER
PROJECT NO. S-938(2) SEC. A (SO) STA. 193+42

HOWELL COUNTY

FINISHED

FINISHED

FINISHED

P-58

108

Drawn Nov. 1950 by W.L.W.
Traced Nov. 1950 by M.E.L.
Checked Feb. 1951 by C.S.A.

Note: This drawing is not to scale. Follow dimensions.

Sheet No. 3 of 6

SEE FINAL PLANS FOR WING LINES

MISSOURI STATE HIGHWAY DEPARTMENT

FED ROAD DIST NO	STATE	FED AID PROJ NO	FISCAL YEAR	SHEET NO	TOTAL SHEETS
5	MO	S-938(2) Sec A (SO)	19		

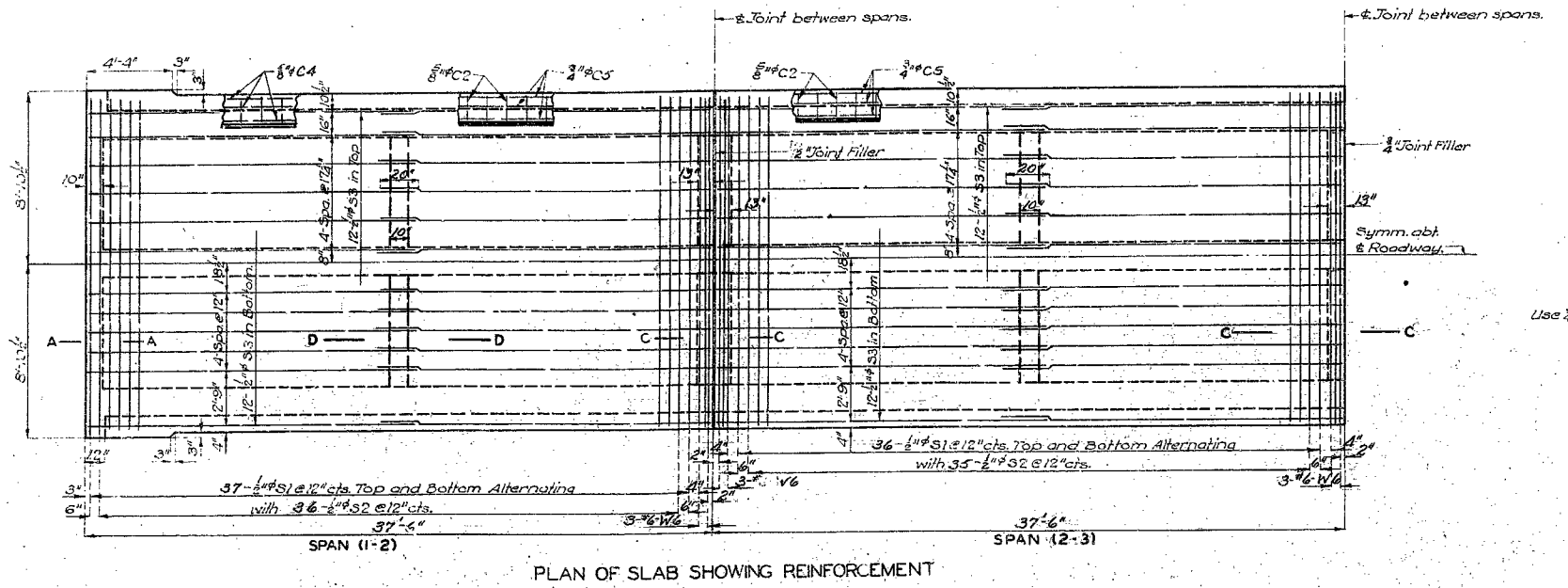

PLAN OF SLAB SHOWING REINFORCEMENT

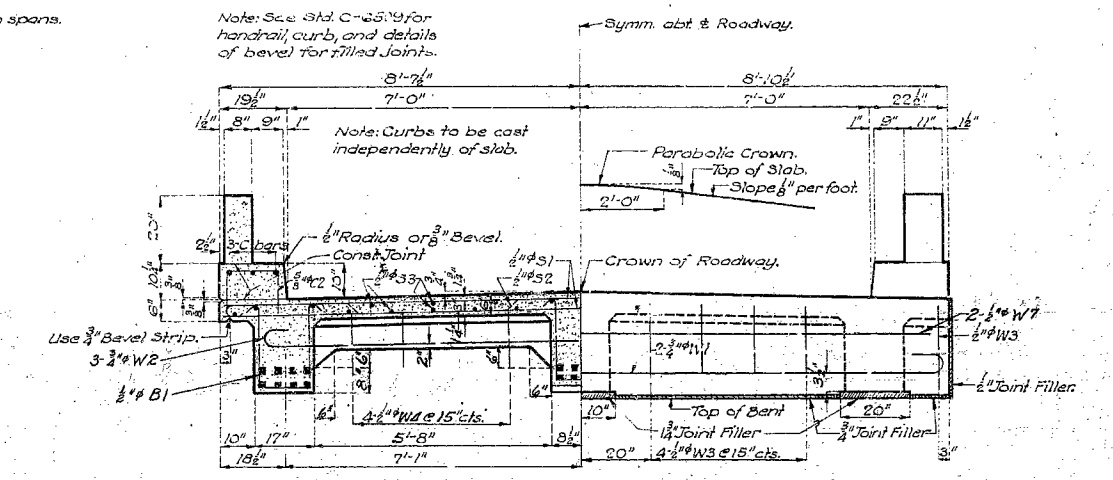

HALF SECTION THRU SPAN (Near Intermediate Bent)

HALF ELEVATION AT END BENT

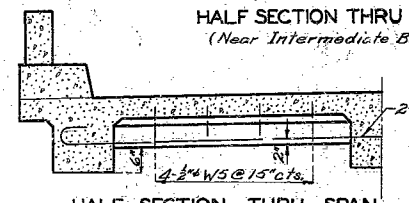

HALF SECTION THRU SPAN (Near Intermediate Web)

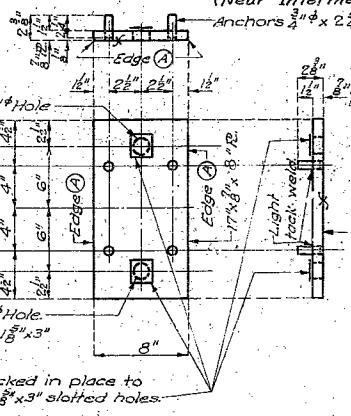

TOP PLATE - EXP.

TOP PLATE - FIX.

Notes for Bearings:
Holes in ⅛" plates for ¾"ϕ x 2½" and 1¼"ϕ x 3" anchors shall be made for driving fit. After anchors are driven in place they shall be lightly tack welded to ⅛" plates.
Surfaces marked "F" shall be finished.
All finished surfaces shall be coated with white lead and tallow in shop and just prior to placing plates in concrete. All finished surfaces shall be thoroughly cleaned and coated with a mixture of graphite and oil.
Edge Ⓐ to be rounded.
Material: Rolled Steel.

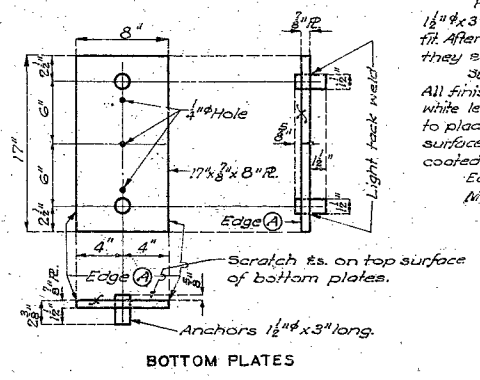

BOTTOM PLATES

DETAILS OF BEARING PLATES

BILL OF REINFORCING STEEL - SPANS (1-2) & (2-3)

No.	Size	Length	Mark	Location
10	⅜"ϕ	3'-6"	C1	Curb
100	⅜"ϕ	3'-3"	C2	"
2	⅜"ϕ	4'-0"	C3	"
6	⅜"ϕ	19'-9"	C4	"
18	⅜"ϕ	20'-0"	C5	"
146	½"ϕ	17'-0"	S1	Slab
71	½"ϕ	18'-9"	S2	"
96	½"ϕ	19'-6"	S3	"
2	½"ϕ	19'-6"	W1	End Web
13	½"ϕ	17'-0"	W2	" "
10	½"ϕ	5'-6"	W3	" "
24	½"ϕ	3'-9"	W4	" "
16	½"ϕ	6'-0"	W5	" "
9	½"ϕ	17'-0"	W6	" "
2	½"ϕ	17'-6"	W7	" "
174	½"ϕ	5'-3"	B1	Girder
24	1¼"ϕ	39'-6"	B2	"
12	1⅛"ϕ	39'-6"	B3	"
12	1⅛"ϕ	37'-0"	B4	"
10	¾"ϕ	6'-0"	R1	Rail
150	⅝"ϕ	4'-9"	R2	"
4	½"ϕ	3'-9"	R3	"
4	½"ϕ	8'-9"	R4	"
4	½"ϕ	6'-9"	R5	"
24	½"ϕ	9'-0"	R6	"
32	½"ϕ	9'-0"	R7	"

Bending Sketches.

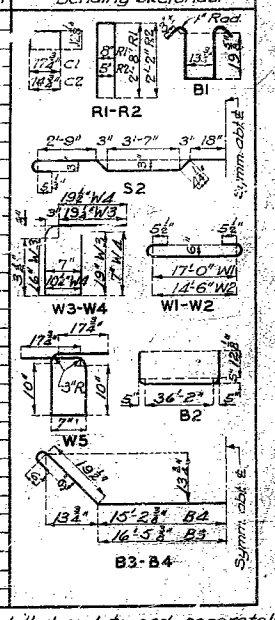

Note: Bars in above unit to be billed and tagged separately.

BAR SIZE EQUIVALENTS	
ϕ 2 = 1¼" Rd.	ϕ 7 = 7/8" Rd.
ϕ 3 = 3/8" Rd.	ϕ 8 = 1" Rd.
ϕ 4 = 1/2" Rd.	ϕ 9 = 1" Sq.
ϕ 5 = 5/8" Rd.	ϕ 10 = 1 1/8" Sq.
ϕ 6 = 3/4" Rd.	ϕ 11 = 1 1/4" Sq.

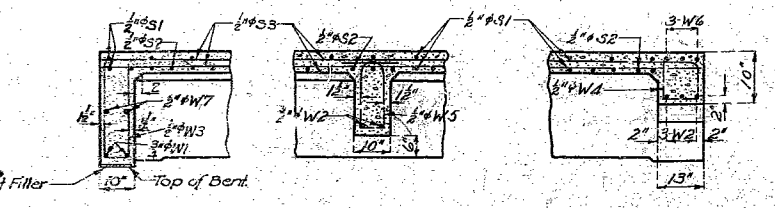

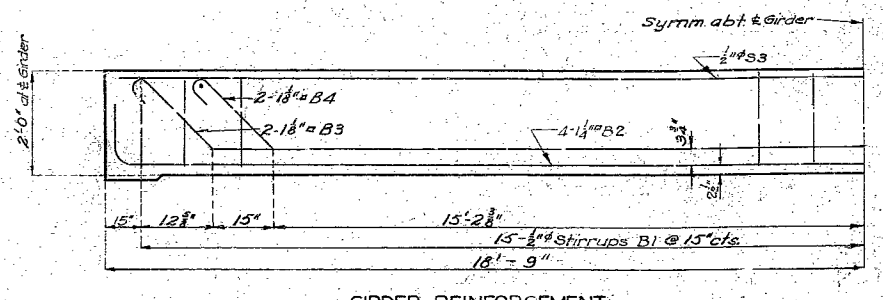

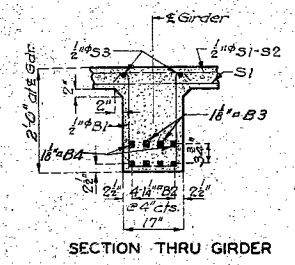

BRIDGE OVER MYATT CREEK

STATE ROAD FROM LANTON EAST TO OREGON CO. LINE

ABOUT 12.3 MILES W. OF THAYER

PROJECT NO. S-938(2) SEC. A (SO) STA. 193+42

HOWELL COUNTY

FINISHED

FINISHED

FINISHED

P-58

Assembled May 1951 by W.L.W. & A.J.K.
Checked May 1951 by C.S.A.
Std. Drawn Sept. 1949 by W.W.S.
Traced Sept. 1949 by K.R.W.

Note: This drawing is not to scale. Follow dimensions.

Sheet No. 4 of 6.

25° thru 40° Dedrs. - Square - 18' Rdwy. - H10

MISSOURI STATE HIGHWAY DEPARTMENT

FED HWAY DEPT NO	STATE	FED AID PROJ NO	FISCAL YEAR	SHEET NO	TOTAL SHEETS
5	MO	S-938(2) Sec. A (SO)	19		

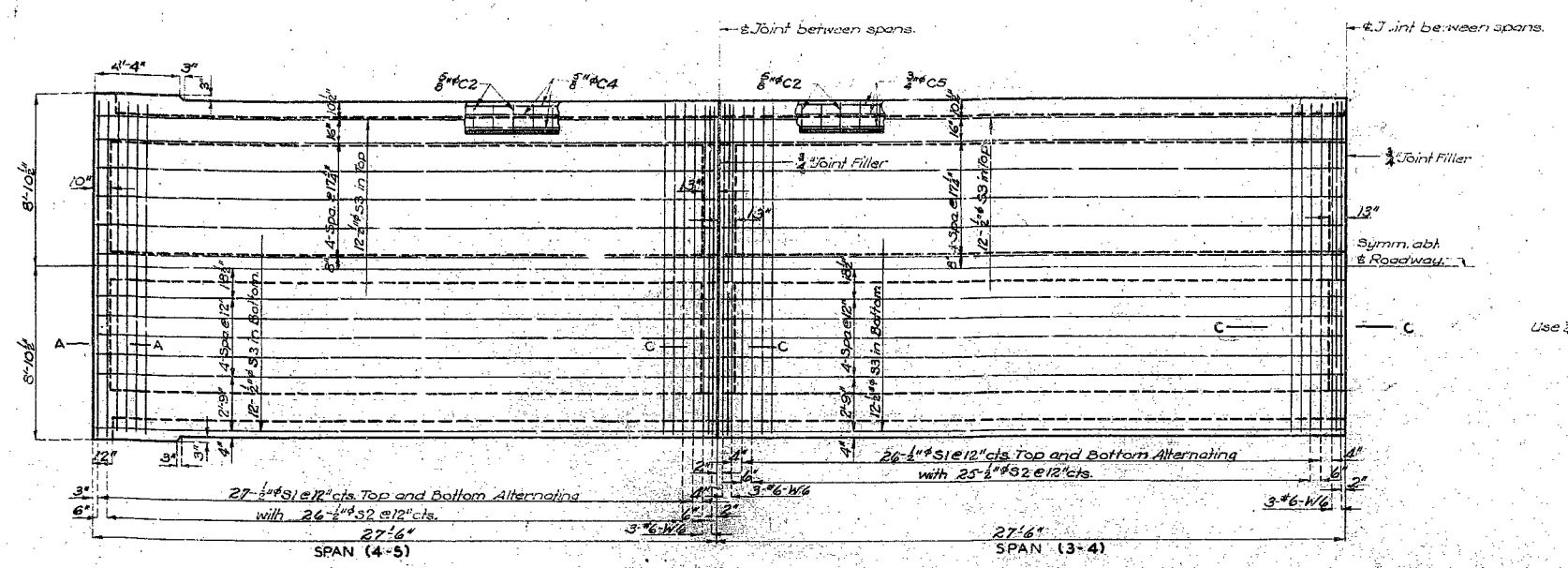

PLAN OF SLAB SHOWING REINFORCEMENT

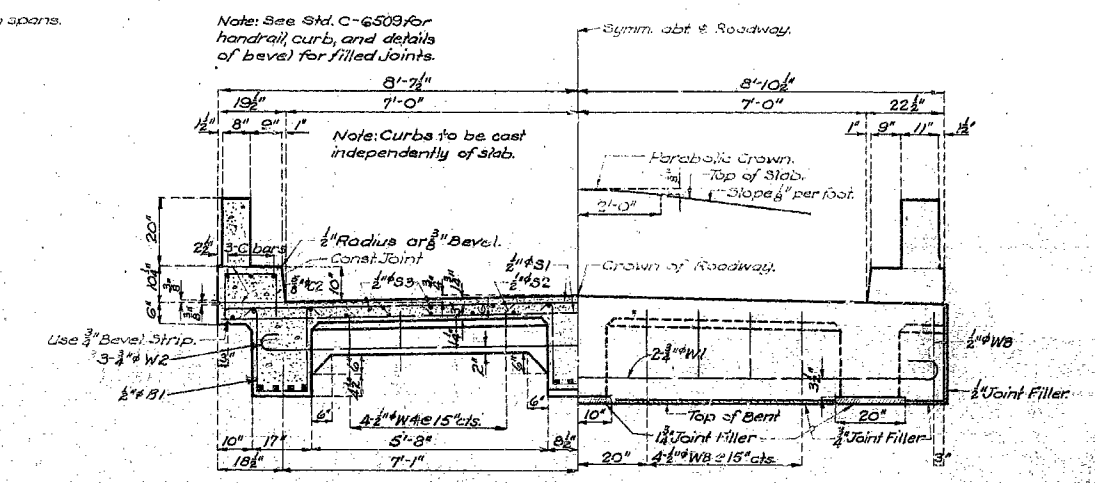

HALF SECTION THRU SPAN

HALF ELEVATION AT END BENT

BILL OF REINFORCING STEEL - SPANS (3-4) & (4-5)

No.	Size	Length	Mark	Location
10	⅜"#	3'-6"	C1	Curb
78	⅜"#	3'-3"	C2	"
2	⅜"#	4'-0"	C3	"
6	⅜"#	15'-0"	C4	"
6	½"#	27'-3"	C5	"
3	½"#	15'-0"	C6	"
106	½"#	17'-0"	S1	Slab
51	½"#	18'-9"	S2	"
48	½"#	27'-3"	S3	"
2	⅝"#	19'-6"	W1	End Web
9	⅝"#	17'-0"	W2	" "
24	½"#	3'-9"	W4	" "
9	½"#	1'-0"	W6	" "
10	½"#	5'-0"	W8	" "
156	½"#	4'-9"	B1	Girder
24	1¼"#	29'-0"	B2	"
10	⅝"#	6'-0"	R1	Rail
110	½"#	4'-9"	R2	"
4	½"#	3'-8"	R3	"
4	½"#	8'-6"	R4	"
4	⅝"#	6'-6"	R5	"
16	½"#	8'-9"	R6	"
24	½"#	8'-9"	R7	"

Bending Skeletons

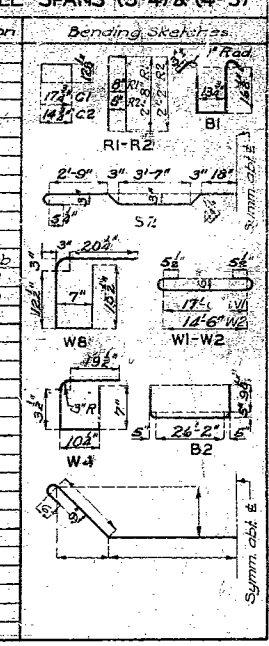

Note: Bars in above unit to be billed & tagged separately.

BAR SIZE EQUIVALENTS	
#2 = 1/4" Rd.	#7 = 7/8" Rd.
#3 = 3/8" Rd.	#8 = 1" Rd.
#4 = 1/2" Rd.	#9 = 1" Sq.
#5 = 5/8" Rd.	#10 = 1 1/8" Sq.
#6 = 3/4" Rd.	#11 = 1 1/4" Sq.

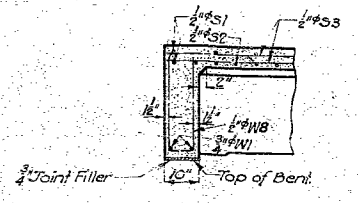

SECTION A-A

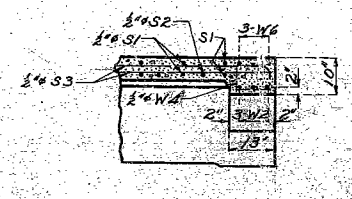

SECTION C-C

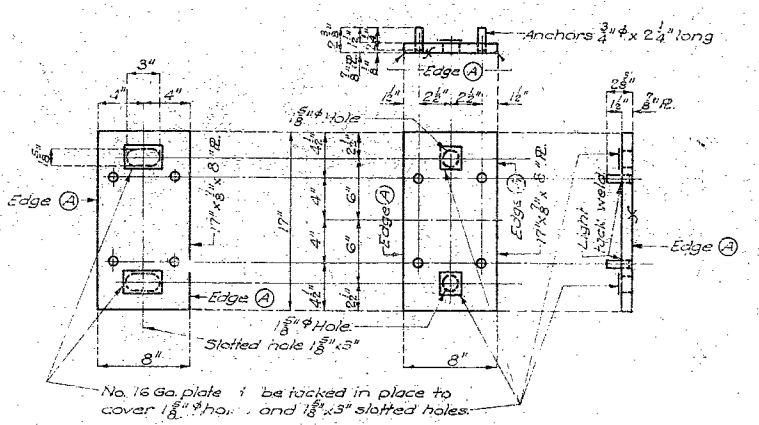

TOP PLATE - EXP.

TOP PLATE - FIX.

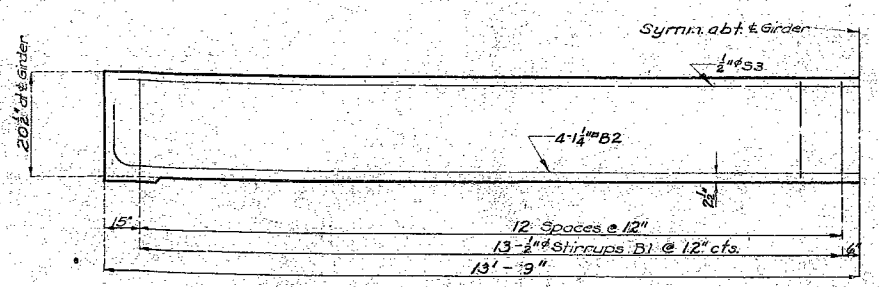

GIRDER REINFORCEMENT

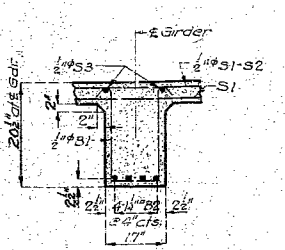

SECTION THRU GIRDER

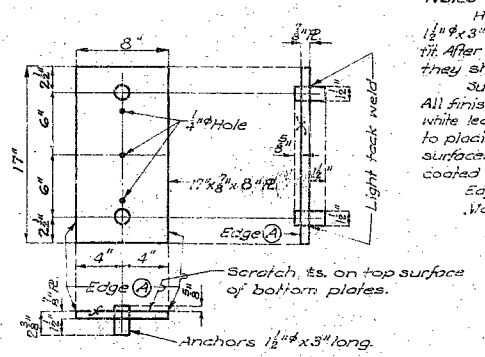

BOTTOM PLATES

DETAILS OF BEARING PLATES

Notes for Bearings:
Holes in ⅜" plates for ¾"#x 2½" and 1¼"#x 3" anchors shall be made for driving fit. After anchors are driven in place they shall be lightly tack welded to ⅜" plates.
Surfaces marked X shall be finished.
All finished surfaces shall be coated with white lead and tallow in shop and just prior to placing plates in concrete. All finished surfaces shall be thoroughly cleaned and coated with a mixture of graphite and oil.
Edge Ⓐ to be rounded.
Material: Rolled steel.

BRIDGE OVER MYATT CREEK

STATE ROAD FROM LANTON EAST TO OREGON CO. LINE

ABOUT 12.3 MILES W. OF THAYER

PROJECT NO. S-938(2) SEC. A (SO) STA. 193+42

HOWELL COUNTY

FINISHED

FINISHED

FINISHED

P-58

110

Assembled May 1951 by W.L.W. & A.J.K.
Checked May 1951 by C.S.A.
Std. Drawn Sept. 1949 by W.W.S.
Traced Sept. 1949 by K.R.W.

Note: This drawing is not to scale. Follow dimensions.

Sheet No. 5 of 6.

NO CONSTRUCTION CHANGES

25' thru 50' D Edge - Square - 14' Roadway - H10

6

MISSOURI STATE HIGHWAY DEPARTMENT

FED. ROAD DIST. NO.	STATE	FED. AID PROJ. NO.	FISCAL YEAR	SHEET NO.	TOTAL SHEETS
5	MO.	S-938(2) Sec.A(50)	19		

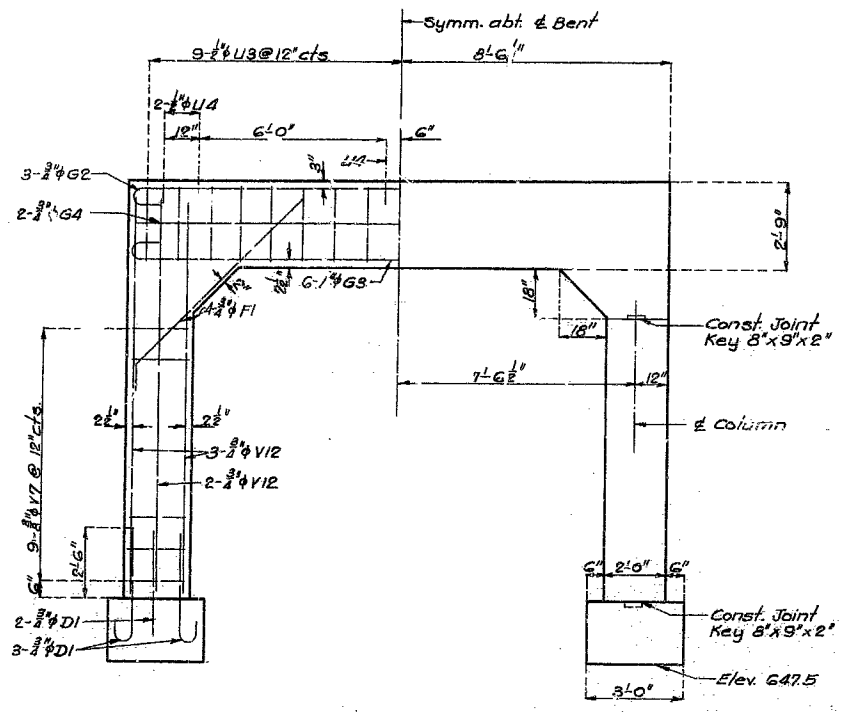

ELEVATION

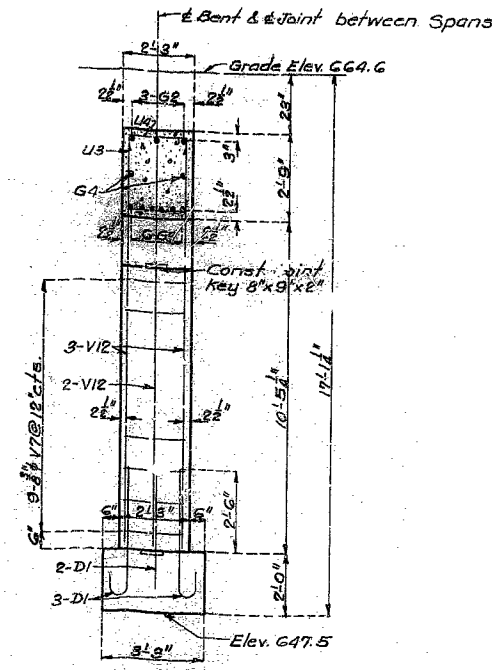

SECTION AT ℄

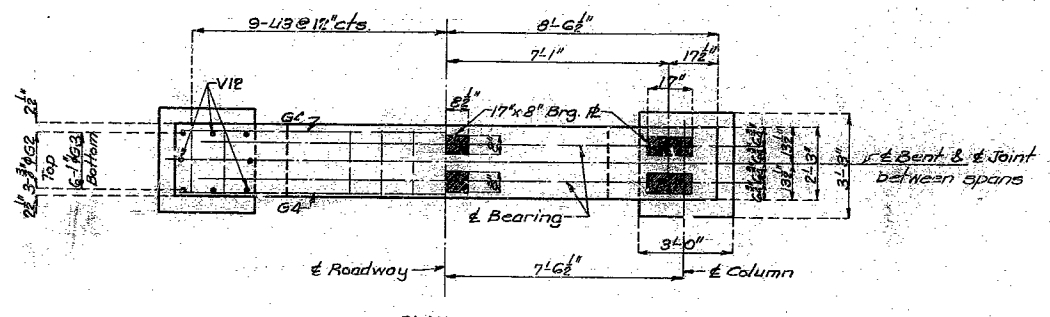

PLAN

DETAILS OF INTERMEDIATE BENT NO. 4.

BRIDGE OVER MYATT CREEK

STATE ROAD FROM LANTON EAST TO OREGON CO. LINE
ABOUT 12.3 MILES W. OF THAYER
PROJECT NO. S-938(2) SEC. A (50) STA. 193+42

HOWELL COUNTY

FINISHED

F-58

Drawn Nov. 1950 by W.L.W.
Traced Dec. 1950 by M.E.L.
Checked Feb. 1951 by C.S.A.

Note: This drawing is not to scale. Follow dimensions.

Sheet No. 6 of 6.

FINISHED

SEE FINAL PLANS BROWN-LINES

MISSOURI STATE HIGHWAY DEPARTMENT

FED. ROAD DIST. NO.	STATE	FED. AID PROJ. NO.	FISCAL YEAR	SHEET NO.	TOTAL SHEETS
5	MO.	S-938(2) Sec. A(SO)	19		

FINAL PLANS

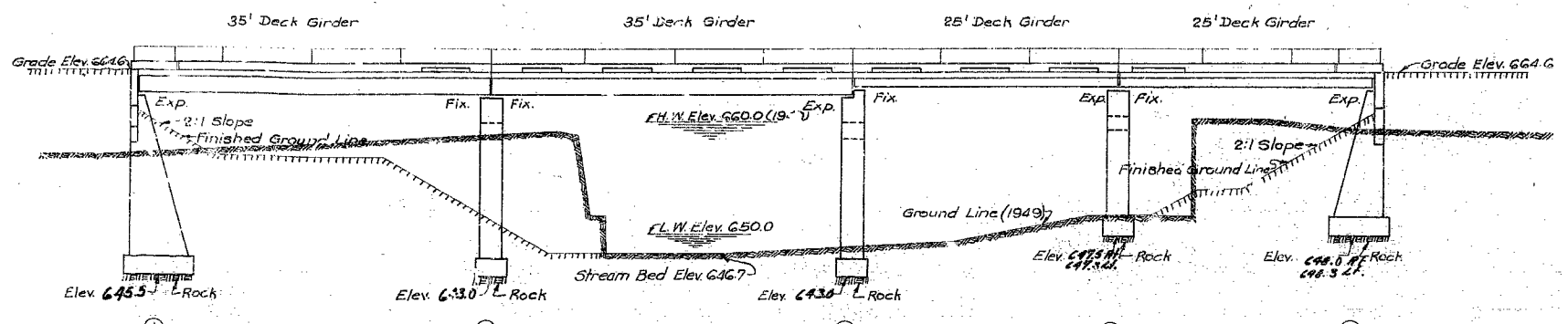

GENERAL ELEVATION

Note: All loose, shelly or disintegrated rock shall be removed and the footings placed on hard, solid undisturbed rock. If soft rock or shale is encountered the footings shall be carried at least 18" into and cast against vertical faces of same. In no case shall footings of Bents No. 2, 3 and 4 be placed higher than elevations shown.

Note: Old roadway fill under ends of bridge shall be removed to natural ground line. Payment for this excavation outside limits of excavation for structure will be made at unit contract price for Roadway Excavation.

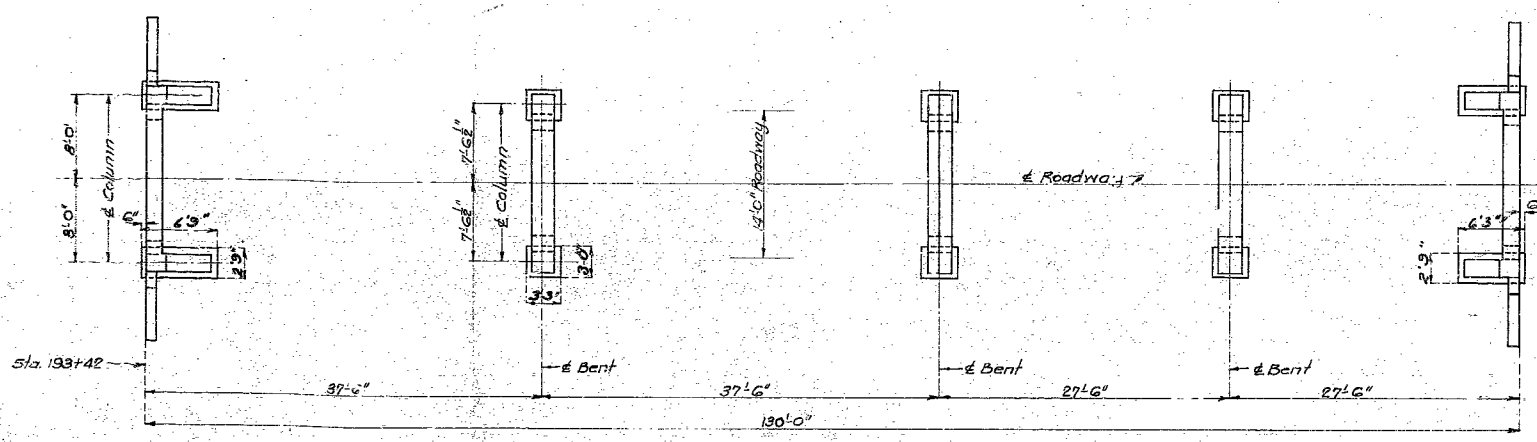

PLAN

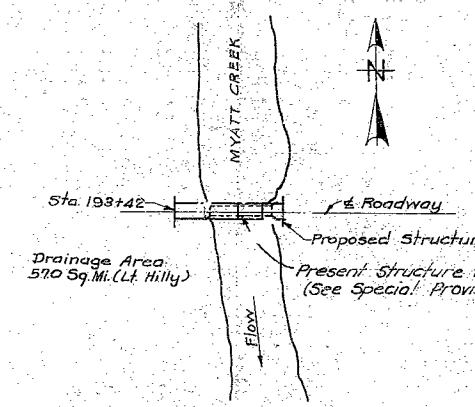

LOCATION SKETCH

FINAL QUANTITIES

Item		Sub str.	Super str.	Total
Class 1 Excavation for Structures	Cu. Yds.	68.5		68.5
Class 2 Excavation for Structures	Cu. Yds.	78.5		78.5
Class "A" Concrete (Handrail)	Cu. Yds.		11.0	11.0
Class "B" Concrete (Except Handrail)	Cu. Yds.	56.6	83.9	142.5
Reinforcing Steel	Lbs.	6950	25118	32068
Structural Steel Bearing Plates	Lbs.		1650	1650
Class 2 Extra Below Plan Elev.	Cu. Yds.	0.5		0.5
Test holes for footings	L. F.	40.0		40.0

Note: Excavation for bridge made above Elev. 651.0 will be paid for as Class 1 Excavation for Structures. Excavation for bridge made below Elev. 651.0 will be paid for as Class 2 Excavation for Structures.

BUREAU OF CONSTRUCTION
OCT 29 1952
HIGHWAY DEPT.

COMPLETE BILL OF SUBSTRUCTURE REINFORCING STEEL

No	Size	Length	Mark	Location
End Bents No. 1 & 5				
28	3/4"	5'-3"	D1	Footing
16	3/4"	8'-0"	F1	Haunch
12	3/4"	17'-6"	H1	Beam
4	1"	19'-6"	H2	Bm. Bl #1
4	3/4"	17'-6"	H3	" " "
16	3/4"	12'-3"	H4	Wing
4	3/4"	19'-6"	H5	Bm. Bl #5
8	3/4"	11'-6"	H6	Wing
6	3/4"	11'-9"	T1	"
8	3/4"	12'-6"	T2	"
18	1/2"	10'-8"	U1	Beam
18	1/2"	2'-8"	U2	"
10	1/2"	8'-6"	V1	Wing
6	3/4"	17'-6"	V2	Col. Bl #1
8	3/4"	17'-0"	V3	" " #1
8	1/2"	11'-9"	V4	" " #1
24	3/4"	14'-0"	V5	" " #1
8	3/4"	12'-9"	V6	Col. Bl #5
6	3/4"	13'-0"	V9	" " #5
16	3/4"	12'-9"	V10	" " #5
8	1/2"	7'-3"	V11	" " #5
6	3/4"	12'-3"	T3	Wing Bl #5
18	5/8"	10'-9"	U6	Bm. Bl #5
Int. Bents 2, 3 & 4				
48	3/4"	5'-3"	D1	Footing
24	3/4"	8'-0"	F1	Haunch
6	1"	19'-3"	G1	Bm. Bl #2
9	3/4"	18'-5"	G2	" " #2
6	1"	18'-9"	G3	Bm. Bl #4
6	3/4"	16'-9"	G4	" " "
2	1"	16'-9"	G5	Bm. Bl #3
5	1"	19'-3"	G6	" " "
51	1/2"	9'-9"	U3	Beam
18	1/2"	3'-0"	U4	"
23	5/8"	2'-0"	U5	Bm. Bl #3
32	3/4"	17'-0"	V6	Col. Bl #2
70	3/4"	8'-3"	V7	" " "
16	3/4"	12'-0"	V12	Col. Bl #4

BAR SIZE EQUIVALENTS

#2 = 1/4" Rd.	#7 = 7/8" Rd.
#3 = 3/8" Rd.	#8 = 1" Rd.
#4 = 1/2" Rd.	#9 = 1" Sq.
#5 = 5/8" Sq.	#10 = 1 1/8" Sq.
#6 = 3/4" Rd.	#11 = 1 1/8" Sq.

Bending Sketches & Cutting Diagrams

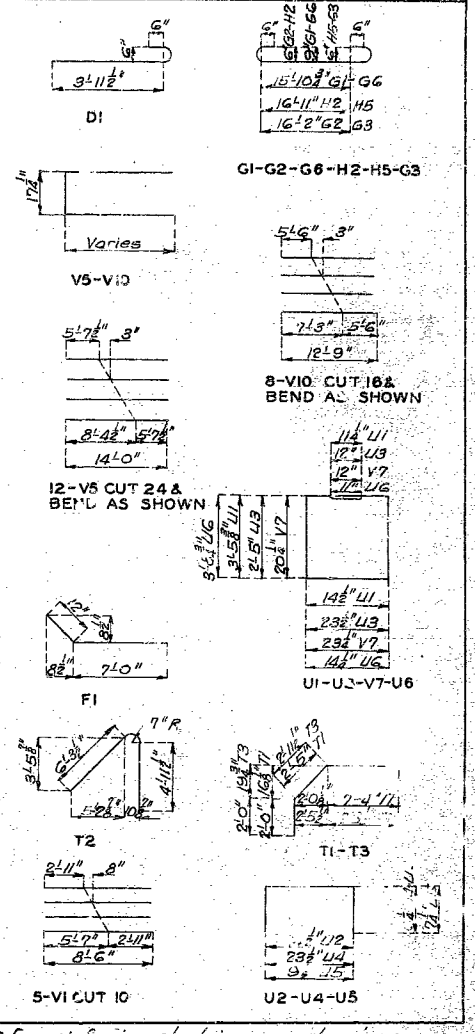

Note: See Sheets No. 4 and 5 of 6 for reinforcing steel in superstructure.

GENERAL NOTES:

Design Specifications A.A.S.H.O. 1949
Loading H 10 - 44
Reinforcing Steel Stress 18,000 #/o"
Class "B" Concrete Stress 1,000 #/o"
All concrete shall be Class "B"
Where Joint Filler is specified on plans it shall conform with the requirements of Section 38-19A (1) of the Standard Specifications for Premoulded Material for Filler.

B.M. Elev. 657.48 N.1.P.P. 162' Lt. Sta. 193+60

BRIDGE OVER MYATT CREEK

STATE ROAD FROM LANTON EAST TO OREGON CO. L.E.

ABOUT 12.3 MILES W. OF THAYER.

PROJECT NO. S-938(2)SEC. A (SO) STA. 193+42

HOWELL COUNTY

FINISHED

SUBMITTED BY V. W. Carnelon BRIDGE ENGINEER DATE 6/5/1951

FINISHED APPROVED BY C.W. Brown CHIEF ENGINEER DATE 6/5/1951

FINISHED

STD. C-6509	
STD. C-110 R3	
P-58	

Drawn Nov. 1950 by W.L.W.
Traced Dec. 1950 by M.E.L.
Checked Feb. 1951 by C.S.H.

Note: This drawing is not to scale. Follow dimensions.

Sheet No. 1A of 4

FINAL PLANS

2

MISSOURI STATE HIGHWAY DEPARTMENT

FED. ROAD DIST. NO.	STATE	FED. AID PROJ. NO.	FISCAL YEAR	SHEET NO.	TOTAL SHEETS
5	MO.	S-938 (2) Sec. A(50))	19		

FINAL PLANS

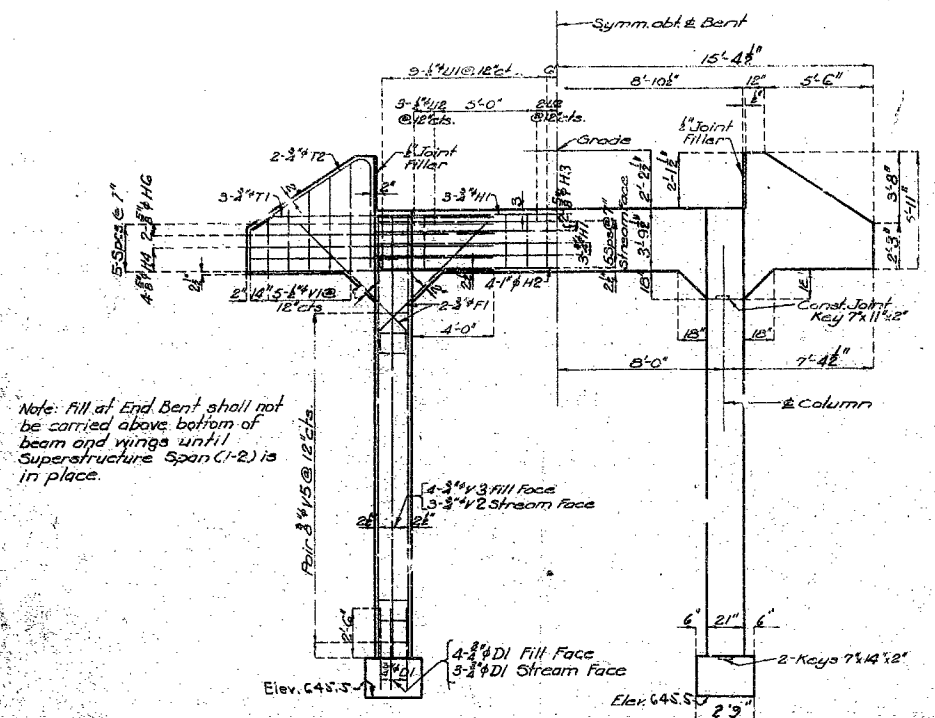

ELEVATION

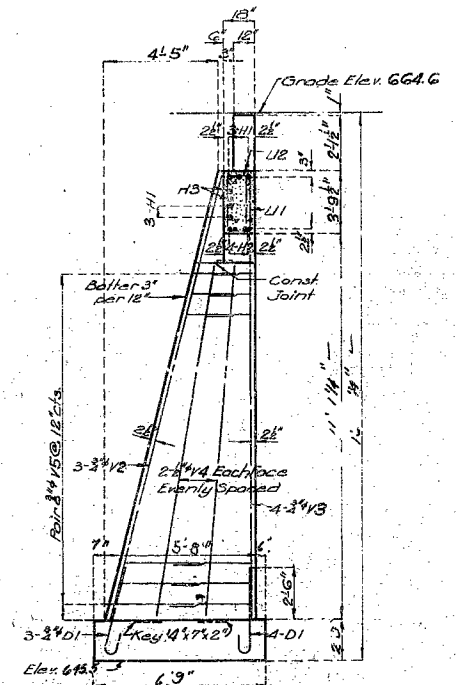

SECTION AT ℄

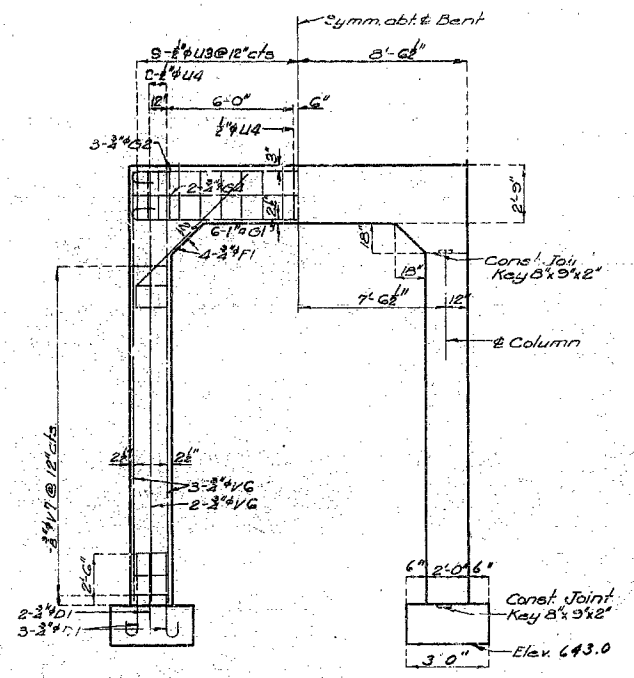

ELEVATION

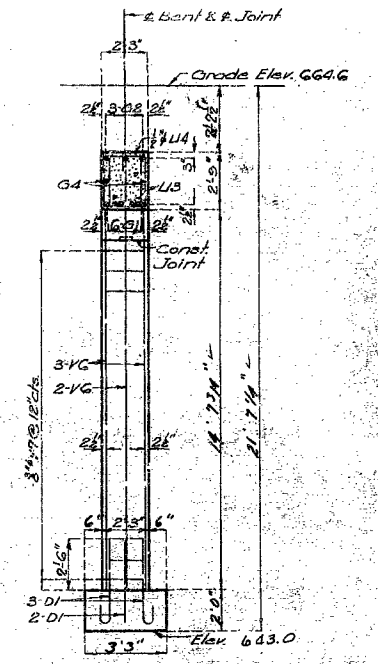

SECTION AT ℄

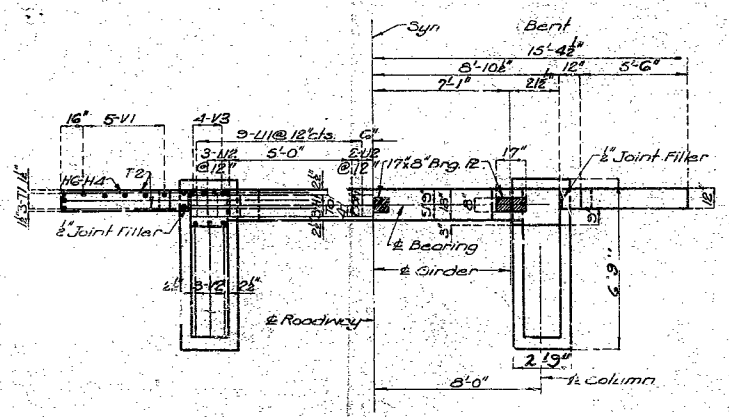

PLAN

DETAILS OF END BENT NO.1

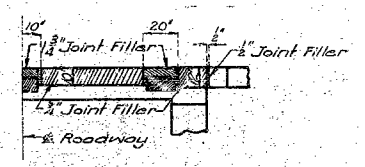

DETAILS OF JOINT FILLER AT END BENTS

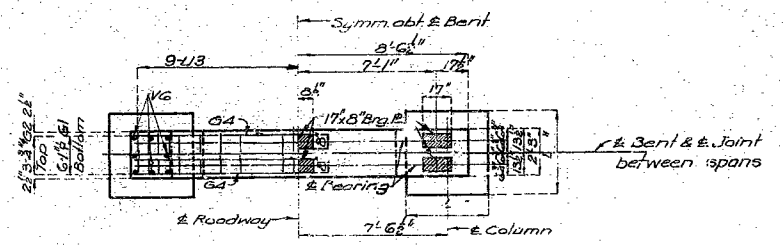

PLAN

DETAILS OF INTERMEDIATE BENT NO. 2

BRIDGE OVER MYATT CREEK

STATE ROAD FROM LANTON EAST TO OREGON CO. LINE

ABOUT 12.3 MILES W. OF THAYER

PROJECT NO. S-938(2) SEC. A(50) STA. 193+42

HOWELL COUNTY

FINISHED FINISHED FINISHED

P-58

Drawn Nov. 1950 by W.L.W.
Traced Nov. 1950 by M.E.L.
Checked Feb. 1951 by C.S.A.

Note: This drawing is not to scale. Follow dimensions.

Sheet No. 2A of 4

FINAL PLANS

MISSOURI STATE HIGHWAY DEPARTMENT

FED. ROAD DIST. NO.	STATE	FED AID PROJ. NO.	FISCAL YEAR	SHEET NO.	TOTAL SHEETS
5	MO.	S-936(2)SEC.A(SO)	19		

FINAL PLANS

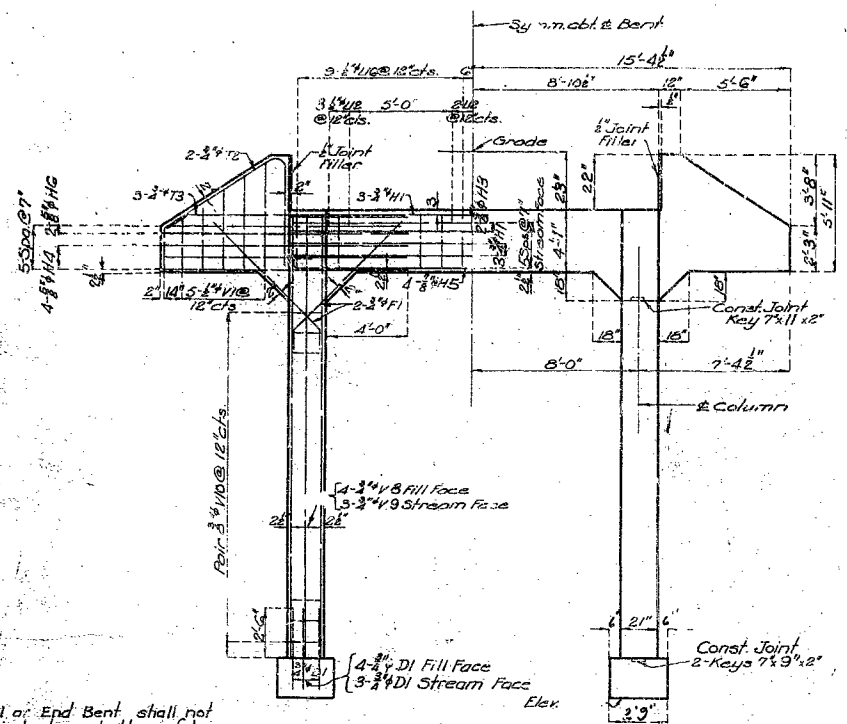

ELEVATION

Note: Fill at End Bent shall not be carried above bottom of beam and wings until superstructure Span (4-5) is in place.

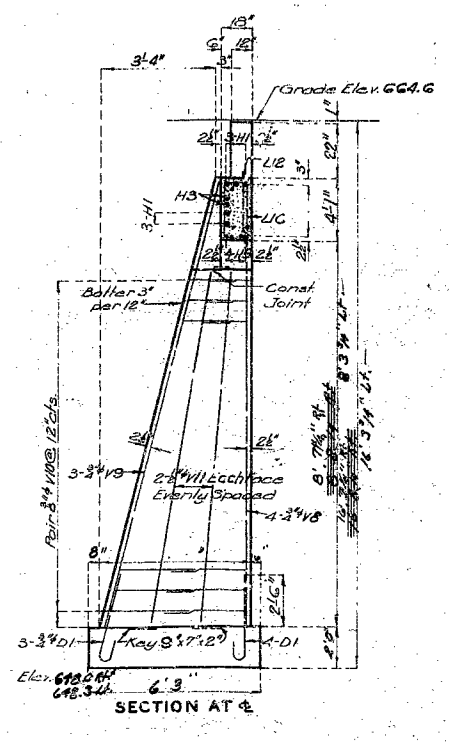

SECTION AT ℄

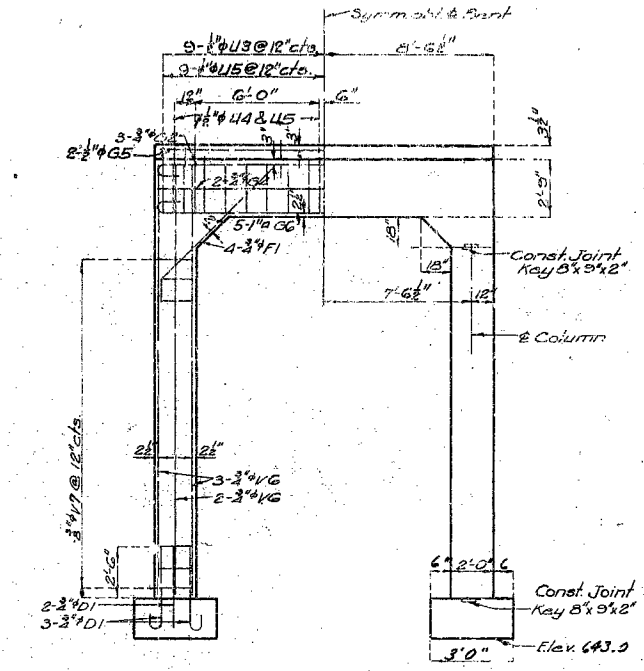

ELEVATION

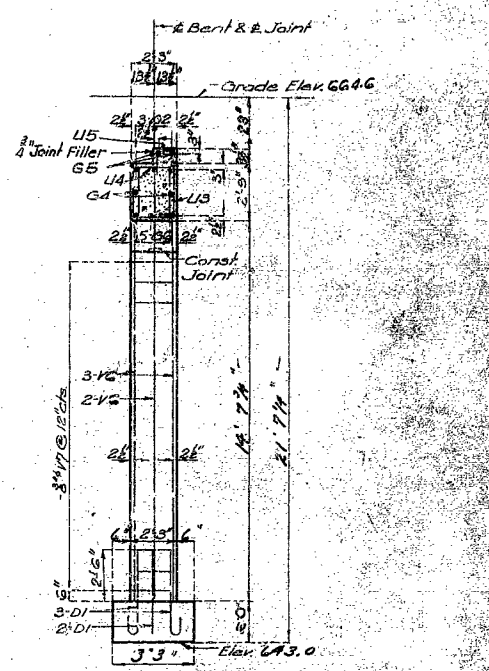

SECTION AT ℄

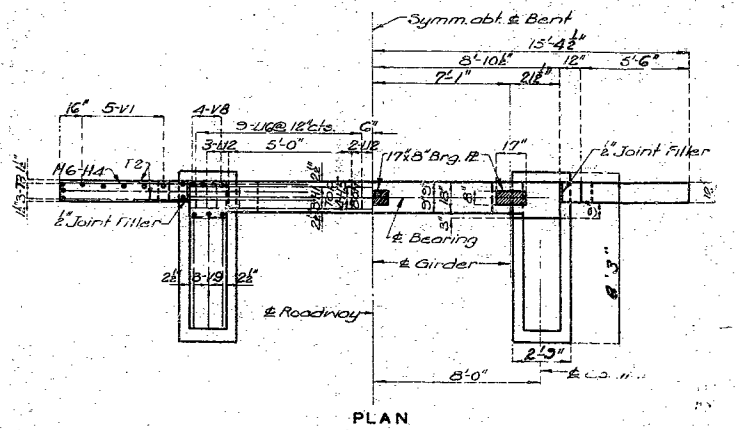

PLAN

DETAILS OF END BENT NO. 5

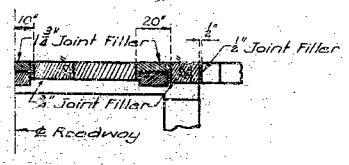

DETAILS OF JOINT FILLER AT END BENTS

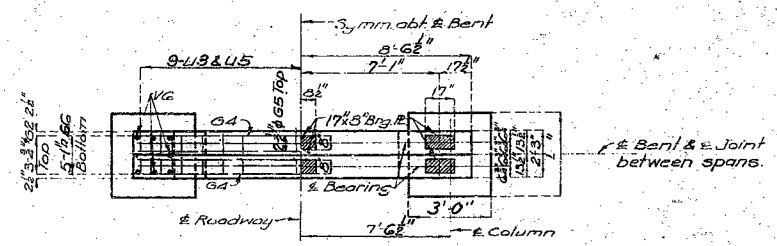

PLAN

DETAILS OF INTERMEDIATE BENT NO. 3

BRIDGE OVER MYATT CREEK

STATE ROAD FROM LANTON EAST TO OREGON CO. LINE.

ABOUT 12.3 MILES W. OF THAYER

PROJECT NO. S-936(2) SEC.A (SO) STA. 193+42

HOWELL COUNTY

FINISHED

FINISHED

FINISHED

P-56

Drawn Nov. 1950 by W.L.W.
Traced Nov. 1950 by M.E.L.
Checked Feb. 1951 by C.S.A.

Note: This drawing is not to scale. Follow dimensions.

Sheet No. 3A of 4

FINAL PLANS

MISSOURI STATE HIGHWAY DEPARTMENT

FED. ROAD DIST. NO.	STATE	FED. AID PROJ. NO.	FISCAL YEAR	SHEET NO.	TOTAL SHEETS
5	MO.	S-938(2) Sec. A(SO)	19		

FINAL PLANS

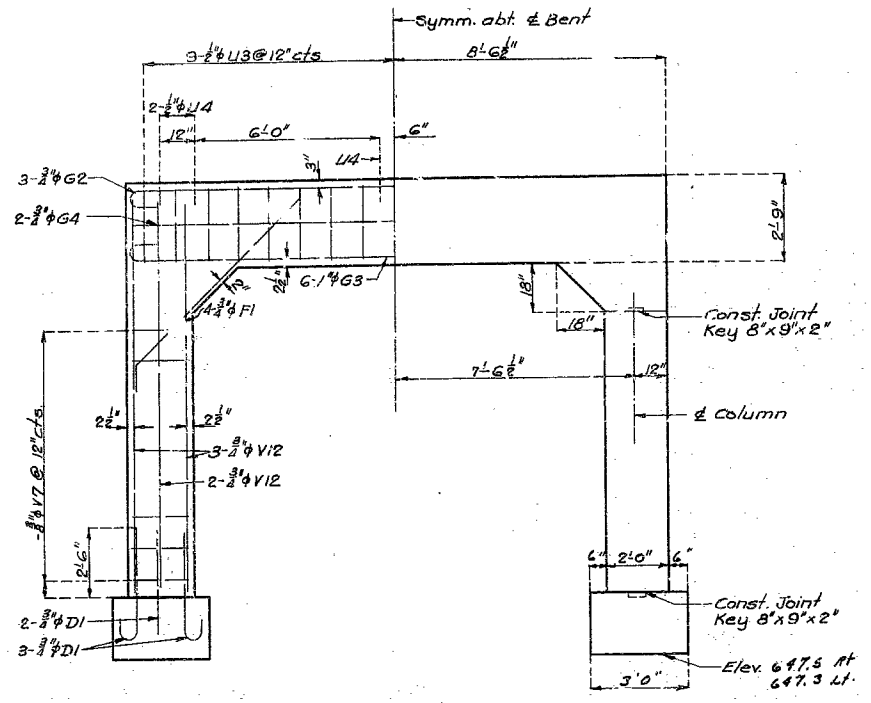

ELEVATION

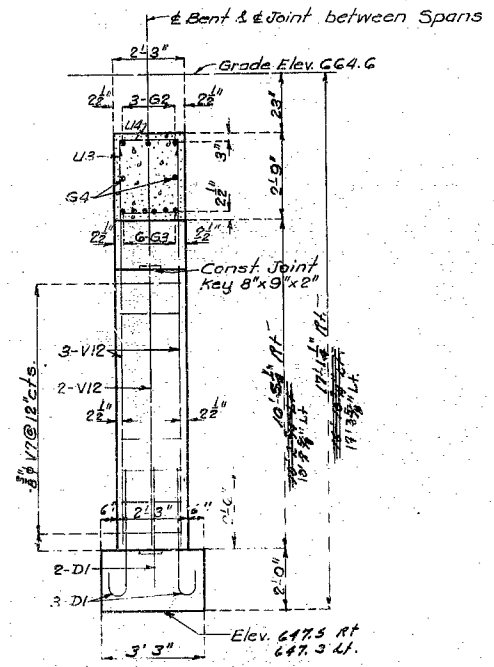

SECTION AT ℄

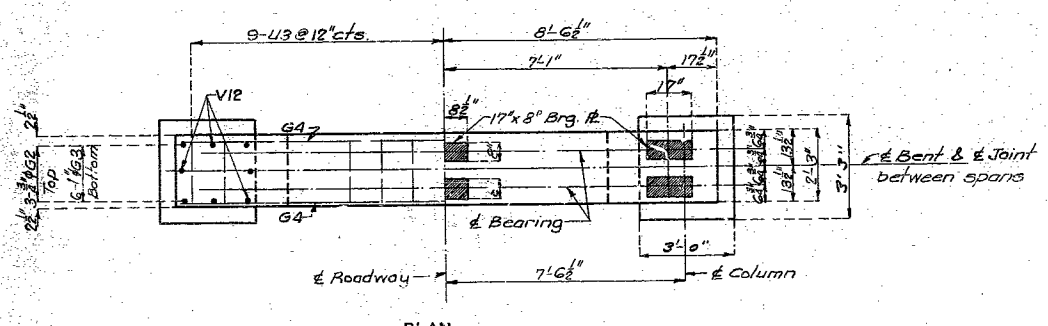

PLAN

DETAILS OF INTERMEDIATE BENT NO. 4.

115

Drawn Nov. 1950 by W.L.W.
Traced Dec. 1950 by M.E.L.
Checked Feb. 1951 by C.S.A.

Note: This drawing is not to scale. Follow dimensions.

Sheet No. 6.A of 4

BRIDGE OVER MYATT CREEK

STATE ROAD FROM LANTON EAST TO OREGON CO. LINE
ABOUT 12.3 MILES W. OF THAYER
PROJECT NO. S-938(2) SEC. A (SO) STA. 193+42

HOWELL COUNTY

FINISHED

FINISHED FINISHED

P-58

FINAL PLANS

APPENDIX B.
ANALYSIS OF EXISTING CAPACITY

Bridge P0058 capacity pre-design

Short spans, interior girder

$L := 26.375ft$

$b_w := 17in$

$h_f := 6in$

$b_e := \min\left(b_w + 2 \cdot 68\frac{in}{2}, b_w + 2 \cdot 8 \cdot h_f, \frac{L}{4}\right) = 79.125 \cdot in$

$h := 20.5in$

$d := h - 2.5in = 18 \cdot in$

$fc := 6000psi$

$\beta_1 := .75$

$f_y := 33000psi$

$A_s := 4 \cdot 1.56in^2 = 6.24 \cdot in^2$

$a := A_s \cdot \frac{f_y}{.85 \cdot fc \cdot b_e} = 0.51 \cdot in$ <hf, OK

Moment Capacity:

$M_n := A_s \cdot f_y \cdot \left(d - \frac{a}{2}\right) = 304.502 \cdot kip \cdot ft$ $\phi_m := .9$

$\phi_m \cdot M_n = 274.052 \cdot kip \cdot ft$

$A_{s_min} := 200\frac{b_w}{in} \cdot \frac{d \cdot psi \cdot in^2}{f_y \cdot in} = 1.855 \cdot in^2$ <As, OK

Shear Capacity:

$A_v := 2 \cdot .2in^2 = 0.4 \cdot in^2$

$s := 12in$

$V_c := \frac{2}{1000} \cdot \left(\frac{fc}{psi}\right)^{\frac{1}{2}} \cdot \frac{b_w}{in} \cdot \frac{d \cdot kip}{in} = 47.405 \cdot kip$ $\phi_v := .75$

$V_s := A_v \cdot f_y \cdot \frac{d}{s} = 19.8 \cdot kip$

$V_n := V_c + V_s = 67.205 \cdot kip$

$\phi_v \cdot V_n = 50.404 \cdot kip$

Short spans, exterior girder

$L := 26.375ft$

$b_w := 17in$

$h_f := 6in$

$b_e := 58in$

$h := 20.5in$

$d := h - 2.5in = 18 \cdot in$

$fc := 6000psi$

$\beta_1 := .75$

$f_y := 33000psi$

$A_s := 4 \cdot 1.56in^2 = 6.24 \cdot in^2$

$a := A_s \cdot \frac{f_y}{.85 \cdot fc \cdot b_e} = 0.696 \cdot in$ <hf, OK

Moment Capacity:

$M_n := A_s \cdot f_y \cdot \left(d - \frac{a}{2} \right) = 302.907 \cdot kip \cdot ft$ $\phi_m := .9$

$\phi_m \cdot M_n = 272.616 \cdot kip \cdot ft$

$A_{s_min} := 200 \frac{b_w}{in} \cdot \frac{d \cdot psi \cdot in^2}{f_y \cdot in} = 1.855 \cdot in^2$ <As, OK

Shear Capacity:

$A_v := 2 \cdot .2in^2 = 0.4 \cdot in^2$

$s := 12in$

$V_c := \frac{2}{1000} \cdot \left(\frac{fc}{psi} \right)^{\frac{1}{2}} \cdot \frac{b_w}{in} \cdot \frac{d \cdot kip}{in} = 47.405 \cdot kip$ $\phi_v := .75$

$V_s := A_v \cdot f_y \cdot \frac{d}{s} = 19.8 \cdot kip$

$V_n := V_c + V_s = 67.205 \cdot kip$

$\phi_v \cdot V_n = 50.404 \cdot kip$

Long spans, interior girder

$L := 36.1875\,ft$

$b_w := 17in$

$h_f := 6in$

$b_e := \min\left(b_w + 2\cdot 68\frac{in}{2}, b_w + 2\cdot 8\cdot h_f, \frac{L}{4}\right) = 85\cdot in$

$h := 24in$

$d_1 := h - 2.5in = 21.5\cdot in$ $\quad$ $d_2 := d_1 - 3.75in = 17.75\cdot in$

$A_{s1} := 4\cdot 1.56in^2 = 6.24\cdot in^2$ $\quad$ $A_{s2} := 4\cdot 1.27in^2 = 5.08\cdot in^2$

$f_y := 33000psi$ $\quad$ $d := \frac{\left(A_{s1}\cdot f_y\cdot d_1 + A_{s2}\cdot f_y\cdot d_2\right)}{A_{s1}\cdot f_y + A_{s2}\cdot f_y} = 19.817\cdot in$

$fc := 6000psi$

$\beta_1 := .75$

$a := \left(A_{s1} + A_{s2}\right)\cdot\frac{f_y}{.85\cdot fc\cdot b_e} = 0.862\cdot in$ $\quad$ <hf, OK

Moment Capacity:

$M_n := \left(A_{s1} + A_{s2}\right)\cdot f_y\cdot\left(d - \frac{a}{2}\right) = 603.495\cdot kip\cdot ft$ $\quad$ $\phi_m := .9$

$\phi_m\cdot M_n = 543.145\cdot kip\cdot ft$

$A_{s_min} := 200\frac{b_w}{in}\cdot\frac{d\cdot psi\cdot in^2}{f_y\cdot in} = 2.042\cdot in^2$ $\quad$ <As, OK

Shear Capacity:

$A_v := 2\cdot .2in^2 = 0.4\cdot in^2$

$s := 15in$

$V_c := \frac{2}{1000}\cdot\left(\frac{fc}{psi}\right)^{\frac{1}{2}}\cdot\frac{b_w}{in}\cdot\frac{d\cdot kip}{in} = 52.191\cdot kip$ $\quad$ $\phi_v := .75$

$V_s := A_v\cdot f_y\cdot\frac{d}{s} = 17.439\cdot kip$

$V_n := V_c + V_s = 69.63\cdot kip$

$\phi_v\cdot V_n = 52.223\cdot kip$

Long spans, exterior girder

$L := 36.1875\,ft$

$b_w := 17in$

$h_f := 6in$

$b_e := 61in$

$h := 24in$

$d_1 := h - 2.5in = 21.5\cdot in$ $\qquad$ $d_2 := d_1 - 3.75in = 17.75\cdot in$

$A_{s1} := 4\cdot 1.56in^2 = 6.24\cdot in^2$ $\qquad$ $A_{s2} := 4\cdot 1.27in^2 = 5.08\cdot in^2$

$f_y := 33000psi$ $\qquad$ $d := \dfrac{\left(A_{s1}\cdot f_y\cdot d_1 + A_{s2}\cdot f_y\cdot d_2\right)}{A_{s1}\cdot f_y + A_{s2}\cdot f_y} = 19.817\cdot in$

$fc := 6000psi$

$\beta_1 := .75$

$a := \left(A_{s1} + A_{s2}\right)\cdot\dfrac{f_y}{.85\cdot fc\cdot b_e} = 1.201\cdot in$ $\qquad$ <hf, OK

Moment Capacity:

$M_n := \left(A_{s1} + A_{s2}\right)\cdot f_y\cdot\left(d - \dfrac{a}{2}\right) = 598.217\cdot kip\cdot ft$ $\qquad$ $\phi_m := .9$

$\phi_m\cdot M_n = 538.396\cdot kip\cdot ft$

$A_{s_min} := 200\dfrac{b_w}{in}\cdot\dfrac{d\cdot psi\cdot in^2}{f_y\cdot in} = 2.042\cdot in^2$ $\qquad$ <As, OK

Shear Capacity:

$A_v := 2\cdot.2in^2 = 0.4\cdot in^2$

$s := 15in$

$V_c := \dfrac{2}{1000}\cdot\left(\dfrac{fc}{psi}\right)^{\frac{1}{2}}\cdot\dfrac{b_w}{in}\cdot\dfrac{d\cdot kip}{in} = 52.191\cdot kip$ $\qquad$ $\phi_v := .75$

$V_s := A_v\cdot f_y\cdot\dfrac{d}{s} = 17.439\cdot kip$

$V_n := V_c + V_s = 69.63\cdot kip$

$\phi_v\cdot V_n = 52.223\cdot kip$

APPENDIX C.
PARAMETRIC STUDY OF FLEXURAL STRENGTHENING

Moment Capacity Parametric (12 inch width)			Long Spans	Short Spans
Unstrengthened			543.15	274.05
FRCM-PBO	1 Ply	New φMn	548.975	278.902
		% increase	1.07%	1.77%
	2 Ply	New φMn	558.994	286.871
		% increase	2.92%	4.68%
	3 Ply	New φMn	569.008	294.84
		% increase	4.76%	7.59%
	4 Ply	New φMn	579.018	302.798
		% increase	6.60%	10.49%
FRCM-Carbon	1 Ply	New φMn	551.224	283.09
		% increase	1.49%	3.30%
	2 Ply	New φMn	565.459	295.245
		% increase	4.11%	7.73%
	3 Ply	New φMn	579.685	307.384
		% increase	6.73%	12.16%
	4 Ply	New φMn	593.905	319.518
		% increase	9.35%	16.59%
SRG	1 Ply	New φMn	538.136	274.679
		% increase	-0.92%	0.23%
	2 Ply	New φMn	543.491	280.136
		% increase	0.06%	2.22%
	3 Ply	New φMn	548.849	285.585
		% increase	1.05%	4.21%
	4 Ply	New φMn	554.206	291.032
		% increase	2.04%	6.20%
CFRP	1 Ply	New φMn	585.397	309.759
		% increase	7.78%	13.03%
	2 Ply	New φMn	608.884	333.596
		% increase	12.10%	21.73%
	3 Ply	New φMn	623.38	346.835
		% increase	14.77%	26.56%
	4 Ply	New φMn	635.661	357.986
		% increase	17.03%	30.63%

Moment Capacity Parametric (17 inch width)			Long Spans	Short Spans
Unstrengthened			543.15	274.05
FRCM-PBO	1 Ply	New φMn	553.143	282.22
		% increase	1.84%	2.98%
	2 Ply	New φMn	567.336	293.513
		% increase	4.45%	7.10%
	3 Ply	New φMn	581.525	304.79
		% increase	7.07%	11.22%
	4 Ply	New φMn	595.693	316.062
		% increase	9.67%	15.33%
FRCM-Carbon	1 Ply	New φMn	557.156	288.153
		% increase	2.58%	5.15%
	2 Ply	New φMn	577.319	305.365
		% increase	6.29%	11.43%
	3 Ply	New φMn	597.456	322.55
		% increase	10.00%	17.70%
	4 Ply	New φMn	617.584	339.721
		% increase	13.71%	23.96%
SRG	1 Ply	New φMn	548.541	276.952
		% increase	0.99%	1.06%
	2 Ply	New φMn	560.77	284.675
		% increase	3.24%	3.88%
	3 Ply	New φMn	572.996	292.391
		% increase	5.50%	6.69%
	4 Ply	New φMn	585.218	300.105
		% increase	7.75%	9.51%
CFRP*	1 Ply	New φMn	605.384	325.909
		% increase	11.46%	18.92%
	2 Ply	New φMn	639.411	359.866
		% increase	17.72%	31.31%
	3 Ply	New φMn	660.582	378.857
		% increase	21.62%	38.24%
	4 Ply	New φMn	678.447	394.813
		% increase	24.91%	44.07%

Highlight = chosen for final design

*for CFRP, 15 in. (381 mm) strips were used

Bridge P0058 CFRP Design

Long spans, interior girder

$L := 36.1875\,ft$

$b_w := 17in$

$h_f := 6in$

$b_e := \min\left(b_w + 2\cdot 68\frac{in}{2}, b_w + 2\cdot 8\cdot h_f, \frac{L}{4}\right) = 85\cdot in$

$h := 24in$

$d_1 := h - 2.5in = 21.5\cdot in$ $\quad$ $d_2 := d_1 - 3.75in = 17.75\cdot in$

$A_{s1} := 4\cdot 1.56in^2 = 6.24\cdot in^2$ $\quad$ $A_{s2} := 4\cdot 1.27in^2 = 5.08\cdot in^2$

$f_y := 33000psi$ $\quad$ $d := \frac{\left(A_{s1}\cdot f_y\cdot d_1 + A_{s2}\cdot f_y\cdot d_2\right)}{A_{s1}\cdot f_y + A_{s2}\cdot f_y} = 19.817\cdot in$

$f'c := 6000psi$ $\quad$ $A_s := A_{s1} + A_{s2} = 11.32\cdot in^2$

$\beta_1 := .75$

$a_0 := \left(A_{s1} + A_{s2}\right)\cdot\frac{f_y}{.85\cdot f'c\cdot b_e} = 0.862\cdot in$ $\quad$ <hf, OK

Moment Capacity before strengthening:

$M_{ns0} := \left(A_{s1} + A_{s2}\right)\cdot f_y\cdot\left(d - \frac{a_0}{2}\right) = 603.495\cdot kip\cdot ft$ $\quad$ $\phi_f := .9$

$\phi_f\cdot M_{ns0} = 543.145\cdot kip\cdot ft$

$A_{s_min} := 200\frac{b_w}{in}\cdot\frac{d\cdot psi\cdot in^2}{f_y\cdot in} = 2.042\cdot in^2$ $\quad$ <As, OK

Shear Capacity before strengthening:

$A_v := 2\cdot .2in^2 = 0.4\cdot in^2$

$s := 15in$

$V_c := \frac{2}{1000}\cdot\left(\frac{f'c}{psi}\right)^{\frac{1}{2}}\cdot\frac{b_w}{in}\cdot\frac{d\cdot kip}{in} = 52.191\cdot kip$ $\quad$ $\phi_v := .75$

$V_s := A_v\cdot f_y\cdot\frac{d}{s} = 17.439\cdot kip$

$V_n := V_c + V_s = 69.63\cdot kip$

$\phi_v\cdot V_n = 52.223\cdot kip$

Fiber Properties

Carbon FRP 5 bridges properties

$t_f := .0065in$ $f_{fuo} := 550ksi$ $\varepsilon_{fuo} := .0167\frac{in}{in}$ $E_f := 33000ksi$ $C_E := .85$

$w_f := 15in$ $f_{fu} := C_E \cdot f_{fuo} = 467.5 \cdot ksi$ $\varepsilon_{fu} := C_E \cdot \varepsilon_{fuo} = 0.014$

$n_f := 2$

$A_f := n_f \cdot w_f \cdot t_f = 0.195 \cdot in^2$ $d_f := h = 24 \cdot in$

Preliminary calcs

$\beta_1 := .75$ $E_c := 57000 \cdot (6000)^{.5} \cdot psi = 4.415 \times 10^6 \cdot psi$ $M_{DL} := 197.3kip \cdot ft$

$E_s := 29000000psi$

Design

$\rho := \frac{A_s}{b_w \cdot d} = 0.034$ $n := \frac{E_s}{E_c} = 6.568$ $k := \left[2 \cdot \rho \cdot n + (\rho \cdot n)^2\right]^{.5} - \rho \cdot n = 0.479$

$I_{cr} := n \cdot A_s \cdot (d - k \cdot d)^2 + \frac{b_w (k \cdot d)^3}{3} = 1.277 \times 10^4 \cdot in^4$

Existing Strain on soffit

$\varepsilon_{bi} := M_{DL} \cdot \frac{\left(d_f - k \cdot d\right)}{I_{cr} \cdot E_c} = 6.088 \times 10^{-4}$

Strain on FRP system

$\varepsilon_{fd1} := .083in^{.5} \cdot \left(\frac{f'c}{n_f \cdot E_f \cdot t_f}\right)^{.5} = 9.816 \times 10^{-3}$ $\varepsilon_{fd2} := .9 \cdot \varepsilon_{fu} = 0.013$

$\varepsilon_{fd} := \min\left(\varepsilon_{fd1}, \varepsilon_{fd2}\right) = 9.816 \times 10^{-3}$

Depth to N.A

$c := 2.209in$ *change c here in iterations

Effective strain in FRP and Concrete

$\varepsilon_{fe1} := .003\left[\frac{\left(d_f - c\right)}{c}\right] - \varepsilon_{bi} = 0.029$ $\varepsilon_{fe2} := \varepsilon_{fd} = 9.816 \times 10^{-3}$

$\varepsilon_{fe} := \min\left(\varepsilon_{fe1}, \varepsilon_{fe2}\right) = 9.816 \times 10^{-3}$ $\varepsilon_c := \left(\varepsilon_{fe} + \varepsilon_{bi}\right) \cdot \frac{c}{d_f - c} = 1.057 \times 10^{-3}$

Strain in Steel

$$\varepsilon_s := \left(\varepsilon_{fe} + \varepsilon_{bi}\right)\cdot\frac{(d - c)}{d_f - c} = 8.424 \times 10^{-3}$$

Stress in Steel and FRP

$$f_{s1} := E_s\cdot\varepsilon_s = 244.282\cdot ksi \qquad f_{s2} := f_y = 33\cdot ksi$$

$$f_s := \min\left(f_{s1}, f_{s2}\right) = 33\cdot ksi$$

$$f_{fe} := \min\left(E_f\cdot\varepsilon_{fe}, f_{fu}\right) = 323.921\cdot ksi$$

Calculate internal force resultants and check equilibrium

$$\varepsilon_{c'} := 1.7\cdot\frac{f'c}{E_c} = 2.31 \times 10^{-3} \qquad \beta_1 := \frac{\left(4\cdot\varepsilon_{c'} - \varepsilon_c\right)}{6\cdot\varepsilon_{c'} - 2\cdot\varepsilon_c} = 0.697 \qquad \alpha_1 := \frac{3\cdot\varepsilon_{c'}\cdot\varepsilon_c - \varepsilon_c^{\,2}}{\left(3\cdot\beta_1\cdot\varepsilon_{c'}^{\,2}\right)} = 0.556$$

$$c = 2.209\cdot in \qquad c' := \frac{\left(A_s\cdot f_s + A_f\cdot f_{fe}\right)}{\alpha_1\cdot\beta_1\cdot f'c\cdot b_e} = 2.209\cdot in \qquad \text{*iterate to force c=c`}$$

Calculate flexural strength components $\qquad a := \beta_1\cdot c = 1.539\cdot in$ <hf, O.K.

$$M_{ns} := A_s\cdot f_s\cdot\left(d - \frac{a}{2}\right) = 592.954\cdot kip\cdot ft$$

$$M_{nf} := A_f\cdot f_{fe}\cdot\left(d_f - \beta_1\cdot\frac{c}{2}\right) = 122.279\cdot kip\cdot ft \qquad \psi_f := .85$$

$$\phi M_n := \phi_f\cdot\left(M_{ns} + \psi_f\cdot M_{nf}\right) = 627.202\cdot kip\cdot ft \qquad \frac{\left(\phi M_n - \phi_f\cdot M_{ns0}\right)\cdot 100}{\left(\phi_f\cdot M_{ns0}\right)} = 15.476$$

Check service stress in FRP and Steel $\qquad \rho_f := \frac{A_f}{b_w\cdot d} = 5.788 \times 10^{-4}$

$$k := \left[\left(\rho_f\cdot\frac{E_f}{E_c} + \rho\cdot\frac{E_s}{E_c}\right)^2 + 2\cdot\left(\rho_f\cdot\frac{E_f\cdot d_f}{E_c\cdot d} + \rho\cdot\frac{E_s}{E_c}\right)\right]^{.5} - \left(\rho_f\cdot\frac{E_f}{E_c} + \rho\cdot\frac{E_s}{E_c}\right) = 0.484$$

$M_s := 383.9 kip\cdot ft$ (anticipated service moment)

$$f_{ss} := \frac{\left[\left[M_s + \varepsilon_{bi}\cdot A_f\cdot E_f\cdot\left(d_f - k\cdot\frac{d}{3}\right)\right]\cdot(d - k\cdot d)\cdot E_s\right]}{A_s\cdot E_s\cdot\left(d - k\cdot\frac{d}{3}\right)\cdot(d - k\cdot d) + A_f\cdot E_f\cdot\left(d_f - k\cdot\frac{d}{3}\right)\cdot\left(d_f - k\cdot d\right)} = 24.085\cdot ksi$$

$.8\cdot f_y = 26.4\cdot ksi$ >f.ss, O.K.

Check creep rupture limit at service of the FRP

$$f_{fs} := \left[f_{ss} \cdot \frac{E_f \cdot (d_f - k \cdot d)}{E_s \cdot (d - k \cdot d)} \right] - \varepsilon_{bi} \cdot E_f = 18.527 \cdot ksi \quad < \quad .55 \cdot f_{fu} = 257.125 \cdot ksi$$

stress is well below limit

Shear Design: 3S2 Truck

$V_u := 57.13kip$

$\varepsilon_{fv} := \min(\varepsilon_{fd}, .004) = 4 \times 10^{-3}$

$f_{fv} := \varepsilon_{fv} \cdot E_f = 132 \cdot ksi$

$n_v := 1$

$d_f := h - h_f = 18 \cdot in$

$t_f = 6.5 \times 10^{-3} \cdot in$

$s_f := 24in$

$w_f := 12in$

$A_{fv} := 2 \cdot n_v \cdot t_f \cdot w_f = 0.156 \cdot in^2$

$$V_f := A_{fv} \cdot f_{fv} \cdot \frac{d_f}{s_f} = 15.444 \cdot kip$$

$\phi_{vn} := \phi_v \cdot (V_c + V_s + V_f) = 63.806 \cdot kip$ >Vu

Check limit on FRCM and Steel

$8 \cdot f'c^{.5} \cdot psi^{.5} \cdot b_w \cdot d = 208.764 \cdot kip$

$V_s + V_f = 32.883 \cdot kip$ <limit, O.K.

Check limit on FRCM

$V_{n_new} := V_n + V_f = 85.074 \cdot kip$

$.5 \cdot V_{n_new} = 42.537 \cdot kip$ >Vf. O.K.

Bridge P0058 C-FRCM Design

Long spans, interior girder

$L := 36.1875\,ft$

$b_w := 17in$

$h_f := 6in$

$b_e := \min\left(b_w + 2\cdot 68\frac{in}{2}, b_w + 2\cdot 8\cdot h_f, \frac{L}{4}\right) = 85\cdot in$

$h := 24in$

$d_1 := h - 2.5in = 21.5\cdot in$ $\qquad$ $d_2 := d_1 - 3.75in = 17.75\cdot in$

$A_{s1} := 4\cdot 1.56in^2 = 6.24\cdot in^2$ $\qquad$ $A_{s2} := 4\cdot 1.27in^2 = 5.08\cdot in^2$

$f_y := 33000psi$ $\qquad$ $d := \frac{\left(A_{s1}\cdot f_y\cdot d_1 + A_{s2}\cdot f_y\cdot d_2\right)}{A_{s1}\cdot f_y + A_{s2}\cdot f_y} = 19.817\cdot in$

$f'c := 6000psi$

$A_s := A_{s1} + A_{s2} = 11.32\cdot in^2$

$\beta_1 := .75$

$a_0 := \left(A_{s1} + A_{s2}\right)\cdot\frac{f_y}{.85\cdot f'c\cdot b_e} = 0.862\cdot in$ $\qquad$ <hf, OK

Moment Capacity before strengthening:

$M_{ns0} := \left(A_{s1} + A_{s2}\right)\cdot f_y\cdot\left(d - \frac{a_0}{2}\right) = 603.495\cdot kip\cdot ft$ $\qquad$ $\phi_f := .9$

$\phi_f\cdot M_{ns0} = 543.145\cdot kip\cdot ft$

$A_{s_min} := 200\frac{b_w}{in}\cdot\frac{d\cdot psi\cdot in^2}{f_y\cdot in} = 2.042\cdot in^2$ $\qquad$ <As, OK

Shear Capacity before strengthening:

$A_v := 2\cdot .2in^2 = 0.4\cdot in^2$

$s := 15in$

$V_c := \frac{2}{1000}\cdot\left(\frac{f'c}{psi}\right)^{\frac{1}{2}}\cdot\frac{b_w}{in}\cdot\frac{d\cdot kip}{in} = 52.191\cdot kip$ $\qquad$ $\phi_v := .75$

$V_s := A_v\cdot f_y\cdot\frac{d}{s} = 17.439\cdot kip$

$V_n := V_c + V_s = 69.63\cdot kip$

$\phi_v\cdot V_n = 52.223\cdot kip$

Fiber Properties

Carbon FRCM

$t_f := .00618in$ $f_{fuo} := 202.2ksi$ $\varepsilon_{fuo} := .0164 \frac{in}{in}$ $E_f := 9210ksi$ $C_E := 1$

$w_f := 17in$ $f_{fu} := C_E \cdot f_{fuo} = 202.2 \cdot ksi$ $\varepsilon_{fu} := C_E \cdot \varepsilon_{fuo} = 0.016$

$n_f := 2$

$A_f := n_f \cdot w_f \cdot t_f = 0.21 \cdot in^2$ $d_f := h = 24 \cdot in$

Preliminary calcs

$\beta_1 := .75$ $E_c := 57000 \cdot (6000)^{.5} \cdot psi = 4.415 \times 10^6 \cdot psi$ $M_{DL} := 197.3kip \cdot ft$

$E_s := 29000000psi$

Design

$\rho := \frac{A_s}{b_w \cdot d} = 0.034$ $n := \frac{E_s}{E_c} = 6.568$ $k := \left[2 \cdot \rho \cdot n + (\rho \cdot n)^2\right]^{.5} - \rho \cdot n = 0.479$

$I_{cr} := n \cdot A_s \cdot (d - k \cdot d)^2 + \frac{b_w (k \cdot d)^3}{3} = 1.277 \times 10^4 \cdot in^4$

Existing Strain on soffit

$\varepsilon_{bi} := M_{DL} \cdot \frac{\left(d_f - k \cdot d\right)}{I_{cr} \cdot E_c} = 6.088 \times 10^{-4}$

Strain on FRP system

$\varepsilon_{fd} := \varepsilon_{fu} - .0043 = 0.012$

STD from Nani

Depth to N.A

$c := 1.9285in$ *change c here in iterations

Effective strain in FRP and Concrete

$\varepsilon_{fe1} := .003\left[\frac{\left(d_f - c\right)}{c}\right] - \varepsilon_{bi} = 0.034$ $\varepsilon_{fe2} := \varepsilon_{fd} = 0.012$

$\varepsilon_{fe} := \min\left(\varepsilon_{fe1}, \varepsilon_{fe2}, .12\right) = 0.012$ $\varepsilon_c := \left(\varepsilon_{fe} + \varepsilon_{bi}\right) \cdot \frac{c}{d_f - c} = 1.11 \times 10^{-3}$

Strain in Steel

$$\varepsilon_s := \left(\varepsilon_{fe} + \varepsilon_{bi}\right)\cdot\frac{(d - c)}{d_f - c} = 0.01$$

Stress in Steel and FRP

$$f_{s1} := E_s\cdot\varepsilon_s = 298.708\cdot ksi \qquad f_{s2} := f_y = 33\cdot ksi$$

$$f_s := \min\left(f_{s1}, f_{s2}\right) = 33\cdot ksi$$

$$f_{fe} := \min\left(E_f\cdot\varepsilon_{fe}, f_{fu}\right) = 111.441\cdot ksi$$

Calculate internal force resultants and check equilibrium

$$\varepsilon_{c'} := 1.7\cdot\frac{f'c}{E_c} = 2.31\times 10^{-3} \qquad \beta_1 := \frac{\left(4\cdot\varepsilon_{c'} - \varepsilon_c\right)}{6\cdot\varepsilon_{c'} - 2\cdot\varepsilon_c} = 0.698 \qquad \alpha_1 := \frac{3\cdot\varepsilon_{c'}\cdot\varepsilon_c - \varepsilon_c^{\,2}}{\left(3\cdot\beta_1\cdot\varepsilon_{c'}^{\,2}\right)} = 0.578$$

$$c = 1.929\cdot in \qquad c' := \frac{\left(A_s\cdot f_s + A_f\cdot f_{fe}\right)}{\alpha_1\cdot\beta_1\cdot f'c\cdot b_e} = 1.928\cdot in$$ *iterate to force c=c`

Calculate flexural strength components

$$a := \beta_1\cdot c = 1.347\cdot in$$ <hf, O.K.

$$M_{ns} := A_s\cdot f_s\cdot\left(d - \frac{a}{2}\right) = 595.942\cdot kip\cdot ft$$

$$\psi_f := 1$$

$$M_{nf} := A_f\cdot f_{fe}\cdot\left(d_f - \beta_1\cdot\frac{c}{2}\right) = 45.518\cdot kip\cdot ft$$

$$\phi M_n := \phi_f\cdot\left(M_{ns} + \psi_f\cdot M_{nf}\right) = 577.313\cdot kip\cdot ft \qquad \frac{\left(\phi M_n - \phi_f\cdot M_{ns0}\right)\cdot 100}{\left(\phi_f\cdot M_{ns0}\right)} = 6.291$$

Check service stress in FRP and Steel

$$\rho_f := \frac{A_f}{b_w\cdot d} = 6.237\times 10^{-4}$$

$$k := \left[\left(\rho_f\cdot\frac{E_f}{E_c} + \rho\cdot\frac{E_s}{E_c}\right)^2 + 2\cdot\left(\rho_f\cdot\frac{E_f\cdot d_f}{E_c\cdot d} + \rho\cdot\frac{E_s}{E_c}\right)\right]^{.5} - \left(\rho_f\cdot\frac{E_f}{E_c} + \rho\cdot\frac{E_s}{E_c}\right) = 0.481$$

$$M_s := 383.9 kip\cdot ft$$ (anticipated service moment)

$$f_{ss} := \frac{\left[\left[M_s + \varepsilon_{bi}\cdot A_f\cdot E_f\cdot\left(d_f - k\cdot\frac{d}{3}\right)\right]\cdot(d - k\cdot d)\cdot E_s\right]}{A_s\cdot E_s\cdot\left(d - k\cdot\frac{d}{3}\right)\cdot(d - k\cdot d) + A_f\cdot E_f\cdot\left(d_f - k\cdot\frac{d}{3}\right)\cdot\left(d_f - k\cdot d\right)} = 24.332\cdot ksi$$

$$.8\cdot f_y = 26.4\cdot ksi$$ >f.ss, O.K.

Check creep rupture limit at service of the FRP

$$f_{fs} := \left[f_{ss} \cdot \frac{E_f \cdot (d_f - k \cdot d)}{E_s \cdot (d - k \cdot d)} \right] - \varepsilon_{bi} \cdot E_f = 5.262 \cdot ksi \quad < \quad .55 \cdot f_{fu} = 111.21 \cdot ksi$$

stress is well below limit

Shear Design: 3S2 Truck

$V_u := 57.13kip$

$\varepsilon_{fv} := \min(\varepsilon_{fd}, .004) = 4 \times 10^{-3}$

$f_{fv} := \varepsilon_{fv} \cdot E_f = 36.84 \cdot ksi$

$n_v := 1$

$d_f := h - h_f = 18 \cdot in$

$t_f = 6.18 \times 10^{-3} \cdot in$

$s_f := 12in$

$w_f := 12in$

$A_{fv} := 2 \cdot n_v \cdot t_f \cdot w_f = 0.148 \cdot in^2$

$$V_f := A_{fv} \cdot f_{fv} \cdot \frac{d_f}{s_f} = 8.196 \cdot kip$$

$\phi_{vn} := \phi_v \cdot (V_c + V_s + V_f) = 58.37 \cdot kip$ >Vu

Check limit on FRCM and Steel

$8 \cdot f'c^{.5} \cdot psi^{.5} \cdot b_w \cdot d = 208.764 \cdot kip$

$V_s + V_f = 25.635 \cdot kip$ <limit, O.K.

Check limit on FRCM

$V_{n_new} := V_n + V_f = 77.826 \cdot kip$

$.5 \cdot V_{n_new} = 38.913 \cdot kip$ >Vf. O.K.

Bridge P0058 PBO Design

Short spans, interior girder

$L := 26.375ft$

$b_w := 17in$

$h_f := 6in$

$b_e := \min\left(b_w + 2 \cdot 68\frac{in}{2}, b_w + 2 \cdot 8 \cdot h_f, \frac{L}{4}\right) = 79.125 \cdot in$

$h := 20.5in$

$d := h - 2.5in = 18 \cdot in$

$f'c := 6000psi$

$\beta_1 := .75$

$f_y := 33000psi$

$A_s := 4 \cdot 1.56in^2 = 6.24 \cdot in^2$

$a := A_s \cdot \frac{f_y}{.85 \cdot f'c \cdot b_e} = 0.51 \cdot in$ <hf, OK

Moment Capacity before strengthening:

$M_{ns0} := A_s \cdot f_y \cdot \left(d - \frac{a}{2}\right) = 304.502 \cdot kip \cdot ft$ $\phi_f := .9$

$\phi_f \cdot M_{ns0} = 274.052 \cdot kip \cdot ft$

$A_{s_min} := 200\frac{b_w}{in} \cdot \frac{d \cdot psi \cdot in^2}{f_y \cdot in} = 1.855 \cdot in^2$ <As, OK

Shear Capacity before strengthening:

$A_v := 2 \cdot .2in^2 = 0.4 \cdot in^2$

$s := 12in$

$V_c := \frac{2}{1000} \cdot \left(\frac{f'c}{psi}\right)^{\frac{1}{2}} \cdot \frac{b_w}{in} \cdot \frac{d \cdot kip}{in} = 47.405 \cdot kip$ $\phi_v := .75$

$V_s := A_v \cdot f_y \cdot \frac{d}{s} = 19.8 \cdot kip$

$V_n := V_c + V_s = 67.205 \cdot kip$

$\phi_v \cdot V_n = 50.404 \cdot kip$

Fiber Properties

PBO FRCM

*Ce for FRP only

$C_E := 1$

$t_f := .002in$ $f_{fuo} := 241.343ksi$ $\varepsilon_{fuo} := .0176\frac{in}{in}$ $E_f := 18656ksi$

$w_f := 17in$ $f_{fu} := C_E \cdot f_{fuo} = 241.343 \cdot ksi$ $\varepsilon_{fu} := C_E \cdot \varepsilon_{fuo} = 0.018$

$n_f := 2$

$A_f := n_f \cdot w_f \cdot t_f = 0.068 \cdot in^2$ $d_f := h$

Preliminary calcs

$\beta_1 := .75$ $E_c := 57000 \cdot (6000)^{.5} \cdot psi = 4.415 \times 10^6 \cdot psi$ $M_{DL} := 94.3kip \cdot ft$

$E_s := 29000000psi$

Design

$\rho := \frac{A_s}{b_w \cdot d} = 0.02$ $n := \frac{E_s}{E_c} = 6.568$ $k := \left[2 \cdot \rho \cdot n + (\rho \cdot n)^2\right]^{.5} - \rho \cdot n = 0.401$

$I_{cr} := n \cdot A_s \cdot (d - k \cdot d)^2 + \frac{b_w (k \cdot d)^3}{3} = 6.896 \times 10^3 \cdot in^4$

Existing Strain on soffit

$\varepsilon_{bi} := M_{DL} \cdot \frac{\left(d_f - k \cdot d\right)}{I_{cr} \cdot E_c} = 4.939 \times 10^{-4}$

Strain on FRP system

$\varepsilon_{fd} := \varepsilon_{fu} - .0013 = 0.016$

STD from Nanni

Depth to N.A

$c := 1.3755in$ *change c here in iterations

Effective strain in FRP and Concrete

$\varepsilon_{fe1} := .003\left[\frac{\left(d_f - c\right)}{c}\right] - \varepsilon_{bi} = 0.041$ $\varepsilon_{fe2} := \varepsilon_{fd} = 0.016$

$$\varepsilon_{fe} := \min(\varepsilon_{fe1}, \varepsilon_{fe2}, .012) = 0.012 \qquad \varepsilon_c := (\varepsilon_{fe} + \varepsilon_{bi}) \cdot \frac{c}{d_f - c} = 8.986 \times 10^{-4}$$

Strain in Steel

$$\varepsilon_s := (\varepsilon_{fe} + \varepsilon_{bi}) \cdot \frac{(d - c)}{d_f - c} = 0.011$$

Stress in Steel and FRP

$$f_{s1} := E_s \cdot \varepsilon_s = 314.959 \cdot ksi \qquad f_{s2} := f_y = 33 \cdot ksi$$

$$f_s := \min(f_{s1}, f_{s2}) = 33 \cdot ksi$$

$$f_{fe} := \min(E_f \cdot \varepsilon_{fe}, f_{fu}) = 223.872 \cdot ksi$$

Calculate internal force resultants and check equilibrium

$$\varepsilon_{c'} := 1.7 \cdot \frac{f'c}{E_c} = 2.31 \times 10^{-3} \qquad \beta_1 := \frac{(4 \cdot \varepsilon_{c'} - \varepsilon_c)}{6 \cdot \varepsilon_{c'} - 2 \cdot \varepsilon_c} = 0.691 \qquad \alpha_1 := \frac{3 \cdot \varepsilon_{c'} \cdot \varepsilon_c - \varepsilon_c^{\,2}}{(3 \cdot \beta_1 \cdot \varepsilon_{c'}^{\,2})} = 0.49$$

$$c = 1.375 \cdot in \qquad c' := \frac{(A_s \cdot f_s + A_f \cdot f_{fe})}{\alpha_1 \cdot \beta_1 \cdot f'c \cdot b_e} = 1.376 \cdot in \qquad \text{*iterate to force c=c`}$$

Calculate flexural strength components

$$a := \beta_1 \cdot c = 0.951 \cdot in \qquad \text{<hf, O.K.}$$

$$M_{ns} := A_s \cdot f_s \cdot \left(d - \frac{a}{2}\right) = 300.719 \cdot kip \cdot ft \qquad \psi_f := 1$$

$$M_{nf} := A_f \cdot f_{fe} \cdot \left(d_f - \beta_1 \cdot \frac{c}{2}\right) = 25.403 \cdot kip \cdot ft \qquad < \qquad .5 \cdot M_{ns0} = 152.251 \cdot kip \cdot ft \qquad \text{O.K.}$$

$$\phi M_n := \phi_f \cdot (M_{ns} + \psi_f \cdot M_{nf}) = 293.51 \cdot kip \cdot ft \qquad \frac{(\phi M_n - \phi_f \cdot M_{ns0}) \cdot 100}{(\phi_f \cdot M_{ns0})} = 7.1$$

$$\frac{\phi M_n}{\phi_f} = 326.122 \cdot kip \cdot ft \qquad \rho_f := \frac{A_f}{b_w \cdot d} = 2.222 \times 10^{-4}$$

Check service stress in FRP and Steel

$$k := \left[\left(\rho_f \cdot \frac{E_f}{E_c} + \rho \cdot \frac{E_s}{E_c}\right)^2 + 2 \cdot \left(\rho_f \cdot \frac{E_f \cdot d_f}{E_c \cdot d} + \rho \cdot \frac{E_s}{E_c}\right)\right]^{.5} - \left(\rho_f \cdot \frac{E_f}{E_c} + \rho \cdot \frac{E_s}{E_c}\right) = 0.402$$

$$M_s := 214.53 kip \cdot ft \qquad \text{(anticipated service moment)}$$

$$f_{ss} := \frac{\left[\left[M_s + \varepsilon_{bi} \cdot A_f \cdot E_f \cdot \left(d_f - k \cdot \frac{d}{3}\right)\right] \cdot (d - k \cdot d) \cdot E_s\right]}{A_s \cdot E_s \cdot \left(d - k \cdot \frac{d}{3}\right) \cdot (d - k \cdot d) + A_f \cdot E_f \cdot \left(d_f - k \cdot \frac{d}{3}\right) \cdot (d_f - k \cdot d)} = 26.319 \cdot ksi$$

$.8 \cdot f_y = 26.4 \cdot ksi$ >f.ss, O.K.

Check creep rupture limit at service of the FRP

$$f_{fs} := f_{ss} \cdot \frac{E_f \cdot (d_f - k \cdot d)}{E_s \cdot (d - k \cdot d)} - \varepsilon_{bi} \cdot E_f = 11.65 \cdot ksi \quad < \quad .3 \cdot f_{fu} = 72.403 \cdot ksi$$

stress is well below limit

Shear Design: H20 Legal truck

$V_u := 46.52kip$ Shear strengthening not needed, but provided for anchorage

$n_v := 2$

$\varepsilon_{fv} := \min(\varepsilon_{fd}, .004) = 4 \times 10^{-3}$

$d_f := h - h_f = 14.5 \cdot in$

$f_{fv} := \varepsilon_{fv} \cdot E_f = 74.624 \cdot ksi$

$t_f = 2 \times 10^{-3} \cdot in$

$s_f := 18in$

$w_f := 12in$

$A_{fv} := 2 \cdot n_v \cdot t_f \cdot w_f = 0.096 \cdot in^2$

$V_c = 210.869 \cdot kN$

$V_s = 88.075 \cdot kN$

$$V_f := A_{fv} \cdot f_{fv} \cdot \frac{d_f}{s_f} = 5.771 \cdot kip$$

$V_f = 25.67 \cdot kN$

$\phi_{vn} := \phi_v \cdot (V_c + V_s + V_f) = 54.732 \cdot kip$ >Vu

Check limit on FRCM and Steel

$8 \cdot f'c^{.5} \cdot psi^{.5} \cdot b_w \cdot d = 189.621 \cdot kip$

$V_s + V_f = 25.571 \cdot kip$ <limit, O.K.

Check limit on FRCM

$V_{n_new} := V_n + V_f = 72.976 \cdot kip$

$.5 \cdot V_{n_new} = 36.488 \cdot kip$ >Vf. O.K.

Bridge P0058 SRG Design

Short spans, interior girder

$L := 26.375ft$

$b_w := 17in$

$h_f := 6in$

$b_e := \min\left(b_w + 2 \cdot 68\frac{in}{2}, b_w + 2 \cdot 8 \cdot h_f, \frac{L}{4}\right) = 79.125 \cdot in$

$h := 20.5in$

$d := h - 2.5in = 18 \cdot in$

$f'c := 6000psi$

$\beta_1 := .75$

$f_y := 33000psi$

$A_s := 4 \cdot 1.56in^2 = 6.24 \cdot in^2$

$a := A_s \cdot \frac{f_y}{.85 \cdot f'c \cdot b_e} = 0.51 \cdot in$ <hf, OK

Moment Capacity before strengthening:

$M_{ns0} := A_s \cdot f_y \cdot \left(d - \frac{a}{2}\right) = 304.502 \cdot kip \cdot ft$ $\phi_f := .9$

$\phi_f \cdot M_{ns0} = 274.052 \cdot kip \cdot ft$

$A_{s_min} := 200\frac{b_w}{in} \cdot \frac{d \cdot psi \cdot in^2}{f_y \cdot in} = 1.855 \cdot in^2$ <As, OK

Shear Capacity before strengthening:

$A_v := 2 \cdot .2in^2 = 0.4 \cdot in^2$

$s := 12in$

$V_c := \frac{2}{1000} \cdot \left(\frac{f'c}{psi}\right)^{\frac{1}{2}} \cdot \frac{b_w}{in} \cdot \frac{d \cdot kip}{in} = 47.405 \cdot kip$ $\phi_v := .75$

$V_s := A_v \cdot f_y \cdot \frac{d}{s} = 19.8 \cdot kip$

$V_n := V_c + V_s = 67.205 \cdot kip$

$\phi_v \cdot V_n = 50.404 \cdot kip$

SRG

Fiber Properties

$t_f := .00333in$ $f_{fuo} := 194.54ksi$ $\varepsilon_{fuo} := .0101 \frac{in}{in}$ $E_f := 13058ksi$ $C_E := 1$

$w_f := 17in$ $f_{fu} := C_E \cdot f_{fuo} = 194.54 \cdot ksi$ $\varepsilon_{fu} := C_E \cdot \varepsilon_{fuo} = 0.01$

$n_f := 2$

$A_f := n_f \cdot w_f \cdot t_f = 0.113 \cdot in^2$ $d_f := h = 20.5 \cdot in$

Preliminary calcs

$\beta_1 := .75$ $E_c := 57000 \cdot (6000)^{.5} \cdot psi = 4.415 \times 10^6 \cdot psi$ $M_{DL} := 94.3kip \cdot ft$

$E_s := 29000000psi$

Design

$\rho := \frac{A_s}{b_w \cdot d} = 0.02$ $n := \frac{E_s}{E_c} = 6.568$ $k := \left[2 \cdot \rho \cdot n + (\rho \cdot n)^2\right]^{.5} - \rho \cdot n = 0.401$

$I_{cr} := n \cdot A_s \cdot (d - k \cdot d)^2 + \frac{b_w (k \cdot d)^3}{3} = 6.896 \times 10^3 \cdot in^4$

Existing Strain on soffit

$\varepsilon_{bi} := M_{DL} \cdot \frac{\left(d_f - k \cdot d\right)}{I_{cr} \cdot E_c} = 4.939 \times 10^{-4}$

Strain on FRP system

$\varepsilon_{fd} := \varepsilon_{fu} - .003 = 7.1 \times 10^{-3}$

STD from Nani

Depth to N.A

$c := 1.701in$ *change c here in iterations

Effective strain in FRP and Concrete

$\varepsilon_{fe1} := .003 \left[\frac{\left(d_f - c\right)}{c}\right] - \varepsilon_{bi} = 0.033$ $\varepsilon_{fe2} := \varepsilon_{fd} = 7.1 \times 10^{-3}$

$$\varepsilon_{fe} := \min(\varepsilon_{fe1}, \varepsilon_{fe2}, .012) = 7.1 \times 10^{-3} \qquad \varepsilon_c := (\varepsilon_{fe} + \varepsilon_{bi}) \cdot \frac{c}{d_f - c} = 6.871 \times 10^{-4}$$

Strain in Steel

$$\varepsilon_s := (\varepsilon_{fe} + \varepsilon_{bi}) \cdot \frac{(d - c)}{d_f - c} = 6.584 \times 10^{-3}$$

Stress in Steel and FRP

$$f_{s1} := E_s \cdot \varepsilon_s = 190.936 \cdot ksi \qquad f_{s2} := f_y = 33 \cdot ksi$$

$$f_s := \min(f_{s1}, f_{s2}) = 33 \cdot ksi$$

$$f_{fe} := \min(E_f \cdot \varepsilon_{fe}, f_{fu}) = 92.712 \cdot ksi$$

Calculate internal force resultants and check equilibrium

$$\varepsilon_{c'} := 1.7 \cdot \frac{f'c}{E_c} = 2.31 \times 10^{-3} \qquad \beta_1 := \frac{(4 \cdot \varepsilon_{c'} - \varepsilon_c)}{6 \cdot \varepsilon_{c'} - 2 \cdot \varepsilon_c} = 0.685 \qquad \alpha_1 := \frac{3 \cdot \varepsilon_{c'} \cdot \varepsilon_c - \varepsilon_c^{\,2}}{(3 \cdot \beta_1 \cdot \varepsilon_{c'}^{\,2})} = 0.391$$

$$c = 1.701 \cdot in \qquad c' := \frac{(A_s \cdot f_s + A_f \cdot f_{fe})}{\alpha_1 \cdot \beta_1 \cdot f'c \cdot b_e} = 1.701 \cdot in \qquad \text{*iterate to force c=c`}$$

Calculate flexural strength components

$$a := \beta_1 \cdot c = 1.165 \cdot in \quad \text{<hf, O.K.}$$

$$M_{ns} := A_s \cdot f_s \cdot \left(d - \frac{a}{2}\right) = 298.883 \cdot kip \cdot ft \qquad \psi_f := 1$$

$$M_{nf} := A_f \cdot f_{fe} \cdot \left(d_f - \beta_1 \cdot \frac{c}{2}\right) = 17.422 \cdot kip \cdot ft \quad < \quad .5 \cdot M_{ns0} = 152.251 \cdot kip \cdot ft \quad \text{O.K.}$$

$$\phi M_n := \phi_f \cdot (M_{ns} + \psi_f \cdot M_{nf}) = 284.675 \cdot kip \cdot ft \qquad \frac{(\phi M_n - \phi_f \cdot M_{ns0}) \cdot 100}{(\phi_f \cdot M_{ns0})} = 3.876$$

Check service stress in FRP and Steel

$$\rho_f := \frac{A_f}{b_w \cdot d} = 3.7 \times 10^{-4}$$

$$k := \left[\left(\rho_f \cdot \frac{E_f}{E_c} + \rho \cdot \frac{E_s}{E_c}\right)^2 + 2 \cdot \left(\rho_f \cdot \frac{E_f \cdot d_f}{E_c \cdot d} + \rho \cdot \frac{E_s}{E_c}\right)\right]^{.5} - \left(\rho_f \cdot \frac{E_f}{E_c} + \rho \cdot \frac{E_s}{E_c}\right) = 0.402$$

$$M_s := 214.53 kip \cdot ft \qquad \text{(anticipated service moment)}$$

$$f_{ss} := \frac{\left[\left[M_s + \varepsilon_{bi}\cdot A_f\cdot E_f\cdot\left(d_f - k\cdot\frac{d}{3}\right)\right]\cdot(d - k\cdot d)\cdot E_s\right]}{A_s\cdot E_s\cdot\left(d - k\cdot\frac{d}{3}\right)\cdot(d - k\cdot d) + A_f\cdot E_f\cdot\left(d_f - k\cdot\frac{d}{3}\right)\cdot\left(d_f - k\cdot d\right)} = 26.297\cdot ksi$$

$.8\cdot f_y = 26.4\cdot ksi$ >f.ss, O.K.

Check creep rupture limit at service of the FRP

$$f_{fs} := f_{ss}\cdot\frac{E_f\cdot\left(d_f - k\cdot d\right)}{E_s\cdot(d - k\cdot d)} - \varepsilon_{bi}\cdot E_f = 8.143\cdot ksi \quad < \quad .3\cdot f_{fu} = 58.362\cdot ksi$$

stress is well below limit

Shear Design: H20 Legal truck

$V_u := 46.52kip$ Shear strengthening not needed, but provided for anchorage

$n_v := 2$

$\varepsilon_{fv} := \min\left(\varepsilon_{fd}, .004\right) = 4 \times 10^{-3}$

$d_f := h - h_f = 14.5\cdot in$

$f_{fv} := \varepsilon_{fv}\cdot E_f = 52.232\cdot ksi$

$t_f = 3.33 \times 10^{-3}\cdot in$ $s_f := 18in$

$w_f := 12in$ $A_{fv} := 2\cdot n_v\cdot t_f\cdot w_f = 0.16\cdot in^2$

$$V_f := A_{fv}\cdot f_{fv}\cdot\frac{d_f}{s_f} = 6.725\cdot kip$$

$\phi_{vn} := \phi_v\cdot\left(V_c + V_s + V_f\right) = 55.448\cdot kip$ >Vu

Check limit on FRCM and Steel

$8\cdot f'c^{.5}\cdot psi^{.5}\cdot b_w\cdot d = 189.621\cdot kip$

$V_s + V_f = 26.525\cdot kip$ <limit, O.K.

Check limit on FRCM

$V_{n_new} := V_n + V_f = 73.931\cdot kip$

$.5\cdot V_{n_new} = 36.965\cdot kip$ >Vf. O.K.

APPENDIX D.
SHEAR STRENGTHENING WRAPPING SCHEME

C-FRCM: (2 girders, 1 ply)

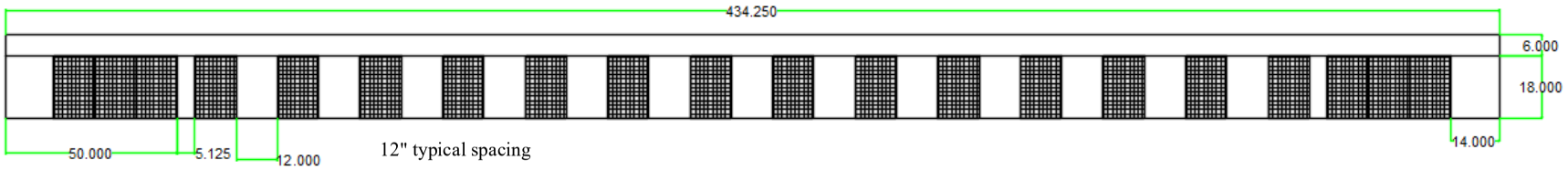

CFRP: (1 girder, 1 ply)

SRG: (2 girders, 2 ply) and PBO: (1 girder, 2 ply)

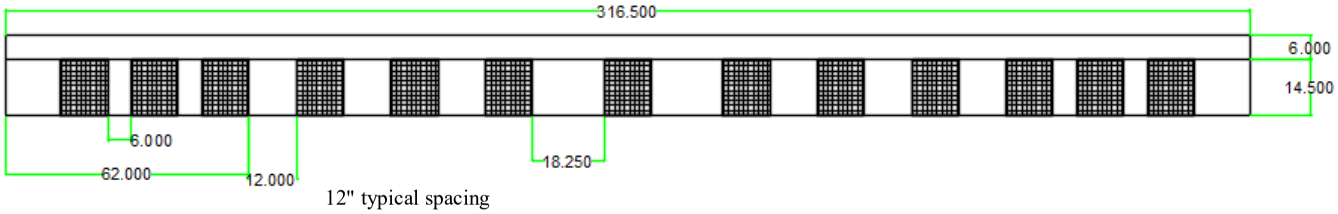

All wraps 12" wide
All schemes symmetric about center line
Dimensions shown in inches. 1 in. = 25.4 mm

APPENDIX E.
BILL OF MATERIALS

Detailed Bill of Materials

1) Carbon FRCM:

1.1) Flexural reinforcement: 2 girders, 2 plies

$A_{fl} := 2 \cdot 2 \cdot 17\,in \cdot 36.1875\,ft = 205.062\,ft^2$ $l_{fl} := 2 \cdot 2 \cdot 36.1875\,ft = 144.75\,f$ **(linear)**

1.2) Shear Reinforcement: 2 girders, 1 ply

$A_{sh} := 2 \cdot 1 \cdot 20 \cdot 12\,in \cdot 4.41666\,ft = 176.666\,ft^2$ $l_{sh} := 2 \cdot 1 \cdot 20 \cdot 4.4166\,ft = 176.66$ **(linear)**

Total:

$A := A_{fl} + A_{sh} = 381.729\,ft^2$ $l := l_{fl} + l_{sh} = 321.414\,ft$ **(linear)**

2) Carbon FRP:

2.1) Flexural reinforcement: 1 girders, 2 plies

$A_{fl} := 1 \cdot 2 \cdot 15\,in \cdot 36.1875\,ft = 90.469\,ft^2$ $l_{fl} := 1 \cdot 2 \cdot 36.1875\,ft = 72.375\,f$ **(linear)**

2.2) Shear Reinforcement: 1 girders, 1 ply

$A_{sh} := 1 \cdot 1 \cdot 18 \cdot 12\,in \cdot 4.41666\,ft = 79.5\,ft^2$ $l_{sh} := 1 \cdot 1 \cdot 18 \cdot 4.4166\,ft = 79.499\,f$ **(linear)**

Total:

$A := A_{fl} + A_{sh} = 169.969\,ft^2$ $l := l_{fl} + l_{sh} = 151.874\,ft$ **(linear)**

3) SRG:

3.1) Flexural reinforcement: 2 girders, 2 plies

$A_{fl} := 2 \cdot 2 \cdot 17\,in \cdot 26.375\,ft = 149.458\,ft^2$ $l_{fl} := 2 \cdot 2 \cdot 26.375\,ft = 105.5\,ft$ **(linear)**

3.2) Shear Reinforcement: 2 girders, 2 ply

$A_{sh} := 2 \cdot 2 \cdot 13 \cdot 12\,in \cdot 3.83333\,ft = 199.333\,ft^2$ $l_{sh} := 2 \cdot 2 \cdot 13 \cdot 3.83333\,ft = 199.333\,ft$ **(linear)**

Total:

$A := A_{fl} + A_{sh} = 348.791\,ft^2$ $l := l_{fl} + l_{sh} = 304.833\,ft$ **(linear)**

4) PBO:

4.1) Flexural reinforcement: 1 girders, 2 plies

$\mathbf{A_{fl}} := 1 \cdot 2 \cdot 17\mathbf{in} \cdot 26.375\mathbf{ft} = 74.729\,\mathbf{ft}^2$ $\mathbf{l_{fl}} := 1 \cdot 2 \cdot 26.375\mathbf{ft} = 52.75\,\mathbf{ft}$ **(linear)**

4.2) Shear Reinforcement: 1 girders, 2 ply

$\mathbf{A_{sh}} := 1 \cdot 2 \cdot 13 \cdot 12\mathbf{in} \cdot 3.83333\,\mathbf{ft} = 99.667\,\mathbf{ft}^2$ $\mathbf{l_{sh}} := 1 \cdot 2 \cdot 13 \cdot 3.83333\,\mathbf{ft} = 99.667$ **(linear)**

Total:

$\mathbf{A} := \mathbf{A_{fl}} + \mathbf{A_{sh}} = 174.396\,\mathbf{ft}^2$ $\mathbf{l} := \mathbf{l_{fl}} + \mathbf{l_{sh}} = 152.417\,\mathbf{ft}$ **(linear)**

APPENDIX F.
MANUFACTURER'S MATERIAL INFORMATION

GeoSteel G600

GeoSteel G600 Hardwire™ is a unidirectional sheet made of ultra-high strength galvanized steel micro-cords, fixed to a fibreglass micromesh to facilitate installation, which can be installed using a GeoCalce® Fino or GeoLite® or GeoLite® Gel matrix according to project and building site requirements.

The structural strengthening GeoSteel sheet is thus extremely easy to handle and shape, and combines excellent mechanical and installation properties with high durability thanks to galvanization of the individual wires. Galvanized steel fiber sheets guarantee unique structural and mechanical properties, much higher than traditional carbon-glass-aramide fibre sheets, making them particularly effective in the various structural strengthening and seismic upgrade or compliance retrofit solutions, as well as the creation of suitable connection systems, when combined with GeoSteel Injector&Connector.

PRODUCT STRENGTHS

- High durability thanks to the special steel wire galvanization process, tested using strict durability tests in a chloride, freeze-thaw and high humidity environment
- Specifically intended for structural strengthening using:
  - GeoCalce® Fino, with pure natural hydraulic NHL 3.5 lime and mineral geo-binder base, ideal for retrofitting structural elements made of brick, natural stone, and tuff masonry and substrates that require advanced breathability along with high mechanical adhesion
  - GeoLite®, with mineral geo-binder base, ideal for retrofitting structural elements in reinforced concrete, prestressed reinforced concrete or good consistency masonry
  - GeoLite® Gel, epoxy-based mineral adhesive, ideal for structural retrofitting sections made of reinforced concrete, prestressed reinforced concrete, wood and steel
- Can be tensioned to create structural reinforcements and active devices using particular mechanical anchoring systems, thanks to the unique characteristics of the textile which do not require advance impregnation of the sheet, and at the same time allow it to be anchored and fastened with metal plates without having to take particular precautions, as is necessary for all the other types of fibre and textile on the market
- Can be shaped using GeoSteel Bender which allows the sheet to be modelled easily without altering its mechanical properties to create surround brackets for beams and pillars and other bent elements required during structural consolidation works

AREAS OF USE

Use

- Static and seismic upgrade or compliance retrofit of structural elements in brick, natural stone, tuff, reinforced concrete, prestressed reinforced concrete, wood, and steel walls
- Consolidation of brick masonry, natural stone and tuff arches, vaults and domes
- Confinement and wrapping of masonry and reinforced concrete structural elements
- Flexural, shear, and confinement strengthening of brick, natural stone, tuff, and masonry panels and reinforced concrete sections
- Flexural, shear, and confinement strengthening for timber elements
- Flexural strengthening for steel girders
- Execution of top ring beams or in breach in reinforced masonry
- Execution of special single- or double-fibre thread connectors for anchoring sheets and grids and executing reinforced injections

INSTRUCTIONS FOR USE

Preparation

The ultra-high strength galvanized steel fibre sheet, GeoSteel G600 Hardwire™, is ready-to-use.
The sheet can be cut at right angles to the cords with manual or electric shears, or parallel with the cords using a normal box cutter. The sheet, cut into strips even just a few cm wide and a number of metres long, ensures perfect stability without in any way compromising the workability of the material and its application.

Preparation of substrates

The substrate must be properly prepared and cleaned, always in accordance with the instructions dictated by the construction supervisor.
When the substrates are not damaged, simply clean and remove any dust or oils that could compromise the adhesion of the system, using compressed air or pressure water.
When the substrate is clearly degraded, uneven, or damaged by significant events, proceed as follows, always in accordance with the construction supervisor:

1. For masonry, tuff, and natural stone substrates:
   - Completely remove residues from previous processes that could compromise adhesion, and any quantity of inconsistent rendering mortars from between the stones;

KERAKOLL
The GreenBuilding Company

INSTRUCTIONS FOR USE

- Saturation, spray, or brush application, if required, of certified natural stabilizing cortical consolidant with base of pure stabilised potassium silicate in aqueous solution such as Biocalce® Silicato Consolidante or water-based eco-friendly solvent-free stabilizing agent, such as Rasobuild® Eco Consolidante;
- Reconstruction, if necessary, of material continuity according to design instructions and the construction supervisor.
- Levelling previously consolidated surfaces with geo-mortar with a base of pure natural hydraulic lime NHL 3.5 and mineral geo-binder such as GeoCalce® or GeoCalce® Fino, depending on the thickness required;

2. For substrates in reinforced concrete or prestressed reinforced concrete:
   - Thorough removal of weakened concrete if necessary, through mechanical scarification or hydro-demolition, making sure to roughen the substrate to a depth of at least 5 mm;
   - Removal of rust, if any, from reinforcing bars, which must be cleaned by brushing (manual or mechanical) or sandblasting;
   - Monolithic reconstruction or smoothing of the section, if needed, using geo-mortar based on a mineral geo-binder such as GeoLite®.
   - When applying the reinforcing system with an inorganic matrix, make sure that the substrate is appropriately dampened (follow the directions on the GeoLite® or GeoCalce® data sheets).
   - When applying the reinforcing system with an organic matrix, the substrate must be dry and free of humidity (follow the instructions on the GeoLite® Gel data sheet).

Application

Execution of steel fibre structural reinforcement in Steel Reinforced Mortar (combination of steel fibre and GeoCalce® Fino or GeoLite®), or Steel Reinforced Polymer (combination of steel fibre and GeoLite® Gel epoxy mineral adhesive) will be followed by application of a first layer of geo-mortar, making sure there is sufficient material for the substrate (average thickness = 3 - 5 mm) to even it out and to lay and incorporate the reinforcing sheet. When using an epoxy mineral adhesive matrix, the substrate can be levelled using GeoLite® or GeoCalce®, taking care to allow the geo-mortar to cure for long enough to ensure that the humidity of the substrate is appropriate for application of GeoLite® Gel. The first layer of adhesive must be an average thickness of = 2 - 3 mm. Afterward, working over the matrix while it is still wet, apply the ultra-high strength galvanized steel fibre sheet GeoSteel G600 Hardwire™, making sure that the sheet is perfectly incorporated into the matrix by pressing with a spreader or steel roller, and also checking that it comes out between the cords to ensure optimum adhesion between the first and second layers of matrix. At longitudinal overlapping points, overlay two layers of steel fibre sheet by least 15 cm for epoxy matrix and 30 cm for inorganic matrices. For organic and inorganic matrix, working wet on wet, perform the final protective smoothing (= 1 -2 mm thick for organic matrix, = 2 -3 mm thick for inorganic), in order to fully incorporate the reinforcement and fill in any underlying voids. If there are additional layers after the first, proceed with laying of the second layer of steel fibre over the matrix while it is still wet, repeating the steps described above. In the event that the system installed with epoxy matrix must be plastered or concealed by smoothing, we recommend that, while the resin is still wet, you apply a spray of mineral quartz to provide better adhesion for subsequent layers.
If the reinforcing system is installed in especially aggressive environments, or you otherwise wish to ensure additional protection beyond that already provided by the matrix, we recommend applying:
- GeoLite® Microsilicato on reinforcement systems with GeoLite® or GeoCalce® Fino matrix;
- Keralover Eco Acrilex Flex on reinforcement systems with GeoLite® Gel matrix.

If the works are in permanent or occasional contact with water, the cycles described above must be replaced with a polyurethane epoxy cycle or an osmotic cement depending on the needs of the worksite and the design specifications.
For technical specifications, application, and preparation of the matrix, as well as protective systems adequate for the matrix type, consult the relevant data sheets.

Creating a GeoSteel Connector

A steel-fibre thread connector system is created by including a band of fabric of appropriate width from the GeoSteel Hardwire™ line to provide the minimum number of cords in the connector according to the design, in order to achieve the required tensile strength; make sure to unravel the end of the fabric band by cutting the supportive mesh, making the cut parallel to the cords themselves to the length of the edge you want to create on the masonry. In the event of a connector with threads on both sides, this operation must be performed on both ends of the duly arranged fibre strip. Once the sheet is cut, roll the band onto itself, taking care to create a cylinder of an appropriate diameter compared to the hole.
Install the connector that has been created into the hole, and then insert the Geosteel glass fibre-reinforced polypropylene GeoSteel Injector&Connector, so that the end of the fibre bends 90°. Finally, using the special hole located on the head of the piece, inject the pourable mortar, such as GeoCalce® Fluido, to grout the fibre-thread connector system. When this phase is complete, the GeoSteel Injector&Connector must be duly sealed with the cap provided.
Depending on the type of substrate (concrete or masonry) for grouting the connector, as an alternative to the use of pourable natural hydraulic lime, the designer may choose to use pourable cement-based mortar Kerabuild® Eco Binder, thixotropic epoxy resin GeoLite® Gel or superfluid Kerabuild® Epofill.

Provided below is a table listing the tensile strength of a connector as a function of the type of GeoSteel Hardwire™ sheet and the corresponding widths of the band adopted:

Sheet	Width of the band (cm)	Number of Cords*	Tensile breaking load
GeoSteel G600	10	16	>24 kN
GeoSteel G600	15	23	>35 kN

*n° cords/cm = 1,57;
tensile breaking load of a cord > 1500 N.

In the event that a connector with another strength or a different number of cords from those listed is required, simply calculate the appropriate width of the band by dividing the required strength by the strength of one cord and then by the number of cords present per unit of width in the type of sheet selected.
Test reports are available upon request to determine the calculation parameters.

SCHEDA GeoSteel G600 Cod. # 08 05 2014/07

KERAKOLL
The GreenBuilding Company

ABSTRACT

SRM-GeoCalce® GeoSteel G600

Execution of structural reinforcement or repair, seismic upgrade of masonry, tuff, or natural stone elements and structures using a composite system based on ultra-high strength galvanized steel fibre sheet GeoSteel G600 Hardwire™ from Kerakoll Spa, with net fibre weight of ≈ 600 g/m², with the following mechanical characteristics: sheet tensile strength > 2600 MPa; sheet elastic modulus > 190 GPa; sheet break deformation > 1.50%; nominal area of a cord 3x2 (5 wires) = 0.536 mm²; no. cords per cm = 1.57; sheet equivalent thickness = 0.064 mm, impregnated with certified inorganic matrix of natural, structural, breathable, eco-friendly geo-mortar based on pure natural hydraulic lime NHL 3.5 and mineral geo-binder, such as GeoCalce® Fino by Kerakoll Spa, to be applied directly on the structure requiring reinforcement.

The procedure is conducted as follows:

1. *Any restoration of degraded, weakened, non-cohesive, or non-planar surfaces with GeoCalce® by Kerakoll Spa, in the case of masonry substrates, or GeoLite® by Kerakoll Spa, in the case of reinforced concrete substrates, and in all cases as dictated and approved by the construction supervisor;*
2. *Lay a first layer, an average of ≈ 3 - 5 mm thick of geo-mortar with pure natural NHL 3.5 and mineral geo-binder base, such as GeoCalce® Fino by Kerakoll Spa;*
3. *While the mortar is still wet, lay the ultra-high strength galvanized steel fibre sheet GeoSteel G600 Hardwire™ by Kerakoll Spa, and by pressing firmly with a smooth spreader or metal roller, make sure that the sheet is completely impregnated and avoid allowing any gaps or air bubbles to form, because these can compromise the adhesion of the sheet to the matrix or to the substrate;*
4. *Working wet on wet, apply the second layer of geo-mortar based on pure natural lime NHL 3.5 and mineral geo-binder, such as GeoCalce® Fino by Kerakoll Spa, ≈ 2 – 3 mm thick to fully incorporate the reinforcing sheet and fill in any remaining underlying gaps;*
5. *Repeat steps ③ and ④ if necessary for all subsequent reinforcing layers called for by the design.*

Delivery and installation of all the materials described above as well as everything else required to finish the job is included. The following are excluded: restoration of degraded areas and repair of the substrate; anchoring devices using connectors or metal plates; material acceptance tests; pre- and post-procedure testing, all aids required to perform the work.

The price is by unit of reinforcing surfaces actually laid, including overlaps and anchoring sections.

SRM-GeoLite® GeoSteel G600

Execution of structural reinforcement or repair, or seismic upgrade or compliance retrofit of reinforced cement, masonry, tuff, or natural stone elements and structures using a composite system based on ultra-high strength galvanized steel fibre sheet GeoSteel G600 Hardwire™ from Kerakoll Spa, with net fibre weight of ≈ 600 g/m², with the following mechanical characteristics: sheet tensile strength > 2600 MPa; sheet elastic modulus > 190 GPa; sheet break deformation > 1.50%; nominal area of a cord 3x2 (5 wires) = 0.536 mm²; no. cords per cm = 1.57; sheet equivalent thickness = 0.064 mm, impregnated with inorganic matrix of eco-friendly, thixotropic, normal-setting certified mineral geo-mortar, based on crystalline reaction geo-binder and zirconium, with very low petrochemical polymer content and free of organic fibres, specifically for passivation, restoration, smoothing, and guaranteed, long-lasting monolithic protection of structures in concrete, such as GeoLite® by Kerakoll Spa, to be applied directly on the structure requiring reinforcement.

The procedure is conducted as follows:

1. *Any restoration of degraded, weakened, non-cohesive, or non-planar surfaces shall be performed with GeoCalce® by Kerakoll Spa, in the case of masonry substrates, or GeoLite® by Kerakoll Spa, in the case of reinforced concrete substrates, and in all cases as dictated and approved by the construction supervisor;*
2. *Spread a first layer of approximate average thickness of ≈ 3 - 5 mm of geo-mortar with mineral geo-binder base, such as GeoLite® by Kerakoll Spa;*
3. *While the mortar is still wet, lay the ultra-high strength galvanized steel fibre sheet GeoSteel G600 Hardwire™ by Kerakoll Spa, and by pressing firmly with a smooth spreader or metal roller, make sure that the sheet is completely impregnated and avoid allowing any gaps or air bubbles to form, because these can compromise the adhesion of the sheet to the matrix or to the substrate;*
4. *Working wet on wet, apply the second layer of geo-mortar, such as GeoLite® by Kerakoll Spa, approximately ≈ 2 -3 mm thick, until the reinforcing sheet is fully incorporated and any underlying voids are filled;*
5. *Repeat steps ③ and ④ if necessary for all subsequent reinforcing layers called for by the design.*

Delivery and installation of all the materials described above as well as everything else required to finish the job is included. The following are excluded: restoration of degraded areas and repair of the substrate; anchoring devices using connectors or metal plates; material acceptance tests; pre- and post-procedure testing, all aids required to perform the work.

The price is by unit of reinforcing surfaces actually laid, including overlaps and anchoring sections.

SRP GeoSteel G600

Execution of structural reinforcement or repair, or seismic upgrade or compliance retrofit of reinforced cement, masonry, wood and steel using a composite system based on ultra-high strength galvanized steel fibre sheet GeoSteel G600 Hardwire™ from Kerakoll Spa, with net fibre weight of ≈ 600 g/m², with the following mechanical characteristics: sheet tensile strength > 2600 MPa; sheet elastic modulus > 190 GPa; sheet break deformation >1.50%; nominal area of a cord 3x2 (5 wires) = 0.536 mm²; no. cords per cm = 1.57; sheet equivalent thickness = 0.064 mm, impregnated with epoxy mineral matrix such as GeoLite® Gel by Kerakoll Spa to be applied directly on the structure requiring reinforcement without any need for primer.

The procedure is conducted as follows:

1. *Any restoration of degraded, weakened, non-cohesive, or non-planar surfaces shall be performed with GeoCalce® by Kerakoll Spa, in the case of masonry substrates, or GeoLite® by Kerakoll Spa, in the case of reinforced concrete substrates, and in all cases as dictated and approved by the construction supervisor;*
2. *Application of a first layer approximately average thickness of ≈ 2 - 3 mm of epoxy mineral adhesive such as GeoLite® Gel by Kerakoll Spa;*
3. *While the epoxy mineral adhesive is still wet, lay the ultra-high strength galvanized steel fibre sheet GeoSteel G600 Hardwire™ by Kerakoll Spa, and by pressing firmly with a smooth spreader or metal roller, make sure that the sheet is completely impregnated and avoid allowing any gaps or air bubbles to form, because these can compromise the adhesion of the reinforcing system to the substrate;*
4. *Working wet on wet, lay the second layer of matrix, such as GeoLite® Gel by Kerakoll Spa, at an average thickness of ≈ 1 – 2 mm, until the reinforcing sheet is completely covered;*
5. *Repeat steps ③ and ④ if necessary for all subsequent reinforcing layers called for by the design.*

Delivery and installation of all the materials described above as well as everything else required to finish the job is included. The following are excluded: restoration of degraded areas and repair of the substrate; anchoring devices using connectors or metal plates; material acceptance tests; pre- and post-procedure testing, all aids required to perform the work.

The price is by unit of reinforcing surfaces actually laid, including overlaps and anchoring sections.

0525Geosteel G600 Code # 88553014/07

KERAKOLL
The GreenBuilding Company

TECHNICAL DATA COMPLIANT WITH KERAKOLL QUALITY STANDARD

Wire			
	- characteristic tensile stress	σ_{wire}	> 2900 MPa
	- elastic modulus	E_{wire}	> 205 GPa
	- area	A_{wire}	0,1076 mm^2
Dry sheet/Cord			
Cord 3x2 obtained by joining 5 filaments, of which 3 straight and 2 wrapped with a high torque angle			
	- actual area of a cord 3x2 (5 wires)	A_{cord}	0,538 mm^2
	- n° cords/cm		1,57 cords/cm
	- mass (inclusive of thermal welding)		≈ 670 g/m^2
	- equivalent thickness of sheet	t_{sheet}	≈ 0,084 mm
	- tensile breaking load of a cord		> 1500 N
	- tensile strength of the sheet	σ_{sheet}	> 2800 MPa
	- tensile strength by unit of width	σ_{sheet}	> 2,35 kN/cm
	- normal elastic modulus of sheet	E_{sheet}	> 198 GPa
	- break warp of the sheet	ε_{sheet}	> 1,50%
Pack	50 m rolls (h 30 cm)		
Weight of 1 roll	≈ 24 kg including packaging		

WARNING

- **Product for professional use**
- abide by any standards and national regulations
- when handling the sheet wear protective clothing and goggles, and follow the instructions regarding methods for applying the material
- contact with the skin: no special measures required
- storage on the work site: store under cover in a dry place, well away from substances that might damage it or its ability to adhere to the chosen matrix
- if necessary, ask for the safety data sheet
- for any other issues, contact the Kerakoll Worldwide Global Service +39 0536 811 516 - globalservice@kerakoll.com

This information was last updated in July 2014: please note that additions and/or amendments may be made over time by KERAKOLL S.p.A. for the latest version, see www.kerakoll.com. KERAKOLL S.p.A. shall therefore be liable for the validity, accuracy and updating of information provided only when taken directly from its institutional website. The technical data sheet given here is based on our technical and practical knowledge. As it is not possible for us to directly check the conditions in your building yard and the execution of the work, this information represents general indications that do not bind Kerakoll in any way. Therefore, it is advisable to perform a preliminary test to verify the suitability of the product for your purposes.

KERAKOLL S.p.a.
Via dell'Artigianato, 9 - 41049 Sassuolo (MO) Italy
Tel +39 0536 816 511 - Fax +39 0536 816 581
info@kerakoll.com - www.kerakoll.com

Ruredil X Mesh Gold

PBO (Poliparafenilenbenzobisoxazolo) mesh in a stabilised inorganic matrix for flexural and shear strenght reinforcement of concrete

Product description

RUREDIL X MESH GOLD is a patented new FRCM (Fibre Reinforced Cementitious Matrix) system, a ground-breaking application of FRP or high performance fibre structural reinforcement systems called FRP.

The RUREDIL X MESH GOLD system consists of a Polyparaphenylene benzobisoxazole (PBO) mesh and a stabilised inorganic matrix designed to connect the mesh with the concrete substrate.

Its outstanding mechanical performance allows this composite material to equal the performance of conventional carbon fibre FRP's with epoxy binders.

Typical applications

RUREDIL X MESH GOLD is suitable for reinforcement of reinforced concrete and pre-compressed reinforced concrete structures, including those subject to the simultaneous action of fire and high temperatures.

RUREDIL X MESH GOLD is applied to reinforced concrete and pre-compressed reinforced concrete structures for:

- Flex reinforcement;
- Shear strength;
- Torsion reinforcement;
- Confinement of beam columns with low eccentricity;
- Confinement and longitudinal reinforcement of beam columns with high eccentricity.

RUREDIL X MESH GOLD is suitable for work in seismic zones for:

- increasing resistance to simple flex fatigue or combined pressing and bending action of pillars and beams;
- increasing resistance to shear stress of pillars and beams;
- increasing the flexibility of the terminal portions of beams and pillars by binding;
- increasing the resistance to tensile stress of the panels of beam-pillar nodes with fibres aligned with tensile stress isostatics.

Packaging, storage, dosage and yield

- RUREDIL X MESH GOLD: roll of PBO fibre mesh 100 cm wide and 15 m long.

  Store in a dry place away from heat.
- RUREDIL X MESH M750: inorganic stabilised matrix, 25 Kg bags.
- For 1 15 m roll of RUREDIL X MESH GOLD about 5 bags of RUREDIL X MESH M750 mortar are required.
- As RUREDIL X MESH M750 is inorganic it is sensitive to damp, and must be kept indoors in a dry place. Use up the whole package once it has been opened.

  Store at temperatures between +5°C and +35°C.

Benefits as compared to conventional FRPs

RUREDIL X MESH GOLD offers the following benefits over an FRP system employing epoxy or polyester resins:

Same resistance to high temperatures as substrate

The structural properties of FRP systems depend on temperature. The glassy transition temperature (Tg) of epoxy resins – normally between 40 and 80 °C – is the chemical/physical quantity determining the performance of an FRP system, independently of the fiber used (carbon, aramid, etc.)

When the outdoor temperature exceeds the glassy transition temperature, the epoxy resin is no longer capable of serving the function of transferring stress from the structure to the high modulus fiber buried in it, making it ineffective as structural reinforcement. This behavior is attributable to total loss of the adhesive bond between the resin and the fiber and/or between the resin and the support.

RUREDIL X MESH GOLD is not influenced by outdoor temperature after it hardens, and is fire-resistant because it is inorganic, like the concrete base. FRP systems not only fail to resist fire, but contribute to it by emitting toxic fumes.

Moisture resistance

RUREDIL X MESH GOLD's adhesion to concrete is not affected by relative humidity, unlike FRP systems. Epoxy resin degrades with prolonged exposure to moisture, losing its adhesive properties and therefore its ability to transfer stress to structural fiber.

Applicability of inorganic material to damp substrates

FRP systems can only be applied to dry substrates, as polyester and epoxy resins will not catalyse in the presence of water.

Ease of handling

The premixed substance is mixed with the amount of water specified in the instructions and applied like a conventional cement mortar, with the PBO structural mesh buried in it.

Workability

There are essentially no differences in workability time between 5 °C and 40 °C. Resins' pot life depends on temperature, which limits applicability of FRPs under unfavourable temperature and humidity conditions.

It is not toxic like the resins used in FRPs

RUREDIL X MESH GOLD is applied under ordinary working conditions applicable to cement mortars.

Tools may be cleaned with water

FRPs require cleaning with special solvents and, in many cases, tools cannot be used again.

Ruredil X Mesh Gold

PBO (Poliparafenilenbenzobisoxazolo) mesh in a stabilised inorganic matrix for flexural and shear strenght reinforcement of concrete

Recommendations for use

a) Preparing the substrate

Eliminate dust and loose parts, then gently sand mechanically or with a high-pressure water jet cleaner to completely eliminate the thin layer of cement grout. Be careful to remove residues from surface treatments such as paint, release agents, insulation, etc. Make sure the surface is flat after this operation.
In the presence of macroscopic surface defects, correct with mortars from the EXOCEM line.Always bevel corners if they are to be bound with composite material.

b) Preparing RUREDIL X MESH M750 matrix

Pour about 90% of the required amount of water into the mixer, then start the mixer and add RUREDIL X MESH M750 uninterruptedly to prevent lumps from forming.Mix for 2-3 minutes; add the rest of the water up to the quantity specified in the technical information sheet and mix for 1-2 minutes more.
Let the mix rest for about 2-3 minutes, then mix again and apply.

c) Applying the RUREDIL X MESH GOLD system

Dampen the substrate, saturating it with water and being sure to remove excess water. Apply RUREDIL X MESH M750 with a smooth metal trowel in a layer about 3-4 mm thick; wait a couple of minutes and then bury RUREDIL X MESH GOLD in it. Apply a second layer of RUREDIL X MESH M750 about 3-4 mm thick to cover the mesh completely.
If the mortar becomes unworkable, do not add any more water, but mix for about 1-2 minutes and then continue applying.
The RUREDIL X MESH GOLD system should not be applied in sunshine, during the hot hours of the day in summer, or with moderate or strong winds.
If it is raining, shelter the structure from the rain.

d) Effect of temperature

The product should be applied at temperatures of between +5 °C and +35 °C; low temperatures (4-10°C) will slow down setting considerably; while high temperatures (35-50 °C) will rapidly cause the mortar to become unworkable.

e) Curing

In environments exposed to sun and wind protection may be required (CURING S or wet non-woven fabric). If it is about to rain, shelter the reinforcement appropriately.

Properties of system RUREDIL X MESH GOLD

PBO fibres properties

Density (g/cm^3)	1,56
Tensile strength (GPa)	5,8
Modulus of elasticity (GPa)	270
Ultimate deformation (%)	2,15
Breakdown temperature (°C)	650
Coefficient of thermal dilation (10^{-6} °C^{-1})	-6

Mesh properties

Weight of PBO fibres in the mesh	88 g/m^2
Equivalent dry fabric thickness in the direction of the warp	0,0455 mm
Equivalent dry fabric thickness in the direction of the weft	0,0115 mm
Ultimate tensile stress of the warp per unit of width	264,0 kN/m
Ultimate tensile stress of the weft per unit of width	66,5 kN/m
Mesh weight (Substrate + PBOfiber)	110 to 126 g/m^2

Inorganic matrix properties

Consistency (UNI EN 13395-1)	175
Specific weight of fresh mortar	1,80 ± 0,05 g/cc
Litres of H_2O for 100 kg of Ruredil X Mesh M750	25 - 27
Yield kg/m^2/mm (dry product)	1,400
Compressive strength (UNI EN 196-1)	≥ 30.0 MPa (at 28 days)
Bending strength (UNI EN 196-1)	≥ 4.0 MPa (at 28 days)
Secant modulus of elasticity (UNI EN 13412)	≥ 7000 MPa (at 28 days)

Durability of the RUREDIL X MESH GOLD system

The mechanical properties of the RUREDIL X MESH GOLD system are not influenced by high temperatures and fire since the binding matrix is inorganic, as in all FRCM systems. The graphic shown in figure N.1 illustrates the load increase of samples reinforced with RUREDIL X MESH GOLD exposed to different temperatures, compared with samples without reinforcement. It should be pointed out that bending strength of concrete drastically decreases at temperatures exceeding +130 °C.

RUREDIL X MESH GOLD: LOAD INCREASE ACCORDING TO TEMPERATURE

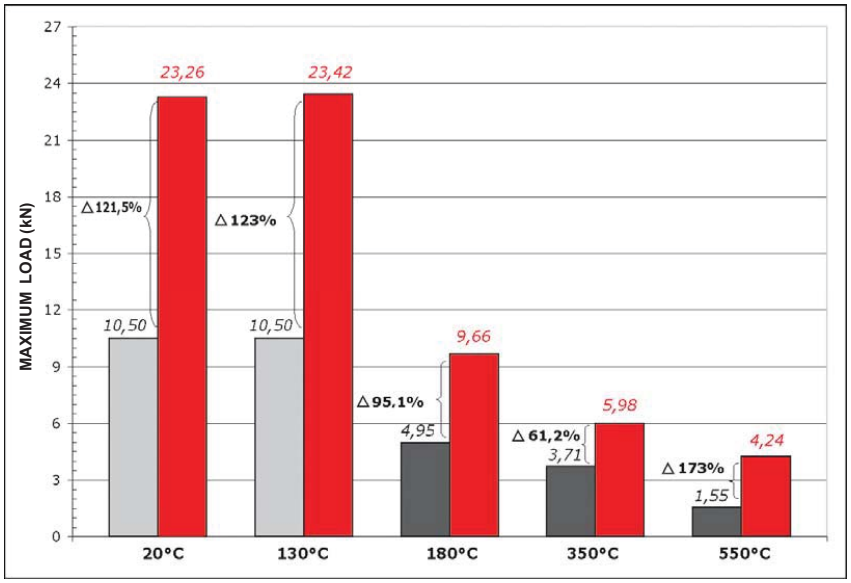

Figure 1

In fact, traditional FRP systems completely lose their mechanical properties after one hour of exposure to +80°C because rigid resin becomes gummy. In addition, resin becomes unable to transfer concrete stress to carbon fibre as from +45°C (Figure N.2).

According to the accelerated tests performed at +80°C thermohygrometric conditions and 100% relative humidity, PBO-FRCM reinforcement does not have any chemical or mechanical alterations whereas C-FRP loses 100% of its efficiency (Figure N.3).

C- FRP: Maximum load according to temperature with equal period of exposure (1h)

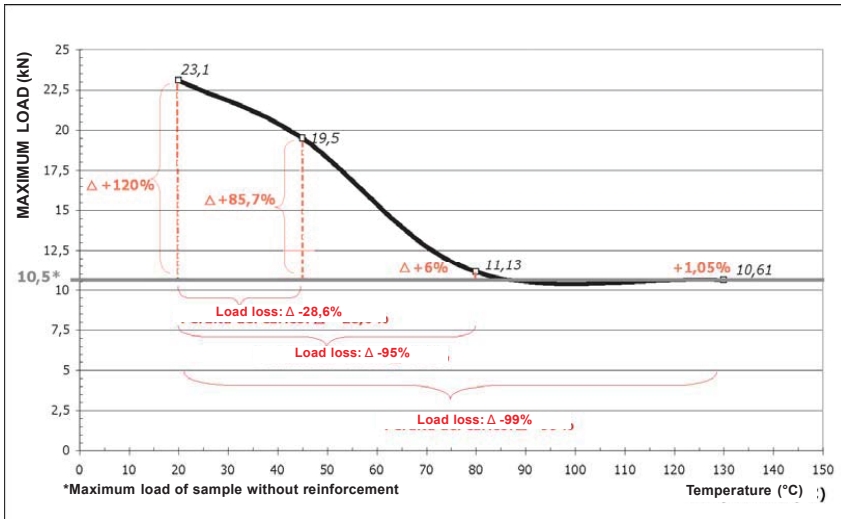

Figure 2

RUREDIL X MESH GOLD vs. C-FRP: Maximum load at +80°C - 100% relative humidity

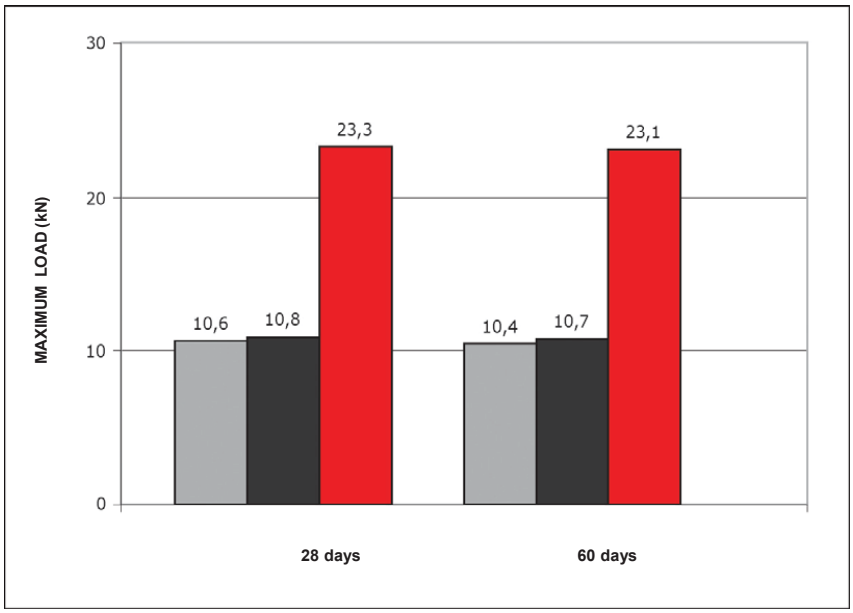

Figure 3

Bending stress reinforcement for concrete beams

The efficiency of concrete beams reinforced with RUREDIL X MESH GOLD has been carefully studied and tested. In fact, bending stress tests were performed on three or four points of concrete beams (40cm x 25cm) with 1.6 and 2.2m clearance. Different types of reinforcement were tested, similar to the ones referred to in figures N.4, N.5, N.6 and N.7. Certain test results concerning load - centre line displacement diagrams have been included in the above mentioned figures. The benefits of fibre reinforcement can be appreciated by the collapse load increase when compared with samples without reinforcement.

- Flex reinforcement of reinforced concrete beams with RUREDIL X MESH GOLD may be achieved with application to areas under tension and bracketing, resulting in an increase in distributed collapse load of around 10-50% or more of the current value.
- The typical reinforcement morphology consists of strips of variable length in the intrados, possibly folded over onto lateral surfaces and, where possible, with at least one U-shaped bracketing strip at the end of the longitudinal cover.

Figures N.4, N.5, N.6 and N.7 represent three possible reinforcement configurations for which the number of intrados layers required must be determined by calculating beam flexing. Some experimental load-arrow charts are illustrated in the same figures. These charts have been obtained by means of bending tests on reinforced concrete beams, adopting similar configurations as those illustrated.

The first configuration (figure N.4) has an intrados reinforcement layer with U-shaped strips at the ends, while the second (figures N.5 and N.6) have two layers of intrados strips and U-shaped strips at the ends, and the third and last configuration (figure N.7) has intrados strips, intrados strips extended to the side surfaces and U-shaped strips for shear strength.

Use of the configuration shown in figure N.7, where possible.

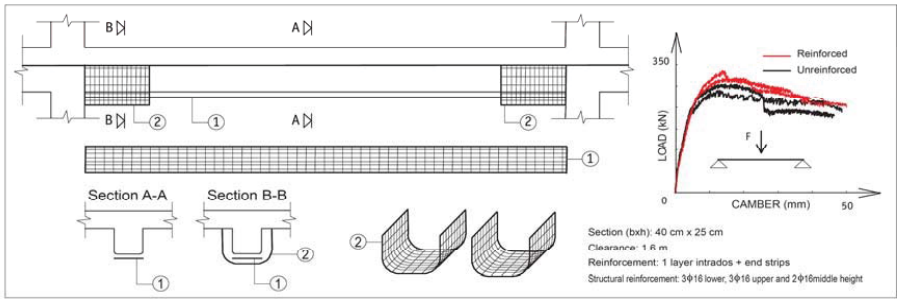

Figure 4

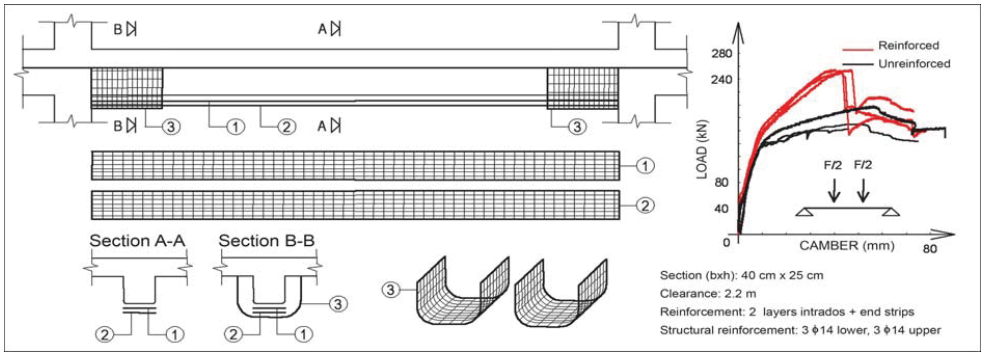

Figure 5

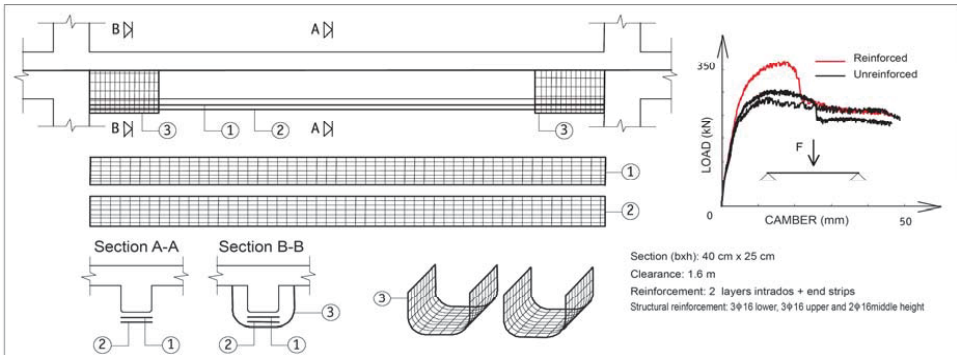

Figure 6

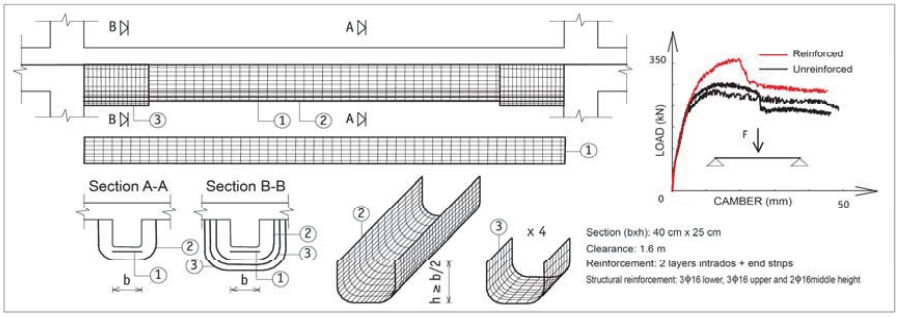

Figure 7

Ruredil X Mesh Gold

PBO (Poliparafenilenbenzobisoxazolo) mesh in a stabilised inorganic matrix for flexural and shear strenght reinforcement of concrete

Design criteria for reinforcement with RUREDIL X Mesh GOLD for inflected reinforced concrete beams

According to the technical document CNR-DT 200/2004, the dimensioning of the flexural reinforcement can be performed at the ultimate state by considering a design resistance of the reinforcement taking the "intermediate peeling" crisis into account. With RUREDIL X MESH GOLD, usually this happens by sliding between fibres and cementitious matrix.

On the basis of these experiments performed, the following figures may be suggested for calculated tensile strength of the reinforcement (taking also the intermediate peeling crisis into account):

- with one reinforcement layer and U-shaped strips at the end (as shown in figure N.4): F_{fd} = 157.5 kN/m (force per width unit of the reinforcement), corresponding to the calculated (warp) tensile strength f_{Fd} = 3500 N/mm^2 and the calculated ultimate dilatation ε_{Fd} = 1,29%.
- with two reinforcement layers and U-shaped strips on the ends (as shown in figures N.5, N.6 and N.7): F_{fd} = 291.6 KN/m (force per width unit of the reinforcement), corresponding to the calculated (warp) tensile strength f_{Fd} = 3240 N/mm^2 and the calculated ultimate dilatation ε_{Fd} = 1,20%.

These figures are to be used exclusively for assessment of the ultimate momentum of reinforced sections.

The verification of peeling at the ends at the ultimate state can be carried out according to the technical document CNR-DT 200/2004, considering, for the various configurations, peeling tensions at the reinforcement end of about 20% of the calculated resistances indicated above.

The peeling of the reinforcement at the end can be prevented with U-shaped bracketing strips shown as □ in figure 5 (which also improve shear strength) and the conformation shown as □ in figure 7 in the surface layer of reinforcement.

The calculated resistances above can be achieved only if the concrete of the metal rod has suitable mechanical properties. Premature breakages of the metal rod might occur, also causing the crisis with sliding of the fibres in the cementitious matrix might not be achieved.

Careful assessment of the mechanical properties of the surface layer of the concrete is therefore recommended, as is reconstruction of the entire area covering the reinforcement rod if it is found to be inadequate and if the metal rods reveal a state of advanced corrosion.

Once the reinforcement section meeting the ultimate state has been determined, it is possible to check the operating limit and that concerning stresses.

Generally the pre-existing stress state (due to the existing loads upon reinforcement application) should be considered, from which a differential dilatation between support and reinforcement derives.

N.B. Reinforcement projects must in all cases, as for all composite materials, be based on careful assessment of the properties of the structure to be reinforced. Specifically, it is important to study the quality of the materials used (concrete and steel), the amount of metal reinforcement present, the condition of the concrete covering the reinforcement rods and corrosion of the rods. It is also essential to assess how the structure reacts to crisis before and after reinforcement.
Designer should be acquainted with the mechanical properties and durability of the structural reinforcement under the different thermohygrometric conditions it will be used.
Before handing over the executive project, the designer must estimate, on the basis of essential tests conducted on the structure, the mechanical properties of the concrete and local damage (cracking and peeling) to be repaired. A total load test is strongly recommended both before and after reinforcement to certify the functioning of the composite-concrete pair.

Before accepting the work the supervisor of works must carefully check the composite material, taking into consideration the mechanical properties and stability under the different environmental conditions of application, compliance with the conditions specified by the engineer on the surfaces for adhesion, and conduct a preventive test in addition to the usual inspections of the installation, including application of the composite material.

Revision 08/2012. The present edition cancels and replaces all the previous ones. The information contained in the present technical data sheet is based on our knowledge and experience and should therefore not be taken as our guarantee. Neither shall we be responsible for the utilisation of the product since the conditions under which it is used are beyond our control.

Ruredil spa
Headquarters and plant: Via B. Buozzi, 1; I-20097 San Donato Milanese - Milan (ITALY)
Phone: +39.02.5276041 Export dept.: ext. 1255 - Fax: +39.02.5272185 e-mail: info@rurcem.it website: www.ruredil.it
Abroad: Algeria, Austria, Canada, Costa Rica, Chile, Cuba, Cyprus, Dominican Republic, Ecuador, Egypt, France, Greece, Iran, Morocco, Panama, Poland, Portugal, Qatar, Romania, Russia, Spain, Switzerland, Tunisia, Ukraine, U.S.A.

Strengthening Solutions

V-Wrap™ C200HM

High Modulus Carbon Fiber Fabric

structural TECHNOLOGIES
structuraltechnologies.com
+1-410-859-6539

Typical Data for V-Wrap C200HM

Storage Conditions:	Store dry at 40°F – 90°F (4°C – 32°C)
Color:	Black
Primary Fiber Direction:	0° (unidirectional)
Weight:	17.7 oz/yd² (600 g/m²)
Shelf life:	10 years

Fiber Properties (Dry)

Tensile Strength:	790,000 psi (5,440 MPa)
Tensile Modulus:	42 x 10^6 psi (289,550 MPa)
Elongation:	1.9 %

Cured Laminate Properties	Average Values	Design Values*
Tensile Strength:	180,000 psi (1,241 MPa)	155,000 psi (1,068 MPa)
Modulus of Elasticity:	14.24 x 10^6 psi (98,181 MPa)	14.0 x 10^6 psi (96,527 MPa)
Elongation at Break:	1.27%	1.1%
Thickness:	0.04 in. (1.02 mm)	0.04 in. (1.02 mm)
Strength per Unit Width:	7,200 lbs/in. (1.26 kN/mm)	6,200 lbs/in. (1.09 kN/mm)

*Design properties are based on ACI 440.2R using average minus three standard deviations.

Description:

V-Wrap C200HM is a unidirectional carbon fiber fabric with fiber oriented in the 0° direction. V-Wrap C200HM system is field laminated using environmentally friendly, two-part 100% solids and high strength structural adhesives to form a carbon fiber reinforced polymer (CFRP) system used to reinforce structural elements.

Product Uses:

V-Wrap strengthening systems can be used to resolve strength deficiencies and increase the load carrying capacity of building, bridges, silos, chimneys, and other structures.

Loading Increases:

- Increasing the live loads capacity of floor systems
- Increasing shear and flexural strengths of reinforced and prestressed beams
- Increasing the axial capacity of columns
- Increasing the live load capacity of parking garages

Seismic Strengthening:

- Column confinement for ductility improvement
- Masonry and concrete shear walls strengthening

Damage to Structural Parts:

- Correct strength deficiency due to deterioration and corrosion
- Restore strength of structural elements damaged by fire

Change in Structural System:

- Load redistribution due to removal of walls, beams or columns
- Removal of slab sections for new openings

Design or Construction Defects:

- Insufficient amount of shear or flexural reinforcement
- Insufficient size and/or layout of reinforcement
- Insufficient reinforcing bar or lap splice length
- Low compressive strength in beams, slabs, and columns

Advantages:

- ICC-ES ESR-3606 listed product
- 0% VOC
- 100% Solvent free
- Non-corrosive reinforcement system
- Lightweight flexible fabric can be wrapped around complex shapes
- Used for shear, confinement or flexural strengthening
- High strength and high modulus
- Light weight
- Reduces crack width
- Alkali resistant
- Low aesthetic impact

Packaging:

Fabric: 24 in. width x 150 ft rolls
0.61 m width x 45.7 m rolls

© 2016 Structural Technologies, LLC

structural TECHNOLOGIES
structuraltechnologies.com
+1-410-859-6539

How To Use:

Design:

Design should comply with ACI 440.2R or recognized design/ specification entity, and is typically based on CFRP contribution determined by detailed analysis. Design values will vary based on project requirements and applicable environmental and strength reduction factors. Contact STRUCTURAL TECHNOLOGIES to determine applicable design factors.

Surface Preparation:

Surfaces to receive V-Wrap C200HM must be clean and sound. It must be dry and free of frost. All dust, laitance, grease, curing compounds, waxes, deteriorated materials, and other bond inhibiting materials must be removed from the surface prior to application. Existing uneven surfaces must be filled with appropriate epoxy putty or repair mortar. Use abrasive blasting, pressure wash, shotblast, grind or other approved mechanical means to achieve an open-pore texture with a concrete surface profile of CSP-3 or better (ICRI). In certain applications and at the engineer's discretion, the bond between the substrate and the fabric may be determined to be non-critical (such as in column confinement applications). All corners must be rounded to 1/2" radius minimum. A minimum overlap [or lap splice] of 6" is required to achieve continuity. The adhesive strength of the concrete may be verified after surface preparation by random pull-off testing (ASTM D7522) at the discretion of the engineer. Minimum tensile strength of 200 psi must be achieved.

Cutting V-Wrap C200HM:

Fabric can be cut to appropriate length by using a commercial quality heavy-duty scissors.

Application:

Installation of the V-Wrap C200HM strengthening system should be performed only by a specially trained, approved contractor. The V-Wrap C200HM strengthening system shall consist of V-Wrap C200HM carbon fabric and V-Wrap epoxy resins such as: V-Wrap 600, V-Wrap 700S, and V-Wrap 770.

Note the specified number of plies, ply widths, and fiber orientation. Mix resin components using recommended procedures on product datasheet. Apply one coat of V-Wrap epoxy as a primer to the surface using a nap roller. Fill minor concrete defects such as bug holes and other imperfections with V-Wrap epoxy putty or V-Wrap epoxy mixed with fumed silica (thickened epoxy). Apply V-Wrap putty or thickened epoxy using a roller or trowel to primed surface. Adjust the gap between saturator rollers to approximately 42 mils. Using a saturator machine, pre-saturate the appropriate length of V-Wrap C200HM with V-Wrap epoxy adhesive as a saturant. Install the saturated FRP sheet. Use a rib roller to remove all air pockets and ensure intimate contact with the surface. If a splice is needed, a minimum 6" overlap is required. On multiple plies with splices, stagger the splice locations. If required, apply topcoat material.

Limitations:

- Design calculations must be approved by a licensed professional engineer.
- System is a vapor barrier.
- Concrete deterioration and steel corrosion must be resolved prior to application.
- Minimum application temperature is 40°F.

Storage:

Store material in a cool, dark space. Low humidity is recommended.

Handling:

Approved personal protection equipment should be worn at all times. Particle mask is recommended for possible airborne particles. Gloves are recommended when handling fabrics and resins to avoid skin irritation. Safety glasses are recommended to prevent eye irritation. Wear chemical resistant clothing/gloves/goggles. Ventilate area. In absence of adequate ventilation, use properly fitted NIOSH respirator.

Cleanup:

Dispose of material in accordance with local disposal regulations. Uncured material can be removed with approved solvents. Cured materials can only be removed mechanically.

First Aid:

In case of skin contact, wash thoroughly with soap and water. For eye contact, flush immediately with plenty of water; contact physician immediately. For respiratory problems, remove to fresh air. Wash clothing before reuse.

STRUCTURAL TECHNOLOGIES, LLC warrants its products to be free from manufacturing defects and to meet STRUCTURAL TECHNOLOGIES' current published properties when applied in accordance with STRUCTURAL TECHNOLOGIES' directions and tested in accordance with ASTM and STRUCTURAL TECHNOLOGIES Standards. User determines suitability of product for use and assumes all risks. Buyer's sole remedy shall be limited to the purchase price or replacement of product and excludes labor or the cost of labor. Any claim for breach of this warranty must be brought within one year of the date of purchase.

No other warranties expressed or implied including any warranty of merchantability or fitness for a particular purpose shall apply. STRUCTURAL TECHNOLOGIES shall not be liable for any consequential or special damages of any kind, resulting from any claim or breach of warranty, breach of contract, negligence or any legal theory. STRUCTURAL TECHNOLOGIES assumes no liability for use of this product in a manner to infringe on another's patent.

© 2016 Structural Technologies, LLC

Strengthening Solutions

V-Wrap™ 770

Epoxy Adhesive

structuraltechnologies.com
+1-410-859-6539

Physical Properties[1]:

Tensile Strength (ASTM D638):	8,800psi (60.7 MPa)
Tensile Modulus (ASTM D638):	400,000 psi (2,760 MPa)
Elongation at Break (ASTM D638):	4.4%
Flexural Strength (ASTM D790):	13,780 psi (95 MPa)
Flexural Modulus (ASTM D790):	380,000 psi (2,620 MPa)
Compressive Strength (ASTM D695):	12,450 psi (85.8 MPa)
Compressive Modulus (ASTM D695):	387,000 psi (2,670 MPa)
Tg (ASTM D4065):	180°F (82°C)
Density:	
Mixed Product	9.17 lbs/gal (1.11 kg/L)
Part A	9.7 lbs/gal (1.16 kg/L)
Part B	7.9 lbs/gal (0.95 kg/L)
VOC Content (ASTM D2369):	0% VOC

(1) Curing schedule: 72 hours post cure at 140°F (60°C)

DESCRIPTION:
V-Wrap 770 is a two-part, 100% solids, epoxy for high strength composite bonding applications. V-Wrap 770 matrix material is combined with V-Wrap carbon and glass fabrics to provide a wet-layup composite for strengthening of structural members. It is formulated to provide high elongation to optimize properties of the V-Wrap composite systems. It provides a long working time for application, with no offensive odor. V-Wrap 770 may be thickened with fumed silica to produce a tack coat/putty or a finishing coat, depending upon the project requirements.

V-Wrap 770 is an environmentally friendly product with no Volatile Organic Compounds (VOC) or solvents.

PRODUCT USES:
V-Wrap 770 is a multi use epoxy that performs as a primer, tack coat/putty, and saturating resin for the V-Wrap carbon and glass fiber systems. For detailed uses see installation guides for V-Wrap strengthening systems. Fumed silica may be added to thicken the resin. The maximum ratio by volume is 1.5 of fumed silica to 1 part of resin.

ADVANTAGES:
- ICC-ES ESR-3606 listed product
- NSF/ANSI Standard 61 listed product for drinking water systems
- 100% solvent free
- Good high / low temperature properties
- High elongation

APPLICATION INFORMATION
Please refer to the NSF Listing for the NSF/ANSI 61 Listed Application.

SURFACE PREPARATION:
V-Wrap 770 should be applied to substrates that are free of protrusions, dry, exhibit an open pore structure, and are free of dust, oils or other surface contaminates or bond inhibiting materials.

BASIC APPLICATION EQUIPMENT:
Application processes for V-Wrap 770 will require mixing drill, mixing paddle, 1/4" nap rollers, steel rollers, paint brushes, trowels and saturator.

MIXING:
Mix ratio: Premix Part A for 2 minutes. Add the full contents of Part B pail to the full contents of Part A pail, or use equal fractions of each pail. Blend Part A and Part B with a mechanical mixer for 3 minutes until uniformly blended.

APPROXIMATE POT LIFE:
3 to 6 hours at 68°F (20°C)

COVERAGE RATES:

AS A PRIMER:

Concrete:	225 ft²/gal (5.5 m²/L)
Masonry: (Concrete)	125 ft²/gal (3.0 m²/L)
Masonry: (Clay)	200 ft²/gal (4.9 m²/L)

AS PUTTY/TACK COAT:

Filler:	60 ft²/gal (1.5 m²/L)

(Depending on surface roughness)

© 2016 Structural Technologies, LLC

Strengthening Solutions

V-Wrap™ 770

Epoxy Adhesive

structuraltechnologies.com
+1-410-859-6539

AS SATURANT:

V-Wrap C100	80 ft²/gal (1.9 m²/L)
V-Wrap C200	60 ft²/gal (1.5 m²/L)
V-Wrap C200H	60 ft²/gal (1.5 m²/L)
V-Wrap C400H	40 ft²/gal (1 m²/L)
V-Wrap EG50	60 ft²/gal (1.5 m²/L)

Coverage rates may vary based on installation procedure and fabric type. Contact STRUCTURAL TECHNOLOGIES for coverage rates.

LIMITATIONS:
Only apply V-Wrap 770 when the ambient temperature is between 40°F and 100°F (4°C to 38°C). Topcoat selection should be based upon requirements for protection from environmental exposures, aesthetics, and fire protection/burn characteristics.

CLEAN UP:
Use methyl ethyl ketone or acetone. Observe fire and health precautions when using solvents. Dispose of in accordance with local regulations.

OBSERVE WORKING TIME LIMITATIONS:
Mix no more material than can be applied within the work time period. Available work time, temperature and complexity of the application will determine how much material should be mixed at one time. Keep material cool and in shaded area, away from direct sunlight in warm weather. During hot weather, work time can be extended by keeping the material cool before and after mixing or by immersing the pot in ice water.

HANDLING PROPERTIES:

Color:	
Mixed	Clear
Part A	Clear
Part B	Clear

SHELF LIFE:
Stored at 70°F (21°C): 24 months (Parts A and B)

PACKAGING:

	Volume	Weight	Package
Part A	2.8 gal	27.3 lbs	5 gal pail
Part B	1.15 gal	9.1 lbs	5 gal pail

STORAGE:
Store in a cool, dry area (40°F and 90°F [4°C to 32°C]) away from direct sunlight, flame or other hazards.

SAFETY:
WARNING: Vapor may be harmful. Contains epoxy adhesive and curing agent. May cause skin sensitivity or other allergic responses. Keep away from heat, sparks or open flame. In enclosed areas or where ventilation is poor use an approved air mask and utilize adequate safety precautions to prevent fire or explosion. In case of sin contact, wash with soap and water. For eyes, flush immediately (seconds count) with water for 15 minutes and CALL A PHYSICIAN. If swallowed, CALL A PHYSICIAN IMMEDIATELY.

HANDLING:
Approved personal protection equipment should be worn at all times. Particles mask is recommended when handling airborne particles. Gloves are recommended when handling fabrics and resins to avoid skin irritation. Safety glasses are recommended to prevent eye irritation. Wear chemical resistant clothing /gloves/goggles. Ventilate area. In absence of adequate ventilation, use properly fitted NIOSH respirator. Product Material Safety Data Sheets (MSDS) are available and should be consulted and on hand whenever handling these products.

These products are for professional and industrial use only and are to be installed by trained and qualified applicators. Trained applicators must follow installation instructions.

MAINTENANCE:
Periodically inspect the applied material and repair localized areas as needed.

STRUCTURAL TECHNOLOGIES, LLC warrants its products to be free from manufacturing defects and to meet STRUCTURAL TECHNOLOGIES' current published properties when applied in accordance with STRUCTURAL TECHNOLOGIES' directions and tested in accordance with ASTM and STRUCTURAL TECHNOLOGIES Standards. User determines suitability of product for use and assumes all risks. Buyer's sole remedy shall be limited to the purchase price or replacement of product and excludes labor or the cost of labor. Any claim for breach of this warranty must be brought within one year of the date of purchase.

No other warranties expressed or implied including any warranty of merchantability or fitness for a particular purpose shall apply. STRUCTURAL TECHNOLOGIES shall not be liable for any consequential or special damages of any kind, resulting from any claim or breach of warranty, breach of contract, negligence or any legal theory. STRUCTURAL TECHNOLOGIES assumes no liability for use of this product in a manner to infringe on another's patent.

© 2016 Structural Technologies, LLC

Simpson Strong-Tie® Composite Strengthening Systems

CSS-CM

Cementitious Matrix

DESCRIPTION

CSS-CM is a one-component, shrinkage-compensated, polypropylene-fiber reinforced cementitious matrix designed to be field installed with CSS-UCG and CSS-BCG carbon grids to create a fabric-reinforced cementitious matrix (FRCM) composite for structural reinforcement applications. This product is part of the tested assembly in UL Design No. N859, which achieved a four-hour fire rating when subjected to ASTM E119 / UL 263 full-scale fire testing. Please refer to UL Online Certifications Directory for the UL listing.

MATERIAL PROPERTIES

Matrix Properties

Unit Weight	140 lb./ft.^{3} (2,240 kg/m^3)
Set Times (ASTM C191)	**Initial Set:** <5 hr. **Final Set:** <8 hr.

Matrix Test Properties[1]

Property	Design Value
Tensile Modulus (ASTM C469)	3,880,000 psi (26.8 GPa) @ 28 days
Rapid Chloride Permeability (ASTM C1202)	<500 coulombs (very low) @ 28 days
Freeze/Thaw Resistance (ASTM C666, Proc. A)	93.7% RDM @ 300 cycles
Salt Scaling Resistance (ASTM C672)	0.06 lb./ft.^{2} (very slight) @ 50 cycles
Sulfate Resistance (ASTM C1012)	+0.02% @ 6 mo.
Direct Tensile Bond Strength (ASTM C1583)	28 day: 390 psi (2.7 MPa)
Direct Shear Bond Strength (Michigan DOT)	28 day: 300 psi (2.1 MPa)
Slant Shear Bond Strength (ASTM C882, mod.)	28 day: 2,630 psi (18.1 MPa)
Splitting Tensile Strength (ASTM C496)	28 day: 700 psi (4.8 MPa)
Flexural Strength (ASTM C348)	28 day: 1,000 psi (6.9 MPa)
Compressive Strength (ASTM C109)	1 day: 3,000 psi (21 MPa) 7 day: 6,300 psi (43 MPa) 28 day: 7,500 psi (52 MPa)
Drying Shrinkage (ASTM C157, mod.[2])	-0.09% @ 28 days

1. The data herein is based on laboratory testing under controlled conditions. Variations may result from mixing methods and jobsite conditions. All testing performed at 73°F (23°C) and 50% R.H., unless otherwise noted. Results were obtained using 0.72 US gallons (2.7 L) water per 55 lb. (25 kg) bag.
2. ASTM C157 modified: 3"x3"x11.25" specimens air cured at 50% RH and 73°F.

PERFORMANCE FEATURES

- High strength
- Ambient cure
- Non-corrosive
- Molds to fit various shapes
- Low aesthetic impact
- Compatible with many finish coatings
- UL listed (www.ul.com/database)

APPLICATIONS

Seismic Retrofit
- Shear strengthening
- Displacement/ductility
- Life safety

Load Rating Upgrade
- Increased live loads
- New equipment
- Change of use

Damage Repair
- Deterioration/corrosion
- Blast/vehicle impact

Defect Remediation
- Size/layout errors
- Low concrete strengths

Blast Mitigation
- Progressive collapse

STRUCTURES

- Buildings
- Bridges
- Parking garages
- Chimneys
- Piers/wharfs
- Tunnels
- Pipes

ELEMENTS

- Columns
- Beams
- Slabs
- Walls
- Piles
- Pier caps

SUBSTRATES

- Concrete
- Masonry

PACKAGING

Bag Size
55 lb. (24.9 kg)

Model No.
CSS-CM

© 2017 Simpson Strong-Tie Company Inc.

Design
The number of layers, dimensions, and detailing of CSS-CM system shall be designed in accordance with ACI 549 or another recognized design guideline/code in order to meet the design performance specified for the application. Contact Simpson Strong-Tie for design and technical support.

Surface Preparation
Prepare surface and any exposed reinforcement per ICRI Guideline No. 310.1R. Concrete shall be prepared to achieve a minimum ¼" (6 mm) amplitude (CSP-6-9 in accordance with ICRI Guideline No. 310.2R) by means of sand blasting, shot blasting, or water blasting. Application surfaces shall be clean, sound, and free of standing water at time of application. All dust, laitance, grease, curing compounds, and other foreign materials that may hinder the bond must be removed before installation. All corners to be covered with grid and matrix shall be rounded to a ¾" (19 mm) minimum radius using a grinder. Wet the substrate for at least 24 hours to a saturated surface dry condition prior to FRCM application.

Mixing
Start with 90% of the total mixing water recommendation depending on the desired consistency of the shot mortar. Consult the printed instructions on the product package for the maximum recommended amount of mixing water. Mix with a mechanical mixer at least 3 minutes adding the remaining 10% of the recommended total water if necessary until a homogeneous mixture with the desired consistency is formed. The mixture should rest 1 minute and then remixed another 10 seconds before applying. Do not add additional water after the setting process is started.

Application
CSS installation shall be performed only by contractors and personnel that have been properly trained by Simpson Strong-Tie. CSS-CM cementitious matrix can be pumped and projected with traditional shotcrete equipment. If required, CSS-CM cementitious matrix may be used to patch voids and defects no deeper than 2" (51 mm). Immediately place ¼"–½" (6–13 mm) layer of CSS-CM cementitious matrix, then immediately set CSS grid into wet CSS-CM layer. Follow with additional layers of CSS grid, if required, set into ¼"–½" (6–13 mm) layers of CSS-CM. Finish with a final layer of CSS-CM at ¼"–½" (6–13 mm) thick and screed/trowel to desired finish. If a layer of matrix is allowed to cure with more layers to follow, the first layer must be cleaned with water pressure before the next matrix layer can be applied.

Curing
Installation shall be kept humid and protected against heat and wind for 3 to 5 days by wet curing or using an ASTM C309 complaint water-based curing compound. The use of curing compounds may affect adhesion of subsequent surface treatments. SSD surface conditions and proper curing procedures are critical at minimum application thickness to prevent premature drying or cracking.

Yield
A 55 lb. (24.9 kg) bag of CSS-CM will yield approximately 0.43 $ft.^3$ (0.012 m^3) of finished material.

Limitations
CSS installation shall take place only when the ambient and substrate temperatures are between 41°F (5°C) and 86°F (30°C).

CAUTION

May cause serious eye and skin irritation or damage. When combined with water may cause moderate to severe alkali burns.

Protective Measures: The use of safety glasses and chemically resistant gloves is recommended. Use appropriate clothing to minimize skin contact. The use of a NIOSH-approved respirator is required to protect respiratory tract when ventilation is not adequate to limit exposure below the permissible exposure limit (PEL). Refer to Safety Data Sheet (SDS) available at **strongtie.com/sds** for detailed information.

FIRST AID

Eye Contact: Immediately flush eyes with plenty of cool water for at least 15 minutes while holding the eyes open. If redness, burning, blurred vision, or swelling persists, **CONSULT A PHYSICIAN**.

Skin Contact: Remove product and wash affected area with soap and water. Do not apply greases or ointments. Remove contaminated clothing. Wash clothing with soap and water before reuse. If redness, burning, or swelling persists, **CONSULT A PHYSICIAN**.

Ingestion: DO NOT INDUCE VOMITING. CONSULT A PHYSICIAN OR POISON CONTROL CENTER IMMEDIATELY FOR CURRENT INFORMATION. Never administer anything by mouth to an unconscious person. Rinse mouth out with water. Never leave affected person unattended. If vomiting occurs spontaneously, lay affected person on their side, keeping head below hips to prevent aspiration of material into lungs.

Inhalation: Remove affected person to fresh air. If affected person continues to experience difficulty breathing, **CONSULT A PHYSICIAN**.

© 2017 Simpson Strong-Tie Company Inc.

CLEAN-UP

Spills: Sweep or vacuum material and place in a suitable container. Keep out of sewers, storm drains, surface waters, and soils.
Surface Clean: Remove any residue with hot soapy water. Cured material can be removed only by mechanical means.
Tools and Equipment: Clean with soap and water immediately after use.
Skin: Use a non-toxic pumice-based soap, citrus-based hand cleaner, or waterless hand-cleaner towel. Never use solvents to remove product from skin.
Disposal: Dispose of container and unused contents in accordance with federal, state, and local requirements. Containers may be recycled; consult local regulations for exceptions.

SHELF LIFE

1 year in unopened packaging.

STORAGE

Store material in a dry area with no exposure to moisture.

LIMITED WARRANTY

See **strongtie.com** for information.

Distributor

IMPORTANT INFORMATION
It is the responsibility of each purchaser and user of each Product to determine the suitability of the Product for its intended use. Prior to using any Product, consult a qualified design professional for advice regarding the suitability and use of the Product, including whether the capacity of any structural building element may be impacted by a repair. As jobsite conditions vary greatly, a small-scale test patch is required to verify product suitability prior to full-scale application. The installer must read, understand, and follow all written instructions and warnings contained on the product label(s), Product Data Sheet(s), Safety Data Sheet(s), and the **strongtie.com** website prior to use. For industrial use only by qualified applicators. KEEP OUT OF REACH OF CHILDREN!
Proposition 65: Products named within this document contain materials listed by the state of California as known to cause cancer, birth defects, or reproductive harm.

© 2017 Simpson Strong-Tie Company Inc.
T-R-CSSCM | 1/16
UPDATED | 12/12/17

Simpson Strong-Tie® Composite Strengthening Systems

CSS-UCG

Unidirectional Carbon Grid

DESCRIPTION

CSS-UCG is a unidirectional, high-strength, non-corrosive carbon grid designed to be field installed with CSS-CM cementitious matrix to create a fabric-reinforced cementitious matrix (FRCM) composite for structural reinforcement applications. This product is part of the tested assembly in UL Design No. N859, which achieved a four-hour fire rating when subjected to ASTM E119 / UL 263 full-scale fire testing. Please refer to UL Online Certifications Directory for the UL listing.

MATERIAL PROPERTIES

Grid Properties

Weight	13 oz./yd.^{2} (440 g/m^2)
Weight of fibers	8.3 oz./yd.^{2} (280 g/m^2)
Equivalent Dry Fabric Thickness (in strong direction)	0.0062 in. (0.157 mm)
Ultimate Tensile Strength	31 kip/ft. (450 kN/m)
Ultimate Tensile Strain	1.5%
Axial Stiffness by width unit	2,067 kip/ft. (30,000 kN/m)
Area by width unit	0.0062 in.^{2}/in. (157 mm^2/m)
Color	Gray

Cured Composite Properties[1]

Property	Design Value[2]
Cracked Tensile Modulus	7.1 x 10^6 psi (49,000 MPa)
Ultimate Tensile Strain	1.1%
Ultimate Tensile Strength	128,300 psi (885 MPa)
Lap Tensile Strength	121,000 psi, 12" lap (834 MPa, 30 cm)
Thickness per Layer	0.5 in. (13 mm)

1. When installed with CSS-CM cementitious matrix.
2. Average tensile strength and strain minus one standard deviation per ACI 549. Modulus values are average.

CLASSIFIED C UL US

STRUCTURAL CONCRETE FIBER-REINFORCED COMPOSITE SYSTEM FIRE RESISTANCE CLASSIFICATION SEE UL FIRE RESISTANCE DIRECTORY < R37897>

PERFORMANCE FEATURES

- High strength
- Ambient Cure
- Non-corrosive
- Molds to fit various shapes
- Low aesthetic impact
- Compatible with many finish coatings
- UL listed (www.ul.com/database)

APPLICATIONS

Seismic Retrofit
- Shear strengthening
- Displacement/ductility
- Life safety

Load Rating Upgrade
- Increased live loads
- New equipment
- Change of use

Damage Repair
- Deterioration/corrosion
- Blast/vehicle impact

Defect Remediation
- Size/layout errors
- Low concrete strengths

Blast Mitigation
- Progressive collapse

STRUCTURES

- Buildings
- Bridges
- Parking garages
- Chimneys
- Piers/wharfs
- Tunnels
- Pipes

ELEMENTS

- Columns
- Beams
- Slabs
- Walls
- Piles
- Pier caps

SUBSTRATES

- Concrete
- Masonry

PACKAGING

Roll Size (Width x Length)	Model No.
77 in. (1.95 m) x 164 ft. (50 m)	CSS-UCG19550

© 2018 Simpson Strong-Tie Company Inc.

Design
The number of layers, dimensions, and detailing of CSS-UCG shall be designed in accordance with ACI 549 or another recognized design guideline/code in order to meet the design performance specified for the application. Contact Simpson Strong-Tie for design and technical support.

Surface Preparation
Prepare surface and any exposed reinforcement per ICRI Guideline No. 310.1R. Concrete shall be prepared to achieve a minimum ¼" (6 mm) amplitude (CSP-6-9 in accordance with ICRI Guideline No. 310.2R) by means of sand blasting, shot blasting, or water blasting. Application surfaces shall be clean, sound, and free of standing water at time of application. All dust, laitance, grease, curing compounds, and other foreign materials that may hinder the bond must be removed before installation. All corners to be covered with grid and matrix shall be rounded to a ¾" (19 mm) minimum radius using a grinder. Wet the substrate for at least 24 hours to a saturated surface dry condition prior to FRCM application.

Application
CSS installation shall only be performed by contractors and personnel that have been properly trained by Simpson Strong-Tie. CSS-CM cementitious matrix is pumped and projected with traditional shotcrete equipment. If required, CSS-CM may be used to patch voids and defects no deeper than 2" (51 mm). Place ¼"–½" (6–13 mm) layer of CSS-CM cementitious matrix, then immediately set CSS-UCG grid into wet CSS-CM layer. Follow with additional layers of CSS-UCG, if required, set into ¼"–½" (6–13 mm) layers of CSS-CM. Finish with a final layer of CSS-CM at ¼"–½" (6–13 mm) thick and screed/trowel to desired finish. If a layer of matrix is allowed to cure with more layers to follow, the first layer must be cleaned with water pressure before the next matrix layer can be applied. See CSS-CM product data sheet for more detailed application and curing recommendations.

Matrix Working and Set Time
See CSS-CM product data sheet for the working time and set times of CSS-CM cementitious matrix.

Limitations
CSS installation shall only take place when the ambient and substrate temperatures are between 41°F (5°C) and 86°F (30°C). Installation shall be kept humid and protected against heat and wind for three to five days after application.

SAFETY PRECAUTIONS

Proper personal protection equipment (PPE) shall be worn at all times. Avoid contact with skin and eyes. Particulate masks, rubber gloves, safety glasses, and coverall suits are recommended. Refer to MSDS for full information.

FIRST AID

Skin: Wash fibers off skin with water and soap. If fibers are embedded in the skin, remove with tweezers. Discard clothing that may contain embedded fibers. **GET MEDICAL ATTENTION** if exposure results in adverse effects.

Eyes: Immediately flush with a continuous water stream for at least 20 minutes. Washing immediately after exposure is expected to be effective in preventing damage to the eyes. **GET MEDICAL ATTENTION.**

Inhalation: If there is inhalation exposure to the fibers of this product, remove source of exposure and move affected person to fresh air. If affected person is not breathing, give artificial respiration. If there is breathing difficulty, give oxygen. **GET IMMEDIATE MEDICAL ATTENTION** for any respiratory problems.

Ingestion: Not expected to occur since ingestion is not a likely route of exposure for this product. If ingestion does occur, **DO NOT INDUCE VOMITING.** Give nothing by mouth if affected person is unconscious. **GET IMMEDIATE MEDICAL ATTENTION.**

CLEAN-UP

Dispose of material in accordance with local regulations.

SHELF LIFE

10 years from date of manufacture

STORAGE

Store material in a dry area with no exposure to moisture.

LIMITED WARRANTY

See **strongtie.com** for information.

IMPORTANT INFORMATION
It is the responsibility of each purchaser and user of each Product to determine the suitability of the Product for its intended use. Prior to using any Product, consult a qualified design professional for advice regarding the suitability and use of the Product, including whether the capacity of any structural building element may be impacted by a repair. As jobsite conditions vary greatly, a small-scale test patch is required to verify product suitability prior to full-scale application. The installer must read, understand, and follow all written instructions and warnings contained on the product label(s), Product Data Sheet(s), Material Safety Data Sheet(s), and the **strongtie.com** website prior to use. For industrial use only by qualified applicators. KEEP OUT OF REACH OF CHILDREN!
Proposition 65: Products named within this document contain materials listed by the state of California as known to cause cancer, birth defects, or reproductive harm.

© 2018 Simpson Strong-Tie Company Inc.
T-R-CSSUCG | 9/15
UPDATED | 6/11/18

REFERENCES

AC434. (2013). “Proposed acceptance criteria for masonry and concrete strengthening using fiber-reinforced cementitious matrix (FRCM) composite systems.” ICC-Evaluation Service, Whittier, CA.

ACI Committee 318. (2014). *Building Code Requirements for Structural Concrete and Commentary*. *American Concrete Institute*. Farmington Hills, Michigan. https://doi.org/10.1016/0262-5075(85)90032-6

ACI Committee 440. (2008). *ACI 440.2R-08 Guide for the Design and Construction of Externally Bonded FRP Systems*. *Guide for the Design and Construction of Externally Bonded FRP Systems for Strengthening Concrete Structures*.

ACI Committee 440. ACI 440.2R-17: Guide for the design and construction of externally bonded FRP systems for strengthening existing structures, American Concrete Institute § (2017).

ACI Committee 549. (2013). *ACI 549.4R-13: Guide to Design and Construction of Externally Bonded Fabric- Reinforced Cementitious Matrix (FRCM) Systems for Repair and Strengthening Concrete and Masonry Structures*. *American Concrete Institute*. Farmington Hills, Michigan.

Aram, M. R., Czaderski, C., & Motavalli, M. (2008). Debonding failure modes of flexural FRP-strengthened RC beams. *Composites Part B: Engineering*, *39*(5), 826–841. https://doi.org/10.1016/j.compositesb.2007.10.006

Arboleda, D. (2014). *Fabric Reinforced Cementitious Matrix (FRCM) Composites for Infrastructure Strengthening and Rehabilitation : Characterization Methods*.

ASCE. (2017). 2017 Infrastructure Report Card. https://doi.org/10.1017/CBO9781107415324.004

Babaeidarabad, S., Loreto, G., & Nanni, A. (2014). Flexural Strengthening of RC Beams with an Externally Bonded Fabric-Reinforced Cementitious Matrix. *Journal of Composites for Construction*, *18*(5), 04014009. https://doi.org/10.1061/(ASCE)CC.1943-5614.0000473

Barton, B., Wobbe, E., Dharani, L. R., Silva, P., Birman, V., Nanni, A., … Tunis, G. (2005). Characterization of reinforced concrete beams strengthened by steel reinforced polymer and grout (SRP and SRG) composites. *Materials Science and Engineering A*, *412*(1–2), 129–136. https://doi.org/10.1016/j.msea.2005.08.151

Brameshuber, W. (2006). *Textile Reinforced Concrete - State-of-the-Art Report of RILEM TC 201-TRC*. *RILEM*.

D'Ambrisi, A., & Focacci, F. (2011). Flexural Strengthening of RC Beams with Cement-Based Composites. *Journal of Composites for Construction*, *15*(5), 707–720. https://doi.org/10.1061/(ASCE)CC.1943-5614.0000218.

Di Tommaso, A., Focacci, F., & Mantegazza, G. (2008). *PBO-FRCM composites to strengthen R . C . beams : mechanics of adhesion and efficiency*. *Fourth International Conference on FRP Composites in Civil Engineering*.

Gonzalez-Libreros, J. H., Sabau, C., Sneed, L. H., Pellegrino, C., & Sas, G. (2017). State of research on shear strengthening of RC beams with FRCM composites. *Construction and Building Materials*, *149*, 444–458. https://doi.org/10.1016/j.conbuildmat.2017.05.128

Hernandez, E.S., & Myers, J. (2019). Evaluation and Strengthening of Missouri Bridge P0058 Using Reinforced Cementitious Materials. Seventh Asia-Pacific Conference on FRP in Structures (APFIS 2019). Gold Coast, Australia.

Hernandez, & Myers. (2018a). Diagnostic Test for Load Rating of a Prestressed SCC Bridge. *Evaluation of Concrete Bridge Behavior Through Load Testing - International Perspective*, ACI SP 323 11.1-11.16.

Hernandez, E.S., & Myers, J. (2018b). Strength evaluation of prestressed concrete bridges by load testing. The Sixth International Symposium on Life-Cycle Civil Engineering (IALCCE 2018). Ghent, Belgium.

Hind, M. K., Özakçab, M., & Ekmekyaparc, T. (2016). A Review on Nonlinear Finite Element Analysis of Reinforced Concrete Beams Retrofitted with Fiber Reinforced Polymers. *Journal of Advanced Research in Applied Mechanics*, *22*(1), 13–48.

Holdener, D. J., Myers, J. J., & Nanni, A. (2004). *Field Strengthening and Validation of FRP Composites Technology in Missouri*.

Huang, X., Birman, V., Nanni, A., & Tunis, G. (2003). Properties and potential for application of steel reinforced polymer and steel reinforced grout composites. *Composites Part B: Engineering*, *36*(1), 73–82. https://doi.org/10.1016/S1359-8368(03)00080-5

Kerakoll S.p.A. (2014). GeoSteel G600, 1–4.

Loreto, G., Babaeidarabad, S., Leardini, L., & Nanni, A. (2015). RC beams shear-strengthened with fabric-reinforced-cementitious-matrix (FRCM) composite. *International Journal of Advanced Structural Engineering*, *7*(4), 341–352. https://doi.org/10.1007/s40091-015-0102-9

Loreto, G., Leardini, L., Arboleda, D., & Nanni, A. (2013). Performance of RC Slab-Type Elements Strengthened with Fabric-Reinforced Cementitious-Matrix Composites. *Journal of Composites for Construction*, *18*(3), A4013003. https://doi.org/10.1061/(ASCE)CC.1943-5614.0000415

Merkle, W. J. (2004). *Load Distribution and Response of Briddges Retrofitted with Various FRP Systems*. University of Missouri- Rolla.

Missouri Department of Transportation. (2005). Preservation of Missouri Transportation Infrastructures : Validation of FRP Composite Technology. *Missouri Depar Transportation Research, Development and Technology*.

Myers, J. J., Holdener, D., & Merkle, W. (2012). Load testing and load distribution of fiber reinforced, polymer strengthened bridges: Multi-year, post construction/post retrofit performance evaluation. *Fiber Reinforced Polymer (FRP) Composites for Infrastructure Applications: Focusing on Innovation, Technology Implementation and Sustainability*, 163–191. https://doi.org/10.1007/978-94-007-2357-3_9

Myers, J. J., Holdener, D., Merkle, W., & Hernandez, E. (2008). *PRESERVATION OF MISSOURI TRANSPORATION INFRASTRUCTURES: IN-SITU LOAD TESTING OF BRIDGES P-962, T-530, X-495, X-596 AND Y-298*.

Nanni, Antonio. "Properties of Materials - Southern Mo Bridge Strengthening: RECAST." 7 Mar. 2018.

Ombres, L. (2015). Structural performances of reinforced concrete beams strengthened in shear with a cement based fiber composite material. *Composite Structures*, *122*, 316–329. https://doi.org/10.1016/j.compstruct.2014.11.059

Petrou, M. F., Parler, D., Harries, K. A., & Rizos, D. C. (2008). Strengthening of Reinforced Concrete Bridge Decks Using Carbon Fiber-Reinforced Polymer Composite Materials. *Journal of Bridge Engineering*, *13*(5), 455–467. https://doi.org/10.1061/(ASCE)1084-0702(2008)13:5(455)

Pino, V. A. (2016). Fabric Reinforced Cementitious Matrix (FRCM) Composites as a Repair System for Transportation Infrastructure.

Rahman, A. H., Kingsley, C. Y., & Kobayashi, K. (2000). SERVICE AND ULTIMATE LOAD BEHAVIOR OF BRIDGE DECK REINFORCED WITH CARBON FRP GRID. *Journal of Composites for Construction*, *45*(February), 16–23.

Ruredil. (2012). Ruredil X Mesh Gold, 1–6. Retrieved from www.ruredil.it

Simpson Strong-Tie. (2017). CSS-CM Product Guide. Retrieved from strongtie.com

Simpson Strong-Tie. (2018). CSS-UCG Product Guide. Retrieved from strongtie.com

Structural Technologies. (2016a). V-Wrap ™ 770 Product Guide, 4–5. Retrieved from structuraltechnologies.com

Structural Technologies. (2016b). V-Wrap ™ C200HM Product Guide, 1–2. Retrieved from structuraltechnologies.com

Wight, J. K., & Macgregor, J. G. (2012). *Reinforced concrete: mechanics and design* (6th ed.). Upper Saddle River, New Jersey: Pearson Education, Inc. https://doi.org/10.1139/l00-087

Wobbe, E., Silva, P., Barton, B. L., Dharani, L. R., Birman, V., Nanni, A., … Tunis, G. (2004). Flexural capacity of RC beams externally bonded with SRP and SRG. *International SAMPE Symposium and Exhibition (Proceedings)*, *49*, 2995–3002. Retrieved from http://www.scopus.com/inward/record.url?eid=2-s2.0-23844538743&partnerID=tZOtx3y1